Doctoral Dissertation (Shinshu University)

Studies on design and characterization of phthalocyanine-based liquid crystals and liquids

March 2020

Yoshiaki Chino

Table of contents

Declaration

I, *Yoshiaki Chino*, declare that this thesis, submitted in fulfillment of the requirements for the degree for Doctor of Engineering, in the Interdisciplinary Graduate School of Science and Technology, Department of Bioscience and Textile Technology, Shinshu University, is completely my own work unless otherwise referenced or acknowledged. This thesis has not been submitted for qualifications at any other academic institution.

Yoshiaki Chino

March 19, 2020

Abbreviations

Col_{ho}: ordered hexagonal columnar phase
Col_{ro}: order rectangular columnar phase
DBU: 1,8-diazabicyclo[5.4.0]undec-7-ene
DMF: *N, N*-Dimethylformamide
DMSO: Dimethylsulfoxide
DSC: Differential scanning calorimetry
FML: Functional molecular liquid
FT-IR: Fourier transform-infrared spectroscopy
HPLC: High performance liquid chromatography
HOMO: Highest occupied molecular orbital
HR-APCI-TOF: High resolution-atmospheric pressure chemical ionization-time of flight
LML: Luminous molecular liquid
LUMO: Lowest unoccupied molecular orbital
MALDI-TOF: Matrix-assisted laser desorption ionization time-of-flight
NIR: Near infrered
NMR: Nuclear magnetic resonance
OFET: Organic field effect transistor
OPV: Organic photovoltaics
Pc: Phthalocyanine
POM: Polarizing optical microscope
Por: Porphyrin
SAXD: Small angle X-ray diffraction
SAXS: Small angle X-ray scattering
T_c: Clearing point (temperature of phase transition from liquid crystal to isotropic liquid)
T_g: Glass transition point
TFA: Trifluoroacetic acid
TGA: Thermogravimetric analysis
THF: Tetrahydrofuran
TLC: Thin layer chromatography
T_m: Melting point (in the case of liquid crystalline sample, T_m means the temperature of phase transition crystal to liquid crystal)

List of figures

List of schemes

List of tables

Chapter 1

Introduction and literature review

1.1. Introduction

1.1.1. Motivation

Intermolecular interactions such as van der Waals force, π-π stacking, and hydrogen bond play key role in organized structure in materials and self-assembled process of molecules as well as physical states.[1] In natural system, there are various organized structures formed through intermolecular interactions. Representative examples are shown in Figure 1-1. Lipid bilayer is formed through van der Waals force among aliphatic units and hydrophobic-hydrophilic interaction between aliphatic units and polar units such as phosphonate.[2] Helical structure of DNA is formed through multiple hydrogen bonds between complementary base pairs in a double strand of polynucleotide chains.[3] Electron transfer system in photosynthetic organism is composed of tubular assembly of chlorophylls formed through multiple molecular interactions such as π-π stacking, hydrogen bond, and coordination bond among chlorophylls.[4] These molecular assemblies in natural system have organized supramolecular structures such as lamellar, helical and column-like structure formed by molecular interactions, which form organs and sustain bioactivity of lives. These nature-inspired systems have been paid much attention of scientists because these structured systems have been optimized to improve efficiency of bioacitivity in the process of their evolution. These structures in natural system have potential to develop high performance materials and devices.[5]

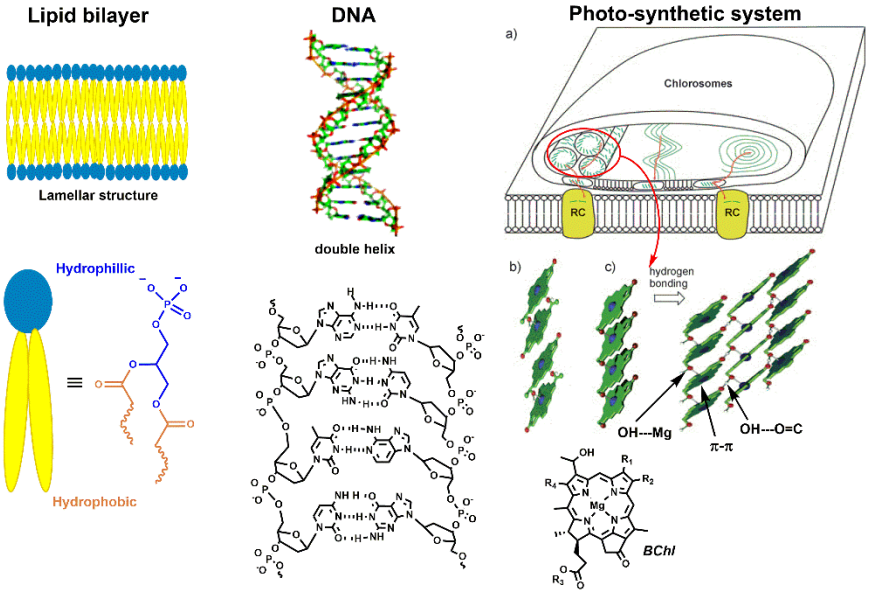

Figure 1-1. Representative examples of superstructures in nature system. Figure of photo-synthetic system was cited from Ref. 5b.

Uncontrollable organization of molecules tends to lose their native properties. In contrast to organized state in nature system, non-organization of molecules in condensed state is seldom found in nature. Non-organized state such as solvent-free liquid was found in semi-artificial biomacromolecules.[6] For example, anionic surfactant-conjugated myoglobin exhibited fluidity, and retained near-native structure and O_2-binding property in the absence of solvents.[7] In addition, the liquid myoglobin exhibited thermal stability of structure and reversible re-folding.[8] The non-organization strategy is crucial to retain native structures and property of molecules. Therefore, this strategy also has been attracted much attention for developing materials with different features to structured ones.

π-Conjugated molecules have attracted much attention due to their potential application as active component in flexible optoelectronic devices such as OPV, OFET, and OLED.[9] Physical state and organized structure among optoelectronic active material affect device performance. Precisely controlling and tuning molecular interactions are crucial issues to improve performance of these devices.[10] Combination of π-conjugated units and flexible chains can not only enhance their solubility to organic solvents but also provide soft materials such as gels[11], polymers[12], supramolecular polymers[13], liquid crystals[14], and molecular liquids[15]. These soft materials have been paid attention for past several decades as active components of organic-based flexible devices.

Phthalocyanines (Pcs) are attractive dyes for optoelectronic devices due to their self-assemble property, NIR absorption, and tunable electronic property.[16] Not only tuning their electronic property but also controlling aggregation structure of Pcs in condensed state are important issue for improving performance of optoelectronic devices. This thesis focus on the control of aggregation and stacking of Pcs in soft condensed states such as solvent-free liquid and liquid crystal. The author synthesized a series of Pcs with bulky yet flexible units, and investigated their relationship between molecular structure-stacking or aggregation structures.

1.2. General introduction and literature review

1.2.1. Combination of π-conjugated units and flexible units

π–Conjugated molecules and polymers have been received attention as active components of light-weighted optoelectronic devices.[9] In general, unsubstituted π–conjugated molecules and polymers have rigid planar structures, which tend to exhibit highly crystallinity and low solubility in common organic solvents due to formation of aggregates through π–π interactions. Considering low cost solution–process for fabrication of devices with large area[17], it is required to enhance their solubility to organic solvents. For solving the issue, various flexible chains are introduced to π–conjugated skeletons.[18] Introducing flexible chains to π–conjugated skeletons can not only enhance their solubility but also provide well-ordered self-assembled state such as a liquid crystalline phase.[10a] On the other hand, introducing bulky yet flexible units to π–conjugated skeletons can provide disordered state such as solvent-free liquids.[19] Performance of devices is affected by not only their optical and electronic property but also their aggregation and stacking state.[10b, c] Therefore, combination of π–conjugated units and flexible units can play a key role in enhancing performance of optoelectronic devices. Moreover, introducing flexible units to π–conjugated skeletons soften their materials because flexible units work as plasticizer, which can lead to realization of practical devices with foldability, bendability and flexibility.[20] In the reason, π–conjugated soft materials have received attention over past decades.

Representative examples of flexible units are aliphatic alkyl chains[3a, 3b], fluoroalkyl chains[21], siloxane chains[22], ethylene glycol chains[23], and crown ethers[24] (Figure 1-2). A melting point of a π–conjugated material is lowered by introducing the flexible units such as alkyl chains and ether-contained flexible units due to π–π interactions reduced by steric hindrance or lower rotational barrier around ether bond. In particular, Guerbet-type[25] branched alkyl chains can dramatically reduce π–π interactions and packing of alkyl chains due to their larger steric hindrance, low crystallinity originated from their asymmetric structure and coexistence of racemic isomers. Therefore, the melting point is effectively lowered by the effect of asymmetric branching. Combination of bulky units and flexible units can provide larger steric hindrance than just flexible units, which can lead to disordered state. In this thesis, the author focuses on the position of alkyl chains on a phenyl group as a bulky unit, and investigated structure-aggregation and stacking relationship of phthalocyanines.

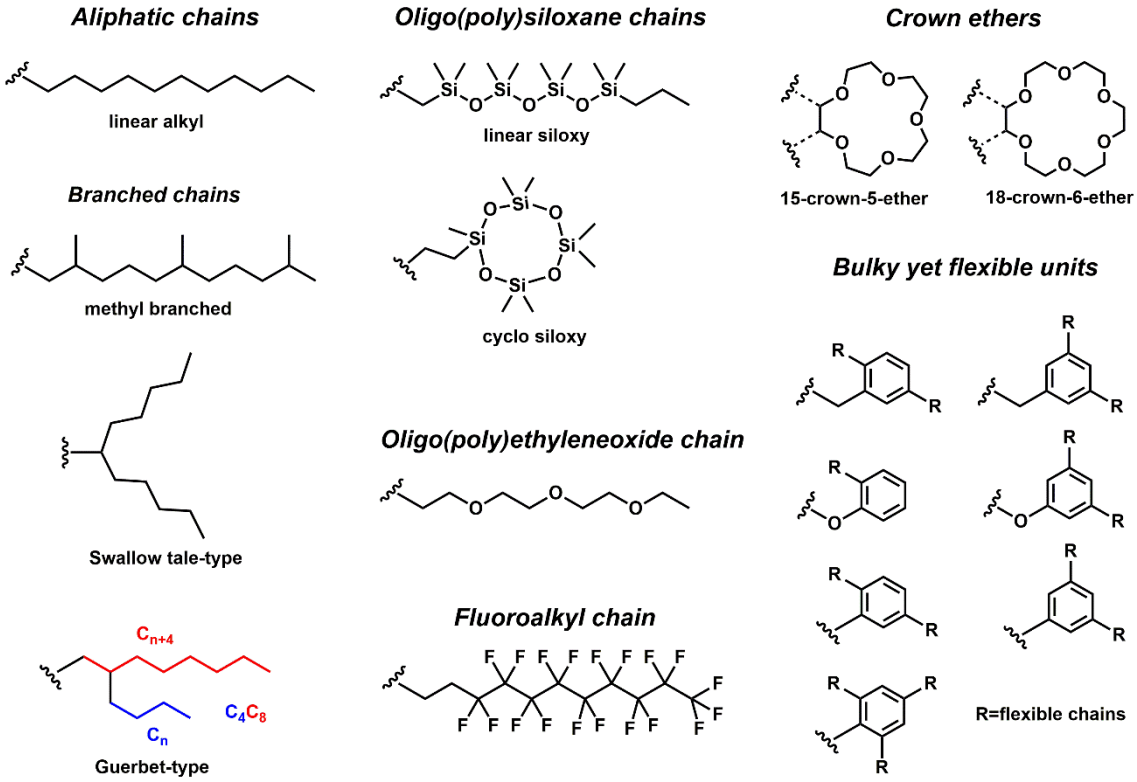

Figure 1-2. Representative types of flexible chains and bulky units.

1.2.2. Liquid crystals

Liquid crystalline phase is intermediate state between crystal and liquid. From the viewpoint of mechanism for inducing the phase, they can be categorized into two types, thermotropic and lyotropic phase. Thermotropic liquid crystalline phase is induced by melting of flexible units among molecules on heating. Lyotropic liquid crystalline phase is induced by changing composition such as adding solvents. Thermotropic liquid crystals have been paid much attention due to their possibility applicable towards optoelectronic devices.[26] First thermotropic liquid crystalline behavior was reported for a cholesteryl benzoate derivative (calamitic molecular structure, later describe) by Friedrich Reinitzer and Otto Lehman in the end of 19th century.[27] Science of liquid crystals started from the findings.

Daniel Vorländer focused on relationship between molecular structure and induction of liquid crystalline behavior.[28] From the viewpoint of molecular shape, liquid crystals can be broadly categorized into two types, calamitics (rod-like molecular structure) and discotics (disk-like molecular structure) (Table 1-1). In general, these liquid crystalline molecules consist of flexible units such as alkyl chains and rigid units such as π-conjugated core. Calamitic liquid crystals have been intensively developed and investigated mainly for display technology. Discotic counterpart was firstly found by Chandrasekhar *et al.* in 1977.[29] Since the finding, various discotic liquid crystals (discogens) have been developed so far.[30] Discogens generally consists of peripheral flexible units such as alkyl chains

and disk-like molecular units based on aromatic macrocycles such as triphenylene, hexabenzocoronen, and phthalocynaine. Discotic liquid crystalline phase can be induced by nano scale-immiscibility between molten flexible units and one-dimensionally stacked π-conjugated units. Discotic liquid crystalline phase also can be called as columnar liquid crystalline phase because disk-like rigid core is stacked and form one-dimensional columnar structure. When disk-like rigid units are aromatic cores, π-orbitals overlap in one-dimensional columns. Consequently, hole and/or electron can be transported along columnar axis. The concept was designed by Simon's group.[6] Later, the concept was demonstrated by Adam *et al*.,[32] discotic liquid crystals based on aromatic cores have been paid much attention as anisotropic semiconductor applicable towards optoelectronic devices.[33] Control of their stacking mode and alignment in liquid crystalline state is essential and a challenging issue for enhancing performance of devices.[33b]

Table 1-1. Molecularly structural classification of liquid crystals.

Molecular shape	Calamitic (rod-like)	Discotic (disk-like)
General structure	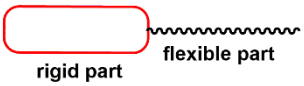	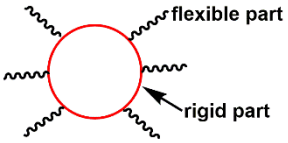
Examples	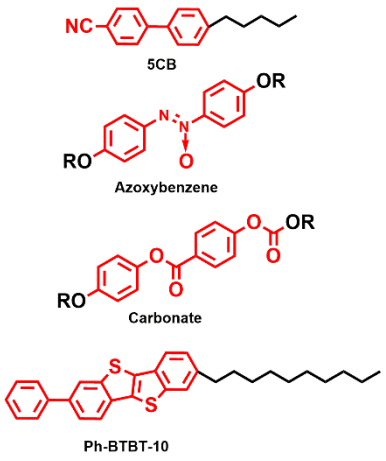	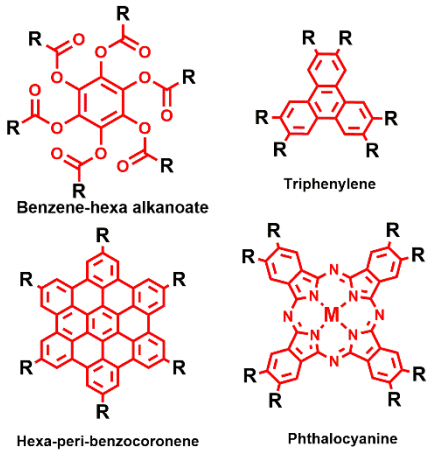

1.2.3. Solvent-free functional molecular liquids

Solvent-free fluidic materials termed as functional molecular liquids (FMLs) have emerged as a new class of soft materials, and attracted much attention as active components of flexible devices.[15] FMLs can freely flow at room temperature due to their low glass transition temperatures. Therefore, they can be directly painted on substrates or filled into micro space through capillary force, which facilitate organic solvents-less process for fabricating devices.[34] In addition, they can be unlimitedly deformable due to their soft amorphous feature. Their free flowing and deformable nature can enable flexible devices[20] to resist mechanical force such as bending, twisting, and stretching. In past decade, FMLs have attracted significant attentions in various research field including luminescent inks[35], vapor-detection of chemicals[36], gas adsorbent[37], photon up conversion system[38], optical limitters[39], optical lasers[40], redox-flow batteries[41] and solvent-like applications[42] as well as flexible electronics[34, 43].

General molecular design for FMLs is based on combination of π-conjugated units and bulky yet flexible units (Figure 1-3). π-Conjugated units govern intrinsic optoelectronic properties of the FMLs. On the other hand, structures and positions of bulky yet flexible units affect liquid physical properties such as viscosity as well as local aggregation in FMLs. Wrapping of π-conjugated units with bulky yet flexible units can isolate the core, which lead to inherent single molecular property in bulk liquid state.[44] In addition, the molecular design for FMLs can enhance their thermal and photochemical stability.[43b] Therefore, precise control of the balance between π-π interactions and van der Waals interactions (governed by flexible chains such as alkyl) is crucial to develop the FMLs with desirable properties.[45]

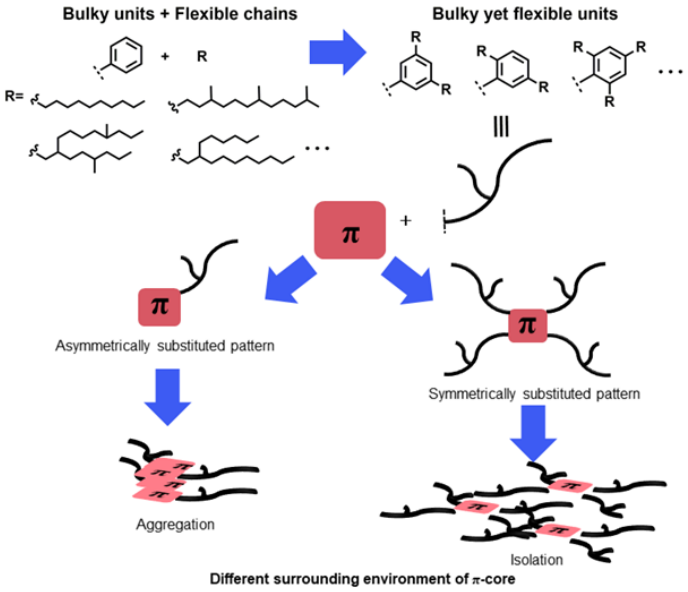

Figure 1-3. General molecular design for FMLs and aggregation properties depending on their substitutional patterns.

1.2.4. Phthalocyanines

1.2.4.1. History of phthalocyanines

In 1907, Braun and Tcherniac isolated blue by-product on a preparation of *o*-cyanobenzamide.[46] The blue by-product was identified later as the metal-free phthalocyanine (H_2Pc). In 1927 after twenty years of the report, Diesbach and Weid isolated blue product in 27% yield on a preparation of 1, 2-dicyanobenzene (phthalonitrile) through nucleophilic attack of cyanide ion to 1, 2-dibromobenzene.[47] They found that the blue product was extremely stable to concentrated H_2SO_4, alkaline, and heat. The blue product was identified later as cupper phthalocyanine (CuPc). In 1928, Dandridge *et al*., scientists at Scottish Dye Ltd (later Imperial Chemical Industries), found that bluish green impurity was formed on preparation of phthalimide from molten phthalic anhydride and ammonia in enameled cast-iron crucible. They revealed that the reaction has been proceeded in the presence of phthalimide product and iron source (chipped enameled cast-iron crucible). The bluish green impurity was identified later as iron(II) phthalocyanine (Fe(II)Pc). They succeeded in replacing the iron with other metals. After recognizing the commercial value of the synthesis, the work was patented in 1929.[48] They sent the samples to Linstead for analyzing their chemical structure. In 1934, Linstead *et al*. analyzed their chemical structure[49], and reported the synthetic method for various metal complexes of Pcs[50]. In 1935, Robertson characterized crystal structure of Pcs by single X-ray crystallography, and demonstrated the chemical structure of Pc reported by Linstead's group.[51] Since these reports, the chemistry of Pcs have been started, and various researches have been reported so far. From 1934 to 2018, a large number of publications has dramatically increased, which have developed new research areas in the chemistry of porphyrinoids (Figure 1-4). Pcs have been industrially utilized as a dyes for jeans and other clothing, pigments for coloring body of super express, photoconductor in laser printer, and recording layer in rewritable compact disk. Recently, Pcs have been paid much attentions due to their unique properties such as absorption of photon in near-infrared (NIR) region, semiconductivity, catalytic ability, and others. Therefore, Pcs have been considered as good candidates of molecular components applicable in various fields such as solar cells[52], optical limiters[53], transistors[54], sensitizers for photo-therapy and diagnosis of cancer[55], catalysts[56], single molecular magnets[57], and chemical sensors[58].

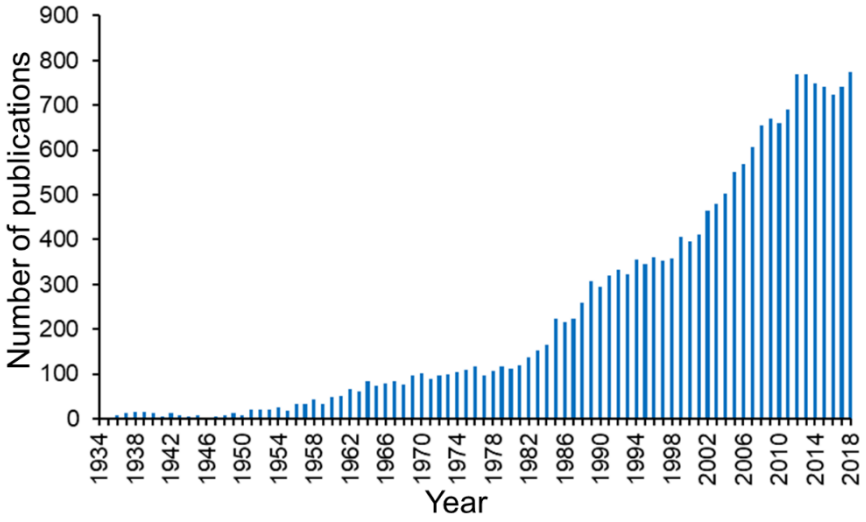

Figure 1-4. Number of publications contained "phthalocyanine" from 1934 to 2018 as counted with SciFinder®.

1.2.4.2. Structure of phthalocyanines

Phthalocyanines (Pcs) are analogues of porphyrins (Pors), which are composed of four isoindole subunits linked together four nitrogen atom at *meso*-position. The carbon atoms at *meso*-positions in porphyrin are replaced with nitrogen atoms, and additional four benzo units are fused at *β*-carbons of pyrrole units in porphyrin ring (Figure 1-5). The two structural change of Pcs leads to a spectral change different from typical porphyrins (Figure 1-6). Pcs have rigid and planar macrocyclic structure constituted from delocalized 18 π-electrons. Electronic properties of Pcs are originated from the π-conjugated system.

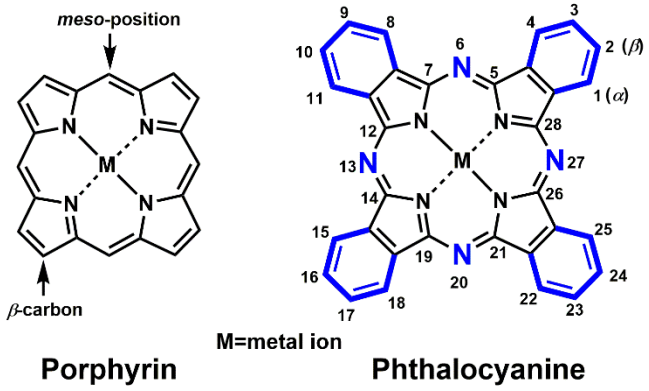

Figure 1-5. Molecular structures of porphyrin and phthalocyanine.

The electronic structure of porphyrinoids including Pcs has been explained by Gouterman's four orbital model.[59] The model can theoretically describe optical properties of porphyrinoids. Pcs and Pors exhibit intense absorption band named as Q-band and Soret-band, respectively. In porphyrins belonging to D_{4h} group, a_{2u} orbital (HOMO) and a_{1u} orbital (HOMO-1) are energetically close, so that transition energies of $a_{2u}\rightarrow e_{gy}$ and $a_{1u}\rightarrow e_{gx}$ are also close, where e_{gx} and e_{gy} are polarized components of doubly degenerated LUMO (Figure 1-7). As the result of strong configuration interaction between the two transitions ($a_{1u}\rightarrow e_{gx}$ and $a_{2u}\rightarrow e_{gy}$), the two new electronic transitions are generated (Q- and Soret-band). These bands are assigned to $S_0\rightarrow S_1$ and $S_0\rightarrow S_2$ transitions, respectively.

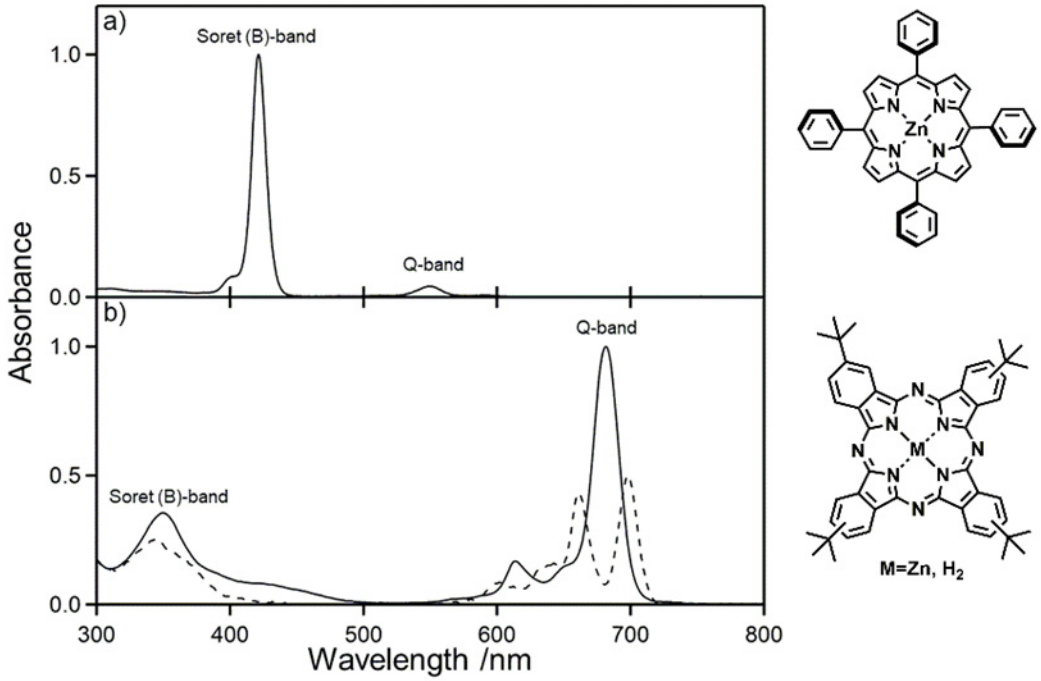

Figure 1-6. UV-vis spectra of zinc tetraphenylporphyrin (a) and (β-tetra-*tert*-Bu)ZnPc (solid line) and the metal-free derivative (dashed line) (b) in THF.

Intensities of these bands are proportional to square of the transition dipole moments (Eq. 1 and 2).[60]

$$\text{Q-band } (S_0\rightarrow S_1)\text{: } |\langle S_0|\mathbf{er}|S_1\rangle|^2=|\alpha\langle S_0|\mathbf{er}|(a_{2u}e_{gy})\rangle - \beta\langle S_0|\mathbf{er}|(a_{1u}e_{gx})\rangle|^2 \quad \text{(Eq. 1)}$$

$$\text{Soret-band } (S_0\rightarrow S_2)\text{: } |\langle S_0|\mathbf{er}|S_2\rangle|^2=|\alpha\langle S_0|\mathbf{er}|(a_{2u}e_{gy})\rangle + \beta\langle S_0|\mathbf{er}|(a_{1u}e_{gx})\rangle|^2 \quad \text{(Eq. 2)}$$

Where, α and β are configuration interaction coefficients of a_{2u}-e_{gy} and a_{1u}-e_{gx}, respectively. In Pors, the value of α is very close to that of β due to strong configuration interaction. Transition dipole moment of Q-band is described as subtraction of α- and β-term in Eq.1, so that intensity of Q-band for

porphyrin is weak. Intensity of Soret-band is strong because transition dipole moment of the band is described as addition of α- and β-term in Eq.2. From these reasons, Pors exhibit strong Soret-band and weak Q-band. In Pcs, a_{2u} orbital (HOMO-1) is dramatically stabilized by replacing carbon atoms with nitrogen atom at *meso*-positions, leading to large energy-difference between ($a_{2u}e_{gy}$) and ($a_{1u}e_{gx}$). As the result, configuration interaction between the two transitions become weak. Therefore, $S_0 \rightarrow S_1$ mainly consists of $a_{1u}e_{gx}$, leading to strong Q-band. For the same reason, $S_0 \rightarrow S_2$ mainly consists of $a_{2u}e_{gy}$, leading to moderate strong Soret-band. This is the reason why absorption of Pcs is different from that of Pors. In lower symmetrical Pcs such as H_2Pcs, splitting of Q-band is generally observed. Considering D_{2h}-symmetrical H_2Pc, the two orbitals (e_{gx} and e_{gy}) in doubly degenerated LUMO are splitting into non-degenerated two orbitals (b_{1g} and b_{2g}) due to the reduction of symmetry from D_{4h} to D_{2h}. Therefore, two splitting Q-bands are observed for H_2Pcs. Optical and electronic properties of Pcs can be tuned by introducing central metals and/or peripheral substituents.[61]

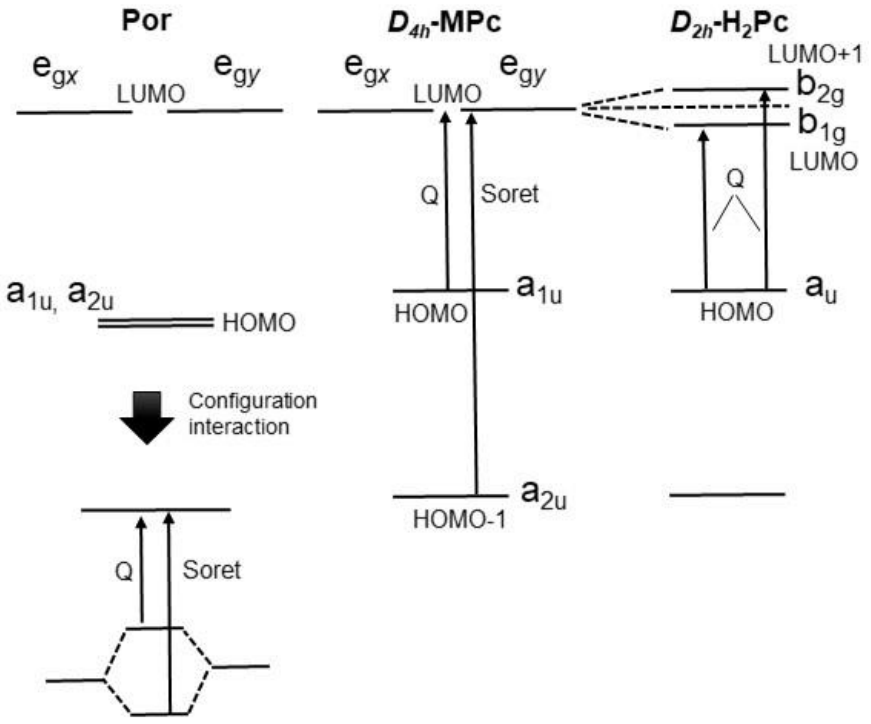

Figure 1-7. Energy diagrams nearby HOMO and LUMO of Por and Pc.

1.2.4.3. Synthetic methods for phthalocyanines

Pcs are synthesized through metal-templated cyclotetramerization of the precursors (Scheme 1-1). These precursors are derivatives of phthalic acid. In general, Pcs are prepared through Wyler's method or Linstead's method[50b]. In the former method, phthalic anhydrides or phtalimides are utilized as starting chemicals, and Pcs are prepared from them in the presence of metal salts, urea, and solvents with high boiling points. In the latter method, 1, 2-dicyanobenzenes (phthalonitriles) are utilized, and Pcs are prepared from them in the presence of metal salts and solvents with high boiling point. In the method, alcohols with high boiling point also can be utilized as solvent and initiator in the presence of alkaline (or alkaline earth) metals such as lithium (lithium method)[62] or organic strong base such as 1,8-diazabicyclo[5.4.0]undec-7-ene (DBU)[63]. The two methods are useful to obtain metal Pcs. Especially, lithium method is helpful to obtain H_2Pcs. The proposed mechanism for formation of Pcs by nucleophilic attack of alkoxide to the nitrile group is shown in Scheme 1-2.[64] The reaction is initiated by nucleophilic attacke of alkoxide to the nitrile group (Step 1). The cyclotetramerization starts with the formation of 1-imido-3-alkoxyindoline, followed by the nucleophilic attack of the intermediate to the nitrile group in another phthalonitrile (Step 2). The resulting dimer reacts with the third phthalonitirle to form the trimer (Step 3a) or another dimer (Step 3b). The reactions in Step 3a and 3b can be mediated by cationic metals as a template. The ring-closing reaction is occurred by intramolecular nucleophilic attack (Step 3c and 4). When lithium alkoxides or lithium salts such as LiBr are utilized as metal source, Li_2Pcs are formed and can be easily converted to H_2Pcs by treatment with acids such as hydrochloric acid and acetic acid. H_2Pcs can be converted to MPcs by reaction with metal salts in solvents such as DMF and THF. In addition, MPcs can be directly prepared by adding metal salts to resulting reaction mixture after Li_2Pcs are formed. The two hydrogen atoms in the center of H_2Pc can be replaced with various elements (more than 70), producing various types of MPcs. In industrial scale, phthalic anhydride or phthalimide are generally utilized as starting chemicals for synthesis of Pcs due to low cost of these chemicals. Cost and reactivity of phthalonitriles are higher than phthalic anhydride and phthalimide. The higher reactivity of phthalonitriles is helpful to obtain Pcs in high purity. Therefore, phthalonitriles are considered as the best precursor for synthesis of Pcs in a laboratory-scale.

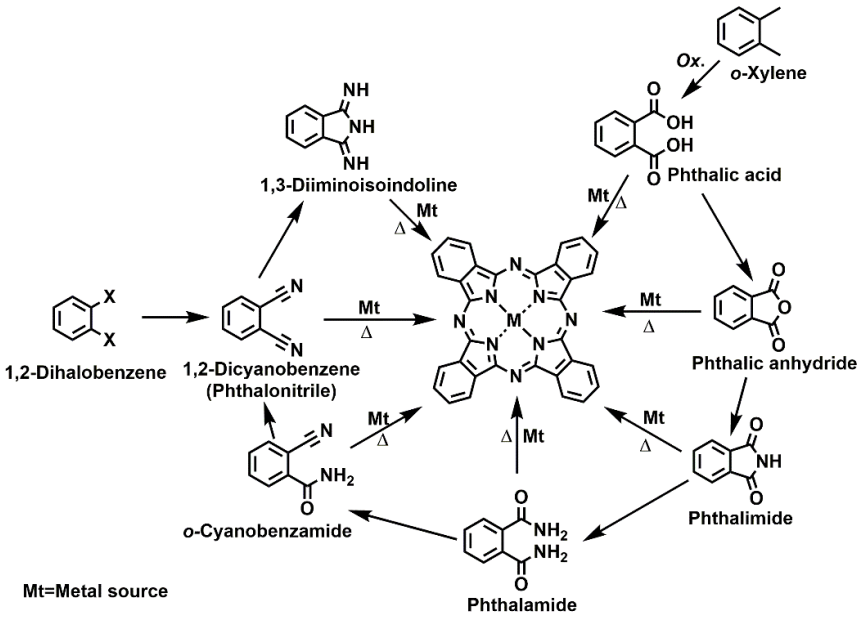

Scheme 1-1. The synthesis of Pcs from various precursors.

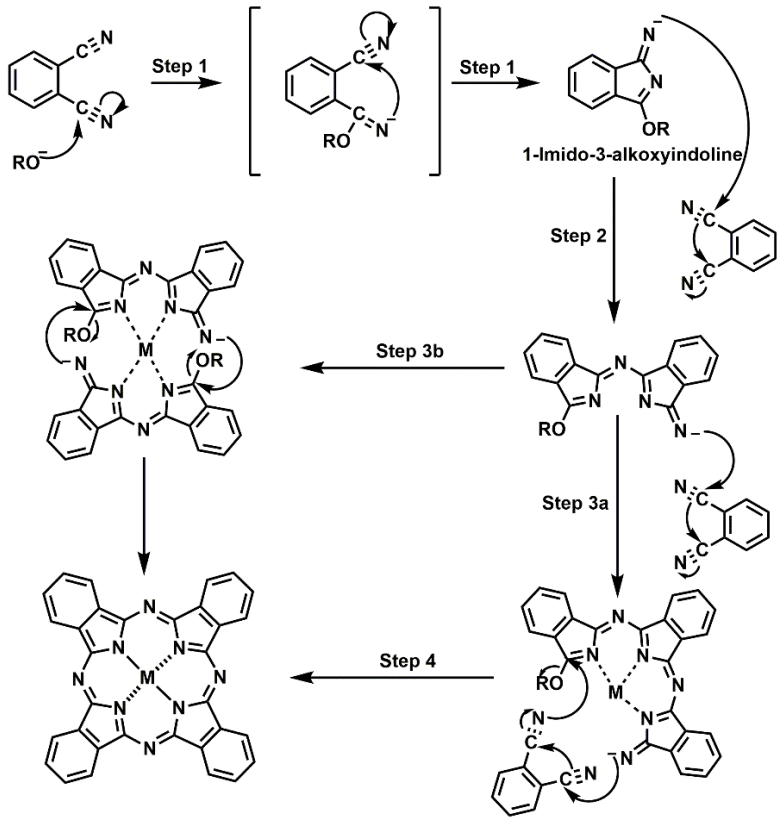

Scheme 1-2. Proposed mechanism for the synthesis of MPcs by cyclotetramerization of phthalonitriles in the presence of a metal salt.[64]

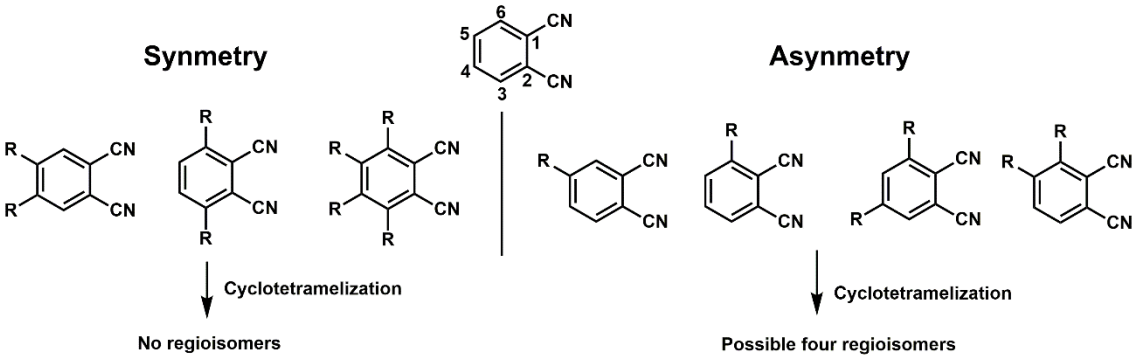

Figure 1-8. Substitutional patterns of side groups on phthalonitirle.

Side groups can be introduced to 3-, 4-, 5-, and 6-positions in phthalonitriles (Figure 1-8). Types and positions of side groups in phthalonitriles affect to Pc's properties such as solubility, aggregation, and electronic state. Cyclotetramerization of asymmetrical substituted phthalonitriles provides a mixture of possible four regioisomers of Pcs (C_{4h}, C_s, C_{2v}, *and* D_{2h}) (Figure 1-9).[65] Co-existence of regioisomers of Pcs affect their aggregation state as well as optical and electronic properties. These four regioisomers can be separated by chromatographic technique[66] or recrystallization[67]. However, the identification of regioisomers needs careful structural characterizations, and it is very difficult to obtain enough amount of single-regioisomer for the fabrication of devices. Therefore, regioselective synthesis of Pcs from asymmetrical substituted phthalonitriles is a crucial issue. Introducing bulky substituents to 3-position in phthalonitrile can control statistical distribution of Pc's regioisomer during cyclotetramerization due to steric repulsion between bulky substituents, and provides single regioisomer of C_{4h}-symmetry.[68] The regioselective approach is important to characterize the properties of resulting Pcs.

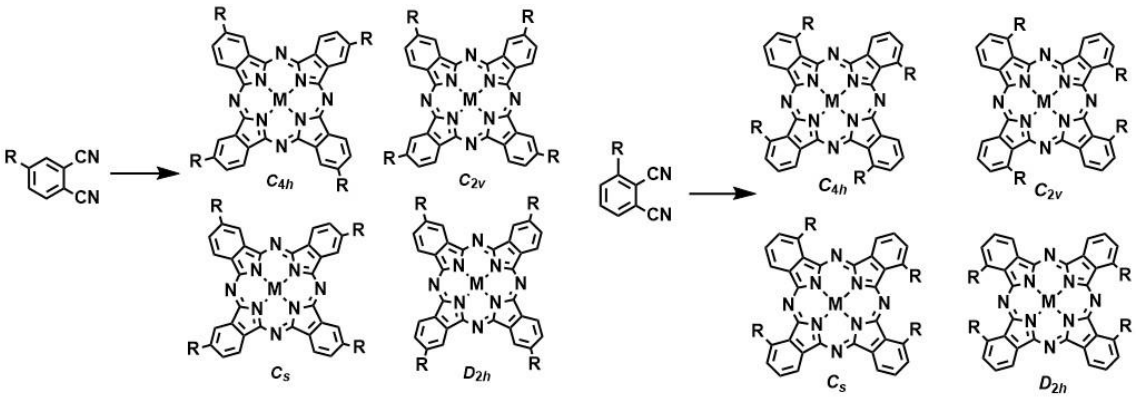

Figure 1-9. Possible four regioisomers obtained from cyclotetramerization of 4- (left) or 3- (right) substituted phthalonitirle.

1.2.4.4. Thermotropic liquid crystalline phthalocyanines

In this section, general types of thermotropic liquid crystalline Pcs are briefly reviewed in the view of their molecular structure.

Since thermotropic liquid crystalline Pcs was reported by Simon's group[31], they have been paid attention as a good candidate for molecular components in molecular devices such as OPV and OFET. Various types of liquid crystalline Pcs have been reported so far, and the reports are summarized in several reviews.[69] Molecular structures of liquid crystalline Pcs can be broadly categorized into five types (Figure 1-10).

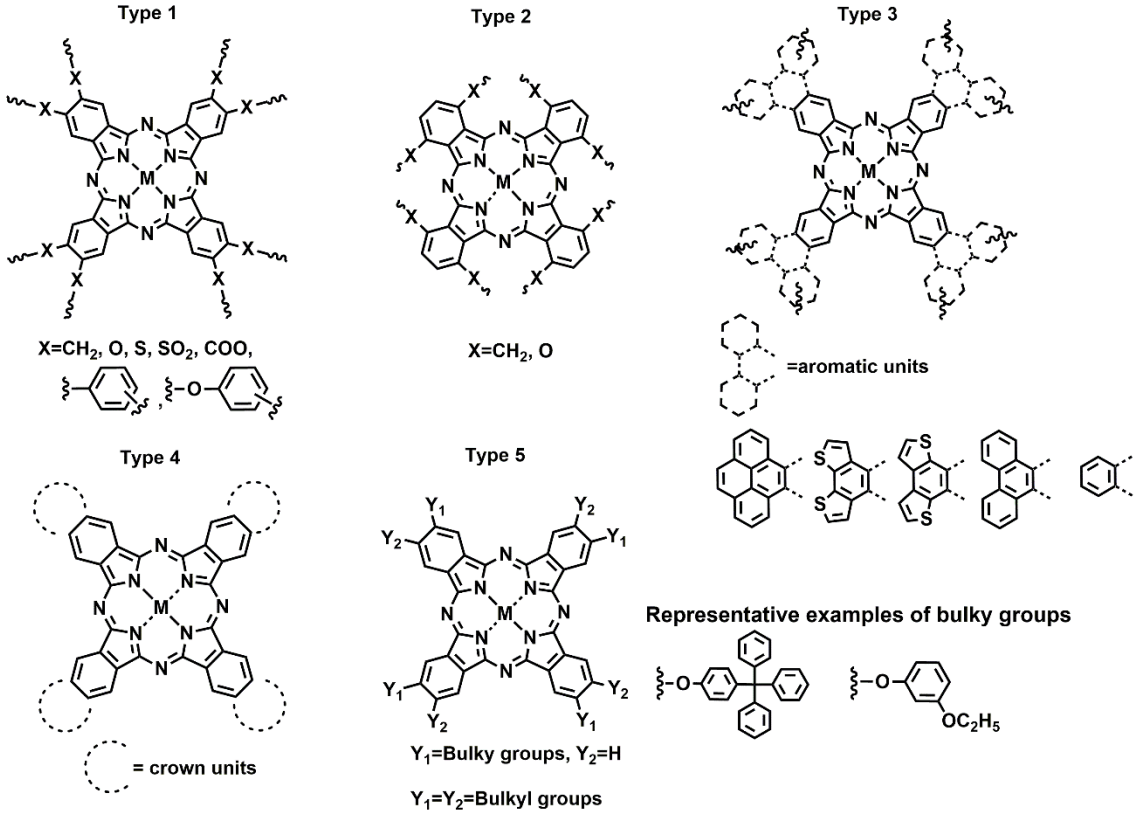

Figure 1-10. Broad categories of liquid crystalline Pcs and their general molecular structures.

Liquid crystalline Pc derivatives in Type 1 has flexible chains such as alkyl, alkoxy, alkylthio, and oligoethyleneglycols at *β*-positions in Pc. The numbers of flexible chains is generally four or eight. Alkylated phenoxy groups can control π-π interaction of Pcs in liquid crystalline phase.[70] Alignment of column made from Pcs in liquid crystalline state can be controlled by side groups. Liquid crystalline Pc having eight 3, 4-dialkoxyphenoxy groups was reported by Ohta's group, and the liquid crystalline Pc exhibit spontaneous perfect homeotropic alignment.[71] The homeotropic alignment is very advantageous for applications in organic semiconductors because charged carriers can rapidly transfer along the one-dimensional column aligned in vertical to surface of electrode. Most of liquid crystalline

Pcs exhibit *p*-type semiconductivity. When alkylsulfonyl group (RSO_2-) are utilized as side chain of Pc, the Pc exhibit *n*-type semiconductivity. Sergeyev and Geerts reported that the liquid crystalline Pc having eight RSO_2-groups at *β*-position exhibit air-stable semiconductivity.[72] The peripheral groups at *β*-position in Pc can affect to aggregation state as well as their electronic state.

Liquid crystalline Pc derivatives in Type 2 heve flexible chains such as alkyl, fluoroalkyl, alkoxy, and siloxyalkoxy chains at *α*-positions in Pc. The number of flexible chains is four or eight. The first liquid crystalline Pc having eight long alkyl chains at *α*-positions was developed by Cook *et al. i*n 1987.[73] The liquid crystalline Pcs having various types of alkyl chains at *α*-positions have been reported.[74] There are several reports of liquid crystallinity for the Pc-derivatives replaced alkyl chains at *α*-positions with siloxyalkoxy[75a] or alkoxy[75b] chains.

Liquid crystalline Pc derivatives in Type 3 have alkylated aromatic rings fused to lateral benzo units in Pc.[76] These liquid crystalline Pcs were developed for aiming to enhance overlapping between π-orbitals in macrocyclic units. Liquid crystalline state of these Pcs was stabilized due to the enhanced overlapping between macrodiscotic cores.

Liquid crystalline Pc derivatives in Type 4 have crown ether units fused to lateral benzo units in Pc.[24] In general, it is believed that both a rigid disk-like core and long alkyl chains are necessary to induce liquid crystalline phase. In 1987, 15-crown-5-ether-fused Pcs having no alkyl chains were reported.[24a] The result of X-ray diffraction indicates the formation of columnar liquid crystalline phase. The result indicates that crown ether can act as a flexible unit instead of long alkyl chains. One-dimensional column made from crown ether-fused Pcs consists from ion-conductive crown-units and carrier-conductive Pc-units.[24a, b] Therefore, the multi-wired molecular cable has been expected to be applicable in ionoelectronics.

Liquid crystalline Pc derivatives in Type 5 have bulky units instead of flexible chains such as alkyl chains.[77] Although the liquid crystalline Pcs have no any flexible chains, they exhibit columnar liquid crystalline phase at higher temperature range over 200 °C. The flip-flop motion of bulky units in these Pcs can be considered as the driving force for inducing the liquid crystalline phase.

1.2.4.5. Phthalocyanine-based solvent-free liquids

In this section, fluidic or liquid Pcs are categorized and briefly reviewed in the view of their molecular structure. The section focuses on Pcs exhibiting fluidic or liquid state around room temperature. Molecular structures of fluidic Pcs having substituents on periphery is shown in Figure 1-11.

Snow *et al.* synthesized liquid Pcs having four or eight oligoethylene oxide ($CH_3(OCH_2CH_2)_nO$, n=8.8) at *β*- or *α*-positions, and investigated their property of optical limiting. Peripheral oligoethylene oxide chains lead to the production of the fluid state.[78] The fluidic Pcs was optically transparent under observation with polarizing optical microscope, indicating that the size of aggregate was reduced. The

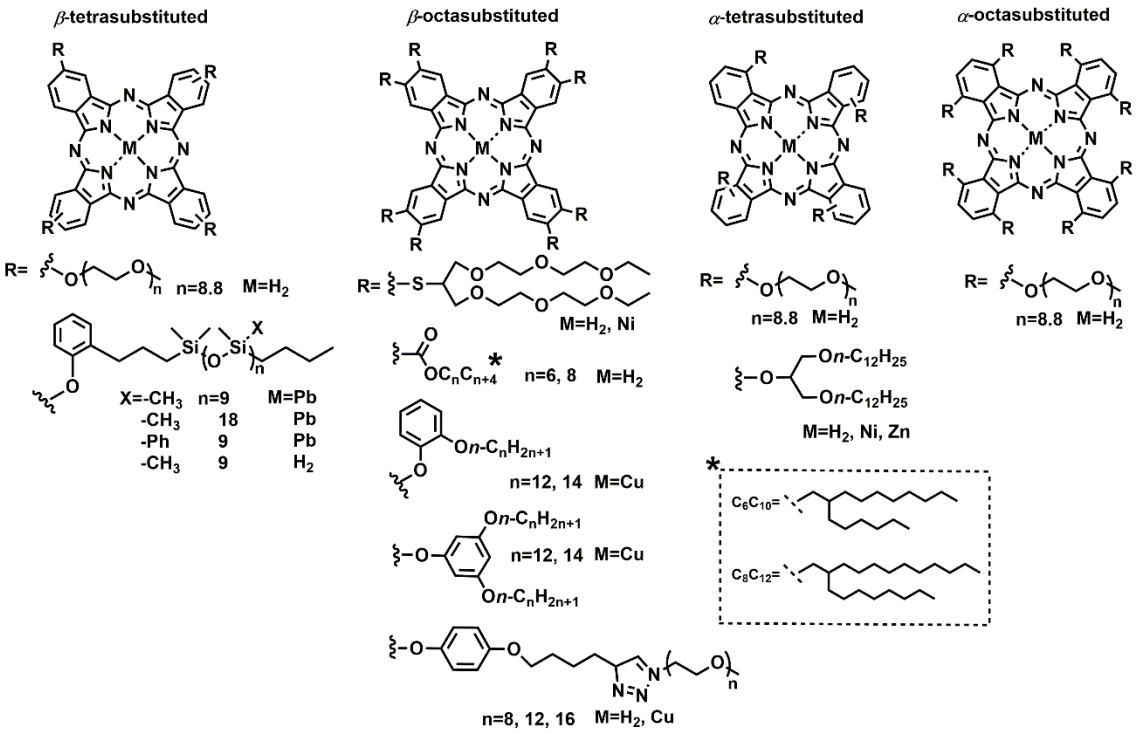

Figure 1-11. Molecular structures of fluidic or liquid Pcs having substituents on periphery.

fluidic Pcs exhibit optical limiting feature at 532 nm. Maya *et al*. reported a series of fluidic Pcs having four oligosiloxane chains at *β*-positions.[79] These fluidic Pcs exhibit unique thermal nonlinear refractive response as well as nonlinear absorption. In addition, de-metalation of the Li_2Pc was difficult to proceed at room temperature. The result indicates that the central regime of Pc core was covered by side chains even in solution state.

Ahsen *et al*. found that Pc derivatives having symmetrical branching four alkyl chains at *α*-position were fluidic at room temperature during their systematical studies on liquid crystalline Pc.[80] In contrast, their *β*-substituted pattern turned them to columnar liquid crystalline phase. Fluidic state was also found in Pc derivatives having eight symmetrical branching triethyleneoxide chains at *β*-position.[81] In aiming to develop n-type liquid crystalline Pcs, Geerts *et al*. synthesized a series of octaalkoxycarbonyl Pcs.[82] Among them, the two derivatives having Guerbet alcohol-based branched alkyl chains (C_6C_{10} and C_8C_{12}) were fluidic at room temperature. Ohta *et al*. investigated the systematic reduction of π-π stacking among CuPc rings by changing the position of liner long alkyl chains at phenoxy units in *β*-position.[83] Among them, 2-substituted and 3, 5-disubstituted CuPc were highly viscous fluids at room temperature. Aiming to develop water-soluble Pcs, Haddleton *et al.* synthesized Pcs having polyethyleneglycol (Mw_{PEG} = 350, 550, 750, and up to 2000 g mol^{-1}) units at *β*-position.[84] Among them, three Pcs with PEG units with molecular weights of 350, 550, and 750 were fluidic around room temperature.

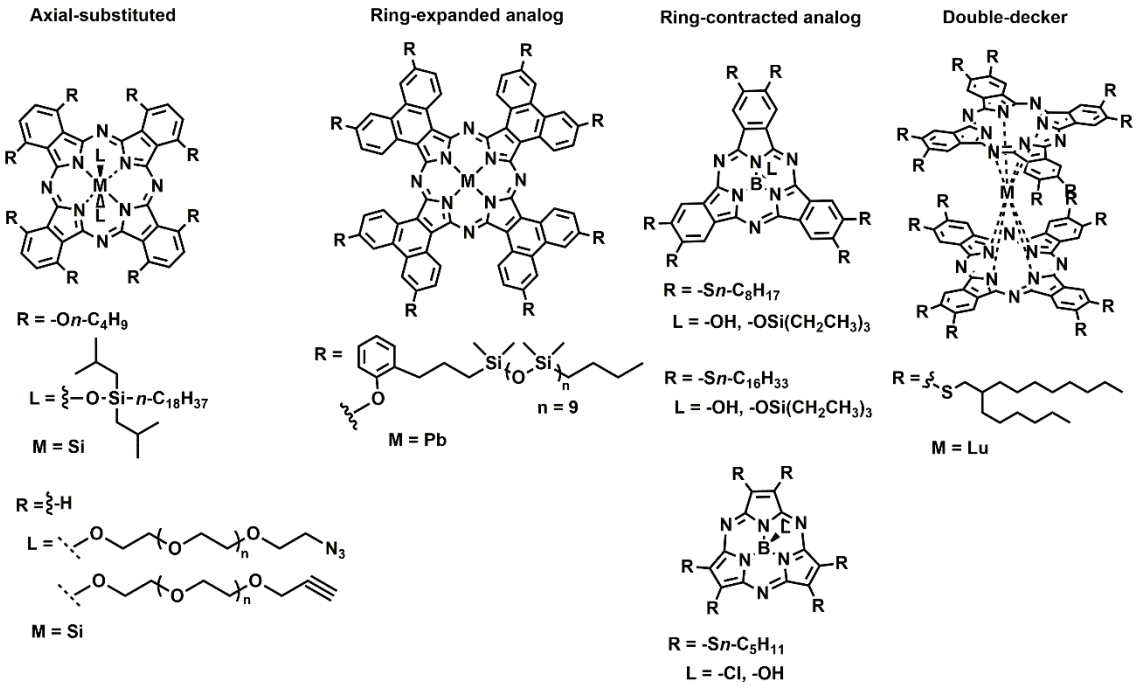

Figure 1-12. Molecular structure for axial substituted fluidic Pc and fluidic Pc-analogues.

There are reports for axial substituted type fluidic Pc and fluidic Pc-analogues (Figure 1-12). Introducing flexible chains to axial position can also produce fluidic Pcs. Kenney *et al.* synthesized SiPc having eight butoxy groups and two (di*iso*-butyloctadecyl)siloxy groups at α- and axial positions, respectively.[85] The SiPc was obtained as green oil. During studies on water-soluble Pcs, Foulger *et al*. synthesized a series of SiPcs having two axial polyethyleneglycol groups with different molecular weights.[86] Among them, two SiPcs with repeated units of from 11 to 13 ethyleneglycol were obtained as blue oil.

Fluidic ring-expanded Pc-analog was reported. Maya *et al*. synthesized a series of phenanthralocyanines (Phcs).[39a] Among them, PbPhc having four 2-oligosiloxyphenyoxy groups in periphery was fluidic at room temperature. The PbPhc had very low glass transition temperature (-125 ^{o}C). In addition, they exhibited optical limiting property originated from their thermorefractive effect.

Fluidic ring-contracted Pc-analogues were reported. Torres *et al*. synthesized a series of boron subphthalocyanines (SubPcs).[87] Among them, hydroxyl and triethylsiloxy SubPcs having six octylthio and hexadecylthio chains were violet gelatine-like viscous fluid. The fluidic SubPcs exhibited temperature-dependent change of their viscosity. Torres *et al*. synthesized a series of boron subporphyrazines (SubPz).[88] Among them, chloro and hydroxy boron SubPzs having six pentylthio chains were dark red syrup at room temperature.

Liquid double-decker Pc was reported. Nakanishi *et al*. synthesized double-decker lutetium Pc ($LuPc_2$) having Guerbet alcohol-based 2-octyldodecylthio chains at β-positions.[89] The $LuPc_2$ was non-

newtonian liquid by confirming with rheology. In addition, the liquid $LuPc_2$ exhibited spin-active and electrochromic feature in the solvent-free liquid state.

1.3. Thesis objectives

The aim of this thesis is design and characterization of Pc-based liquid crystals (**Chapter 3**) and liquids (**Chapter 4** and **5**). The states exhibit opposite assembled structures, which provides different functions. In addition, considering their application to materials and devices, the states have benefits such as the absence of solvents and their soft feature. The tune of structures in molecular assemblies plays a key role for enhancing performance of Pc-based materials and devices. How do the molecular structures affect their molecular assembled structures? Especially, the relationship between the molecular structures and aggregation structures in Pc-based liquids is still frontier in material chemistry and the chemistry of Pcs. It is a crucial issue for their applications to provide guidelines for the open question.

In this thesis, the author focused on structures and positions of side groups in Pcs. The author aims to reveal their molecular structures-assembled structures relationship. For this purpose, the author focuses on control of intermolecular interactions through the molecular design based on combination of Pc core and flexible units. Pcs having three types of side groups have been designed and synthesized, and their structures of molecular assembly have been characterized by polarizing optical microscopy, X-ray scattering / diffraction, and UV-vis absorption / fluorescence spectra. In addition, the relationship between the structures of molecular assembly and the functions such as stimuli-responsive rheological property and fluorescence in NIR spectral region. These works are summarized in the sections as follows:

Chapter 3 describes the design and characterization of novel phenylthio-substituted Pcs. The effect of alkyl chain-length and sulfur-replacement to π-π stacking structures in liquid crystalline state was investigated.

Chapter 4 describes the detailed investigation for liquid Pcs. The author investigated their rheological property and aggregation structure in liquid state. The stimuli-response of aggregates was also investigated.

Chapter 5 describes the design, synthesis, and characterization of novel tetra α-substituted Pcs. The author investigated relationship between their molecular structure and aggregation property. The near-infrared fluorescent property in liquid state was also investigated.

References

1. a) J. M. Lehn, *Supramolecular Chemistry*, John Wiley&Sons, Inc., NewYork; b) T. F. A. De Greef, M. M. J. Smulders, M. Wolffs, A. P. H. J. Schenning, R. P. Sijbesma, and E. W. Meijer, *Chem. Rev.*, 2009, **109**, 5687.
2. D. M. Engelman, *J. Mol. Biol*., 1971, **58**, 153.
3. a) R. E. Franklin and R. G. Gosling, *Nature*, 1953, **171**, 740; b) A. G. Leslie and S. Arnott, *J. Mol. Biol.*, 1980, **143**, 49.
4. G. McDermott, S. M. Prince, A. A. Freer, A. M. Hawthornthwaite-Lawless, M. Z. Papiz, R. J. Cogdell, and N. W. Isaacs, *Nature*, 1995, **374**, 517.
5. a) F. J. M. Hoeben, P. Jonkheijm, E. W. Meijer, and A. P. H. J. Schenning, *Chem. Rev.*, 2005, **105**, 1491; b) S. Sengupta and F. Würthner, *Acc. Chem. Res.*, 2013, **46**, 2498; c) K. Liu, Y. Kang, Z. Wang, and X. Zhang, *Adv. Mater.*, 2013, **25**, 5530.
6. K. Liu, C. Ma, R. Gostl, L. Zhang, and A. Herrmann, *Acc. Chem. Res.*, 2017, **50**, 1212.
7. A. W. Perriman, A. P. S. Brogan, H. Colfen, N. Tsoureas, G. R. Owen, and S. Mann, *Nat. Chem.*, 2010, **2**, 622.
8. A. P. S. Brogan, G. Siligardi, R. Hussain, A. W. Perriman, and S. Mann, *Chem. Sci.*, 2012, **3**, 1839.
9. a) A. Pron, P. Gawrys, M. Zagorska, D. Djurado, and R. Demadrille, *Chem. Soc. Rev*., 2010, **39**, 2577; b) C. Wang, H. Dong, W. Hu, Y. Liu, and D. Zhu, *Chem. Rev.*, 2012, **112**, 2208; c) H. Dong, H. Zhu, Q. Meng, X. Gong, and W. Hu, *Chem. Soc. Rev*., 2012, **41**, 1754.
10. a) W. Pisula, X. Feng, and K. Müllen, *Adv. Mater.*, 2010, **22**, 3634; b) P. M. Beaujuge and J. M. Fréchet, *J. Am. Chem. Soc*., 2011, **133**, 20009; c) Z. B. Henson, K. Müllen, and G. C. Bazan, *Nat. Chem.*, 2012, **4**, 699.
11. a) A. Dawn, T. Shiraki, S. Haraguchi, S. Tamaru, and S. Shinkai, *Chem. –Asian J*., 2011, **6**, 266; b) S. S. Babu, V. K. Praveen, and A. Ajayaghosh, *Chem. Rev.*, 2014, **114**, 1973.
12. a) Y-J. Jin, J-E. Bae, K-S. Cho, W-E. Lee, D-Y. Hwang, and G. Kwak, *Adv. Funct. Mater*., 2014, **24**, 1928; b) A. T. Kleinschmidt and D. J. Lipomi, *Acc. Chem. Res*., 2018, **51**, 3134; c) A. Shinohara, C. Pan, Z. Guo, L. Zhou, Z. Li, L. Dei, Z. Yan, F. J. Stadler, L.Wang, and T. Nakanishi, *Angew. Chem. Int. Ed.*, 2019, **58**, 9581.
13. T. Aida, E. W. Meijer, S. I. Stupp, *Science*, 2012, **335**, 813.
14. a) H. K. Bisoyi and Q. Li, *Chem. Rev.*, 2016, **116**, 15089; b) T. Kato, J. Uchida, T. Ichikawa, and T. Sakamoto, *Angew. Chem. Int. Ed.*, 2018, **57**, 4355-4371
15. a) A. Ghosh and T. Nakanishi, *Chem. Commun.*, 2017, **53**, 10344; b) F. Lu and T. Nakanishi, *Adv. Opt. Mater.*, 2019, 1900176.
16. G. de la Torre, C. G. Claessens, and T. Torres, *Chem. Commun.*, 2007, 2000.
17. M. Berggren, D. Nilsson, and N. D. Robinson, *Nat. Mater.*, 2007, **6**, 3.
18. a) M. J. Hollamby and T. Nakanishi, *J. Mater. Chem. C*, 2013, **1**, 6178; b) H. Li, J. Choi, and T.

Nakanishi, *Langmuir*, 2013, **29**, 5394-5406; c) T. Lei, J-Y. Wang, and I. Pei, *Chem. Mater.*, 2014, **26**, 594.

19. a) A. Ghosh and T. Nakanishi, *Chem. Commun.*, 2017, **53**, 10344; b) F. Lu and T. Nakanishi, *Adv. Opt. Mater.*, 2019, 1900176.
20. a) G. Gustafsson, Y. Cao, G. M. Treacy, F. Klavetter, N. Colaneri, and A. J. Heeger, *Nature*, 1992, **357**, 477; b) T. Someya, Z. Bao, and G. G. Malliaras, *Nature*, 2016, **540**, 379.
21. a) A. Facchetti, M. Mushrush, M-H. Yoon, G. R. Hutchison, M. A. Ratner, and T. J. Marks, *J. Am. Chem. Soc.*, 2004, **126**, 13859; b) L. Sosa-Vargas, F. Nekelson, D. Okuda, M. Takahashi, Y. Matsuda, Q-D. Dao, H. Yoshida, A. Fujii, M. Ozaki, and Y. Shimizu, *J. Mater. Chem. C*, 2015, **3**, 1757.
22. a) J. Newton, H. Coles, P. Hodge, and J. Hannington, *J. Mater. Chem.*, 1994, **4**, 869; b) A. Zelcer, B. Donnio, C. Bourgogne, F. D. Cukiernik, and D. Guillon, *Chem. Mater.*, 2007, **19**, 1992; c) M. Funahashi, M. Yamaoka, K. Takenami, and A. Sonoda, *J. Mater. Chem. C*, 2013, **1**, 7872; d) T. G. Plint, B. A. Kamino, and T. P. Bender, *J. Phys. Chem. C*, 2015, **119**, 1676; e) J-C. Ribierre, L. Zhao, M. Inoue, P-O. Schwartz, J-H. Kim, K. Yoshida, A. S. D. Sandanayaka, H. Nakanotani, L. Mager, S. Méry, and C. Adachi, *Chem. Commun.*, 2016, **52**, 3103.
23. a) T. Ogoshi, T. Aoki, R. Shiga, R. Iizuka, S. Ueda, K. Demachi, D. Yamafuji, H. Kayama, and T. Yamagishi, *J. Am. Chem. Soc.*, 2012, **134**, 20322; b) A. Shimizu, K. Takenaka, N. Handa, T. Nokami, T. Itoh, and J. Yoshida, *Adv. Mater.*, 2017, 1606592.
    c) Y. Sagara, C. Weder, and N. Tamaoki, *Chem. Mater*., 2017, **29**, 6145.
24. a) C. Sirlin, L. Bosio, J. Simon, V. Ahsen, E. Yilmazer, and Ö. Bekâroğlu, *Chem. Phys. Lett.*, 1987, **139**, 362; b) C. F. van Nostrum, S. J. Picken, A-J. Schouten, and R. J. M. Nolte, *J. Am. Chem. Soc*., 1995, **117**, 9957; d) S. Kawano, Y. Yamada, S. Rongfang, Y. Ishihara, and K. Tanaka, *Chem. Lett.*, 2018, **47**, 1262.
25. M. Guerbet, *C. R. Chim.*, 1909, **149**, 129.
26. a) M. O'Neill and S. M. Kelly, *Adv. Mater*., 2003, **15**, 1135. b) M. Funahashi, *J. Mater. Chem. C*, 2014, **2**, 7451.
27. a) F. Reinitzer, *Monatsh. Chem.*, 1888, **9**, 421; b) O. Lehmann, *Z. Phys. Chem.*, 1889, **4**, 462; c) H. Kelker, *Mol. Cryst. Liq. Cryst.*, 1973, **21**, 1; d) F. Reinitzer, *Liq. Cryst*., 1989, **5**, 7; e) V. Vill, *Mol. Cryst. Liq. Cryst.*, 1992, **213**, 67.
28. D. Vorländer, *Ber. Dtsch. Chem. Ges.*, 1907, **40**, 1970.
29. S. Chandrasekhar, B. K. Sadashiva, and K. A. Suresh, *Pramana*, 1977, **9**, 471.
30. a) S. Kumar, *Chem. Soc. Rev.*, 2006, **35**, 83; b) T. Wöhrle, I. Wurzbach, J. Kirres, A. Kostidou, N. Kapernaum, J. Litterscheidt, J. C. Haenle, P. Staffeld, A. Baro, F. Giesselmann, and S. Laschat, *Chem. Rev.*, 2016, **116**, 1139.
31. C. Piechocki, J. Simon, A. Skoulios, D. Guillon, and P. Weber, *J. Am. Chem. Soc.*, 1982, **104**,

5245.

32. D. Adam, P. Schuhmacher, J. Simmerer, L. Häussling, K. Siemensmeyer, K. H. Etzbach, H. Ringsdorf, and D. Haarer, *Nature*, 1994, **371**, 141.
33. a) S. Laschat, A. Baro, N. Steinke, F. Giesselmann, C. Hägele, G. Scalia, R. Judele, E. Kapatsina, S. Sauer, A. Schreivogel, and M. Tosoni, *Angew. Chem. Int. Ed.*, 2007, **46**, 4832; b) S. Sergeyev, W. Pisula, and Y. H. Geerts, *Chem. Soc. Rev.*, 2007, **36**, 1902.
    c) B. R. Kaafarani, *Chem. Mater.*, 2011, **23**, 378; d) T. Kato, J. Uchida, T. Ichikawa, and T. Sakamoto, *Angew. Chem. Int. Ed.*, 2018, **57**, 2.
34. a) D. Xu and C. Adachi, *Appl. Phys. Lett.*, 2009, **95**, 053304; b) S. Hirata, K. Kubota, H. H. Jung, O. Hirata, K. Goushi, M. Yahiro, and C. Adachi, *Adv. Mater.*, 2011, **23**, 889; c) N. Kobayashi, T. Kasahara, T. Edura, J. Oshima, R. Ishimatsu, M. Tsuwaki, T. Imato, S. Shoji, and J. Mizuno, *Sci. Rep.*, 2015, **5**, 14822.
35. a) S. S. Babu, J. Aimi, H. Ozawa, N. Shirahata, A. Saeki, S. Seki, A. Ajayaghosh. H. Möhwald, and T. Nakanishi, *Angew. Chem. Int. Ed.*, 2012, **51**, 3391; b) S. S. Babu, M. J. Hollamby, J. Aimi, H. Ozawa, A. Saeki, S. Seki, K. Kobayashi, K. Hagiwara, M. Yoshizawa, H. Möhwald, and T. Nakanishi, *Nat. Commun.*, 2013, **4**, 1969; c) C. Allain, J. Piard, A. Brosseau, M. Han, J. Paquier, T. Marchandier, M. Lequex, C. Boissière, and P. Audebert, *ACS Appl. Mater. Interfaces*, 2016, **8**, 19843; d) M. J. Hollamby, A. E. Danks, Z. Schnepp, S. E. Rogers, S. R. Hart, and T. Nakanishi, *Chem. Commun*., 2016, **52**, 7344; e) T. Machida, R. Taniguchi, T. Oura, K. Sada, and K. Kokado, *Chem. Commun*., 2017, **53**, 2378; f) B. Narayan, K. Nagura, T. Takaya, K. Iwata, A. Shinohara, H. Shinmori, H. Wang, Q. Li, X. Sun, H. Li, S. Ishihara, and T. Nakanishi, *Phys. Chem. Chem. Phys.*, 2018, **20**, 2970; g) Goudappagouda, A. Manthanath, V. C. Wakchaure, K. C. Ranjeesh, T. Das, K. Vanka, T. Nakanishi, S. S. Babu, *Angew. Chem. Int. Ed.*, 2019, 58, 2284; h) F. Lu, K. Hagiwara, M. Yoshizawa, K. Nagura, S. Ishihara, and T. Nakanishi, *J. Mater. Chem. C*, 2019, **7**, 2577.
36. a) K. Isoda, Y. Sato, and D. Matsukuma, *ChemistrySelect*, 2017, **2**, 7222; b) Y. Sato, Y. Mutoh, D. Matsukuma, M. Nakagawa, T. Kawai, K. Isoda, *Chem. –Asian J*., 2018, 13, 2619; c) T. Ogoshi, K. Maruyama, Y. Sakatsume, T. Kakuta, T. Yamagishi, T. Ichikawa, and M. Mizuno, *J. Am. Chem. Soc.*, 2019, **141**, 785.
37. N. Giri, M. G. Del Pópolo, G. Melaugh, R. L. Greenaway, K. Ratzke, T. Koschine, L. Pison, M. F. Costa Gomes, A. I. Cooper, and S. L. James, *Nature*, 2015, **527**, 216.
38. P. Duan, N. Yanai, and N. Kimizuka, *J. Am. Chem. Soc.*, 2013, **135**, 19056.
39. a) E. M. Maya, A. W. Snow, J. S. Shirk, S. R. Flom, R. G. S. Pong, and J. H. Callahan, *J. Porphyrins Phthalocyanines*, 2002, **6**, 463; b) E. M. Maya, A. W. Snow, J. S. Shirk, R. G. S. Pong, S. R. Flom, and G. L. Roberts, *J. Mater. Chem.*, 2003, **13**, 1603.
40. A. S. D. Sandanayaka, L. Zhao, D. Pitrat, J-C. Mulatier, T. Matsushima, C. Andraud, J-H. Kim, J.

C. Ribierre, and C. Adachi, *Appl. Phys. Lett*., 2016, **108**, 223301.

41. A. Shimizu, K. Takenaka, N. Handa, T. Nokami, T. Itoh, and J. Yoshida, *Adv. Mater.*, 2017, 29, 1606592.
42. a) T. Ogoshi, T. Aoki, R. Shiga, R. Iizuka, S. Ueda, K. Demachi, D. Yamafuji, H. Kayama, and T. Yamagishi, *J. Am. Chem. Soc.*, 2012, **134**, 20322; b) V. C. Wakchaure, L. V. Pillai, Goudappagouda, K. C. Ranjeesh, S. Chakrabarty, S. Ravindranathan, P. R. Rajamohana, and S. S. Babu, *Chem. Commun*., 2019, **55**, 9371.
43. a) H. J. Snaith, S. M. Zakeeruddin, Q. Wang, P. Péchy, and M. Grätzel, *Nano Lett.*, 2006, **6**, 2000; b) J. C. Ribierre, T. Aoyama, T. Muto, and P André, *Org. Electron.*, 2011, **12**, 1800; c) T. G. Plint, B. A. Kamino, and T. P. Bender, *J. Phys. Chem. C*, 2015, **119**, 1676; d) A. Ghosh, M. Yoshida, K. Suemori, H. Isago, N. Kobayashi, Y. Mizutani, Y. Kurashige, I. Kawamura, M. Nirei, O. Yamamuro, T. Takaya, K. Iwata, A. Saeki, K. Nagura, S. Ishihara, and T. Nakanishi, *Nat. Commun*., 2019, **10**, 1.
44. F. Lu, T. Takaya, K. Iwata, I. Kawamura, A. Saeki, M. Ishii, K. Nagura, and T. Nakanishi, *Sci. Rep.*, 2017, **7**, 3416.
45. F. Lu and T. Nakanishi, *Sci. Technol. Adv. Mater.*, 2015, **16**, 014805.
46. A. Braun and J. Tcherniac, *Ber. Deut. Chem. Ges*., 1907, **40**, 2709.
47. H. de Diesbach and E. von der Weid, *Helv. Chim. Acta.*, 1927, **10**, 886-888.
48. A. G. Dandridge, H. A. Drescher, and J. Thomas, British Patent 322169 (1929).
49. a) R. P. Linstead, *J. Chem. Soc.*, 1934, 1016; b) R. P. Linstead and A. R. Lowe, *J. Chem. Soc.*, 1934, 1031; c) C. E. Dent, R. P. Linstead, and A. R. Lowe, *J. Chem. Soc.*, 1934, 1033.
50. a) G. T. Byrne, R. P. Linstead, and A. R. Lowe, *J. Chem. Soc.*, 1934, 1017; b) R. P. Linstead and A. R. Lowe, *J. Chem. Soc.*, 1934, 1022; c) C. E. Dent and R. P. Linstead, *J. Chem. Soc.*, 1934, 1027.
51. J. M. Robertson, *J. Chem. Soc.*, 1935, 615.
52. a) M. V. Martínez-Díaz, G. de la Torre, and T. Torres, *Chem. Commun.*, 2010, **46**, 7090; b) G. de la Torre, G. Bottari, and T. Torres, *Adv. Energy Mater.*, 2017, **7**, 1601700; c) M. Urbani, M-E. Ragoussi, M. K. Nazeeruddin, and T. Torres, Coord. *Chem. Rev.*, 2019, **381**, 1; d) M. Urbani, G. de la Torre, M. K. Nazeeruddin, and T. Torres, *Chem. Soc. Rev.,* 2019, **48**, 2738.
53. a) G. de la Torre, P. Vázquez, F. Agulló-López, and T. Torres, *Chem. Rev.*, 2004, **104**, 3723; b) Y. Chen, M. Hanack, Y. Araki, and M. Hanack, *Chem. Soc. Rev*., 2005, **34**, 517; c) M. O. Senge, M. Fazekas, E. G. A. Notaras, W. J. Blau, M. Zawadzka, O. B. Locos, and E. M. Ni Mhuircheartaigh, *Adv. Mater*., 2007, **19**, 2737; d) D. Dini, M. J. F. Calvete, and M. Hanack, *Chem. Rev.*, 2016, **116**, 13043.
54. a) L. Li, Q. Tang, H. Li, W. Hu, X. Yang, Z. Shuai, Y. Liu, and D. Zhu, *Pure. Appl. Chem*., 2008, **80**, 2231; b) O. A. Melville, B. H. Lessard, and T. P. Bender, *ACS Appl. Mater. Interfaces*, 2015,

7, 13105.

55. a) M. Mitsunaga, M. Ogawa, N. Kosaka, L. T. Rosenblum, P. L. Choyke, and H. Kobayashi, *Nat. Med.*, 2011, **17**, 1685; b) T. Nyokong, *Pure Appl. Chem*., 2011, **83**, 1763; c) K. Ishii, *Coord. Chem. Rev.*, 2012, **256**, 1556; d) S. Singh, A. Aggarwal, N. V. S. D. K. Bhupathiraju, G. Arianna, K. Tiwari, and C. M. Drain, *Chem. Rev.*, 2015, **115**, 10261; e) R. C. H. Wong, P-C. Lo, D. K. P. Ng, *Coord. Chem. Rev.*, 2019, **379**, 30.
56. a) A. B. Sorokin, *Chem. Rev.*, 2013, **113**, 8152; b) S. Kusama, T. Saito, H. Hashiba, A. Sakai, and S. Yotsuhashi, *ACS Catal*., 2017, **7**, 8382; c) J. Bian, J. Feng, Z. Zhang, Z. Li, Y. Zhang, Y. Liu, S. Ali, Y. Qu, L. Bai, J. Xie, D. Tang, X. Li, F. Bai, J. Tang, and L. Jing, *Angew. Chem. Int. Ed*., 2019, **58**, 10873; d) M. Wang, K. Torbensen, D. Salvatore, S. Ren, D. Joulié, F. Dumoulin, D. Mendoza, B. Lasslle-Kaiser, U. Isci, C. P. Berlinguette, and M. Robert, *Nat. Commun.*, 2019, **10**, 3602; e) S. Ren, D. Joulié, D. Salvatore, K. Torbensen, M. Wang, M. Robert, and C. P. Berlinguette, *Science*, 2019, **365**, 367; f) R. Matheu, E. Gutierrez-Puebla, M. Á. Monge, C. S. Diercks, J. Kang, M. S. Prévot, X. Pei, N. Hanikel, B. Zhang, P. Yang, and O. M. Yaghi, *J. Am. Chem. Soc.*, 2019, **141**, 17081.
57. a) N. Ishikawa and Y. Kaizu, *Coord. Chem. Rev.*, 2002, **226**, 93; b) K. Katoh, H. Isshiki, T. Komeda, and M. Yamashita, *Chem. –Asian J.*, 2012, **7**, 1154; c) T. Fukuda and N. Ishikawa, *J. Porphyrins Phthalocyanines,* 2014, **18**, 615.
58. R. Paolesse, S. Nardis, D. Monti, M. Stefanelli, and C. D. Natale, *Chem. Rev.*, 2017, **117**, 2517.
59. a) M. Gouterman, *J. Chem. Phys.*, 1959, **30**, 1139; b) M. Gouterman, *J. Mol. Spectrosc.*, 1961, **6**, 138.
60. K. Ishii and N. Kobayashi in *Phthalocyanines as Functional Dyes* (機能性色素としてのフタロシアニン [in Japanese]), (Eds.: R. Hirohashi, K. Sakamoto, and E. Okumura), IPC, 2004, pp. 103-110, ISBN4-901493-49-3 C3043.
61. a) N. Kobayashi, H. Ogata, N. Nonaka, and E. A. Luk'yanets, *Chem. –Eur. J.*, 2003, **9**, 5123; b) T. Fukuda and N. Kobayashi in *Handbook of Porphyrin Science*, (Eds.: K. M. Kadish, K. M. Smith, and R. Guilard), World Scientific, Singapore, 2010, Vol. 9*,* pp1-664.
62. P. A. Barrett, D. A. Frye, and R. P. Linstead, *J. Chem. Soc.*, 1938, 1157.
63. H. Tomoda, S. Saito, S. Ogawa, and S. Shiraishi, *Chem. Lett.*, 1980, 1277.
64. S. W. Oliver and T. D. Smith, *J. Chem. Soc. Perkin Trans. II*, 1987, 1579.
65. a) G. Schmid, M. Sommerauer, M. Geyer, and M. Hanack in *Phthalocyanines: Properties and Applications,* (Eds.: C. C. Leznoff and A. B. P. Lever), VCH, Weinheim, 1996, Vol. 4, pp5-18; b) N. B. Mckeown in *The Porphyrin Handbook*, (Eds.: K. M. Kadish, K. M. smith, R. Guilard), Elsevier Science, San diego, USA, 2003, Vol. 15, pp61-124.
66. a) M. Hanack, G. Schmid, and M. Sommerauer, *Angew. Chem. Int. Ed. Engl.*, 1993, **32**, 1422; *Angew. Chem*., 1993, **105**, 1540; b) M. Sommerauer, C. Rager, and M. Hanack, *J. Am. Chem. Soc.*,

1996, **118**, 10085; c) M. Bai, Y. Zhang, R. Song, S. Han, P. Wan, and C. Zhang, *Dyes Pigm.*, 2013, **97**, 469.

67. Y. Chen, W. Fang, K. Wang, W. Liu, and J. Jiang, *Inorg. Chem.*, 2016, **55**, 9289.
68. a) C. Leznoff, M. Hu, C. R. McArthur, and Y. Qin, *Can. J. Chem.*, 1994, **72**, 1990; b) J. Ranta, T. Kumpulainen, H. Lemmetyinen, and A. Efimov, *J. Org. Chem*., 2010, **75**, 5178; c) P. Apostol, A. Bentaleb, M. Rajaoarivelo, R. Clérac, and H. Bock, *Dalton Trans.*, 2015, **44**, 5569. d) S. Yamamoto, K. Kuribayashi, T. N. Murakami, E. Kwon, M. J. Stillman, N. Kobayashi, H. Segawa, and M. Kimura, *Chem. –Eur. J*., 2017, **23**, 15446.
69. a) H. Eichhorn, *J. Porphyrins Phthalocyanines*, 2000, **4**, 88; b) K. Ohta, H-D. Nguyen-Tran, L. Tauchi, Y. Kanai, T. Megumi, and Y. Takagi in *Handbook of Porphyrin Science*, (Eds.: K. M. Kadish, K. M. Smith, R. Guilard), World Scientific, Singapore, 2010, Vol. 12*,* pp1-120; c) A. Yu. Tsivadze, L. A. Nosikova, and Z. A. Kudryashova, *Prot. Met. Phys. Chem. Surf*., 2012, **48**, 135; d) T. Basova, A. Hassan, M. Durmuş, A. G. Gürek, and V. Ahsen, *Coord. Chem. Rev.*, 2016, **310**, 131.
70. a) M. Ichihara, A. Suzuki, K. Hatsusaka, and K. Ohta, *J. Porphyrins Phthalocyanines*, 2007, **11**, 503; b) M. Ichihara, A. Suzuki, K. Hatsusaka, and K. Ohta, *Liq. Cryst.*, 2007, **34**, 555.
71. K. Hatsusaka, K. Ohta, I. Yamamoto, and H. Shirai, *J. Mater. Chem*., 2001, **11**, 423.
72. B. Tylleman, G. Gbabode, C. Amato, C. Buess-Herman, V. Lemaur, J. Cornil, R. G. Aspe, Y. H. Geerts, and S. Sergeyev, *Chem. Mater.*, 2009, **21**, 2789.
73. M. J. Cook, M. F. Daniel, K. J. Harrison, N. B. McKeown, and A. J. Thomson, *J. Chem. Soc., Chem. Commun.*, 1987, 1086.
74. a) M. J. Cook, *J. Mater. Sci. -Mater. El*., 1994, **5**, 117; b) N. B. Chaure, C. Pal, S. Barard, T. Kreouzis, A. K. Ray, A. N. Cammidge, I. Chambrier, M. J. Cook, C. E. Murphy, and M. G. Cain, *J. Mater. Chem.*, 2012, **22**, 19179; c) D. J. Tate, R. Anémian, R. J. Bushby, S. Nanan, S. L. Warriner, and B. J. Whitaker, *Beilstein J. Org. Chem.*, 2012, **8**, 120.
75. a) R. Yamaoka and M. Funahashi, *ChemistrySelect*, 2017, **2**, 11934; b) M. Yatabe, A. Kajitani, M. Yasutake, and K. Ohta, *J. Porphyrins Phthalocyanines*, 2017, **21**, 1.
76. a) B. Mohr, G. Wegner, and K. Ohta, *J. Chem. Soc., Chem. Commun.*, 1995, 995; b) D. K. P. Ng, Y. Yeung, W. K. Chan, and S. Yu, *Tetrahedron Lett.*, 1997, **38**, 6701; c) M. Ichihara, M. Miida, B. Mohr, and K. Ohta, *J. Porphyrins Phthalocyanines*, 2006, **10**, 1145; d) A. N. Cammidge and H. Gopee, *J. Porphyrins Phthalocyanines*, 2009, **13**, 235; e) L. Zöphel, K. S. Mali, P. S. Raddy, M. Wagner, S. De Feyter, W. Pisula, and K. Müllen, *Chem. Eur. J*., 2012, **18**, 3264; f) H. Suzuki, K. Kawano, K. Ohta, Y. Shimizu, N. Kobayashi, and M. Kimura, *ChemistryOpen*, 2015, **5**, 150.
77. a) N. Zharnikova, N. Usol'tseve, E. Kudrick, and M. Thelakkat, *J. Mater. Chem*., 2009, **19**, 3169; b) Y. Takagi, K. Ohta, S. Shimosugi, T. Fujii, and E. Itoh, *J. Mater. Chem.*, 2012, **22**, 14418; c) H. Nakamura, K. Sugiyama, K. Ohta, and M. Yasutake, *J. Mater. Chem. C*, 2017, **5**, 7297.

78. A. W. Snow, J. S. Shirk, and R. G. S. Pong, *J. Porphyrins Phthalocyanines*, 2000, **4**, 518.
79. E. M. Maya, J. S. Shirk, A. W. Snow, and G. L. Roberts, *Chem. Commun*., 2001, 615.
80. M. Durmuş, C. Lebrun, and V. Ahsen, *J. Porphyrins Phthalocyanines*, 2004, **8**, 1175.
81. A. G. Gürek, M. Durmuş, and V. Ahsen, *New J. Chem.*, 2004, **28**, 693.
82. S. Sergeyev, E. Pouzet, O. Debever, J. Levin, J. Gierschner, J. Cornil, R. G. Aspe, and Y. H. Geerts, *J. Mater. Chem.*, 2007, **17**, 1777.
83. M. Ichihara, A. Suzuki, K. Hatsusaka, and K. Ohta, *J. Porphyrins Phthalocyanines*, 2007, **11**, 503.
84. M. Li, E. Khoshdel, and D. M. Haddleton, *Polym. Chem.*, 2013, **4**, 4405.
85. G. Cheng, X. Peng, G. Hao, V. O. Kennedy, I. N. Ivanov, K. Knappenberger, T. J. Hill, M. A. J. Rodgers, and M. E. Kenny, *J. Phys. Chem. A*, 2003, **107**, 3503.
86. Y. Bandera, M. K. Burdette, J. A. Shetzline, R. Jenkins, S. E. Creager, and S. H. Foulger, *Dyes Pigm.*, 2016, **125**, 72.
87. B. Del Rey, M. V. Martínez-Díaz, J. Barbera, and T. Torres, *J. Porphyrins Phthalocyanines*, 2000, **4**, 569.
88. M. S. Rodríguez-Morgade, S. Esperanza, T. Torres, and J. Barberá, *Chem. -Eur. J.*, 2005, **11**, 354.
89. A. Zielinska, A. Takai, H. Sakurai, A. Saeki, M. Leonowicz, and T. Nakanishi, *Chem. –Asian J.*, 2018, **13**, 770.

Chapter 2

General experimental

2.1. Syntesis and characterizations

2.1.1. Materials and synthesis

All starting chemicals were purchased from commercial suppliers and used without further purifications unless otherwise noted. Column chromatography was performed with silica (WAKO gel C-200) or activated alumina (WAKO 200 mesh). Recycling preparative gel permeation chromatography was carried out by a recycling high performance liquid chromatography (HPLC, Japan Analytical Industry Co., Ltd.) using chloroform as an eluent. Analytical thin layer chromatography was performed with commercial Merck plates coated with silica gel $60F_{254}$ or aluminum oxide.

2.1.2. Characterization of compounds

High resolution atmospheric pressure chemical ionization time-of-flight (HR-APCI-TOF) mass spectra were recorded with Bruker micrOTOF-II. ^{1}H and ^{13}C NMR spectra were recorded with Bruker BioSpin AVANCE NEO 400 ONEBAY at 400.13 and 100.61 MHz, respectively. Chemical shift was reported relative to internal standard (tetramethylsilane (TMS), 0.00 pppm). Chemical shifts were expressed in δ (ppm) values, and coupling constants (J) were expressed in hertz (Hz). The following abbreviations of multiplicity are used: s=singlet, d=doublet, dd=double doublet, t=triplet, quin=quintet, m=multiplet, brs=broad singlet, br=broad. Fourier transfer infrared (FT-IR) absorption spectra were recorded on Shimadzu IR Prestige-21 with Dura Sample IR II.

2.1.3. UV-vis absorption and fluorescence spectroscopy

The absorption spectra in solution state were recorded with Shimadzu UV-2600. The molar absorption (or extinction) coefficient (ε) were calculated from absorption measurements in solution state:

$$A = \log(\frac{I}{I_0}) = \varepsilon cl \qquad \text{(Lambert-Beer's law)}$$

Where A is the measured absorbance, I is transmitted intensity, I_0 is the intensity of the incident light at a given wavelength, c is the molar concentration of samples in solvents, l is the pass length through the sample. Plotting A against to c, if the relationship A and c is linear, Lambert-Beer's law is satisfied. If not linear, aggregates are formed in the solution.

The absorption spectra in thin film were recorded with JASCO V-650. In general, π-conjugate molecules tend to form aggregates in condensed state. The absorption spectra in condensed state powerful technique for analyzing structure of aggregates. According to Kasha's exciton coupling theory[1], the shape and position of absorption spectra are affected by relative configurations of π-

conjugate molecules (Figure 2-1). Therefore, aggregation structures of π-conjugate molecules can be determined with this theory. The absorption bands originated from highest occupied molecular orbital (HOMO)-lowest unoccupied molecular orbital (LUMO) transition are dramatically affected by formation of aggregates. In the case of Pcs, the Q-bands are HOMO-LUMO transition. Hence, the author focused the position and shape of the Q-bands in this thesis. When face-to-face (H-) dimers are formed, the absorption bands are blue-shifted (shift to higher energy region). On the other hand, the absorption bands are red-shifted (shift to lower energy region) in parallel arrangement of the π-conjugate molecules. When slipped stacked dimers are formed, the shift of bands depends on tilt angle θ between the monomers. In the case of θ>54.7°, the bands are blue-shifted. In the case of θ<54.7°, the bands are red-shifted. In the case of θ=54.7°, the bands are not shifted. When herringbone dimers are formed, the bands are splitting.

The fluorescence spectra were recorded with JASCO FP-750. Fluorescence spectra is sensitive to surrounding environment around the molecules at excited state. The fluorescence spectra in condensed state provide an information about intermolecular interactions.

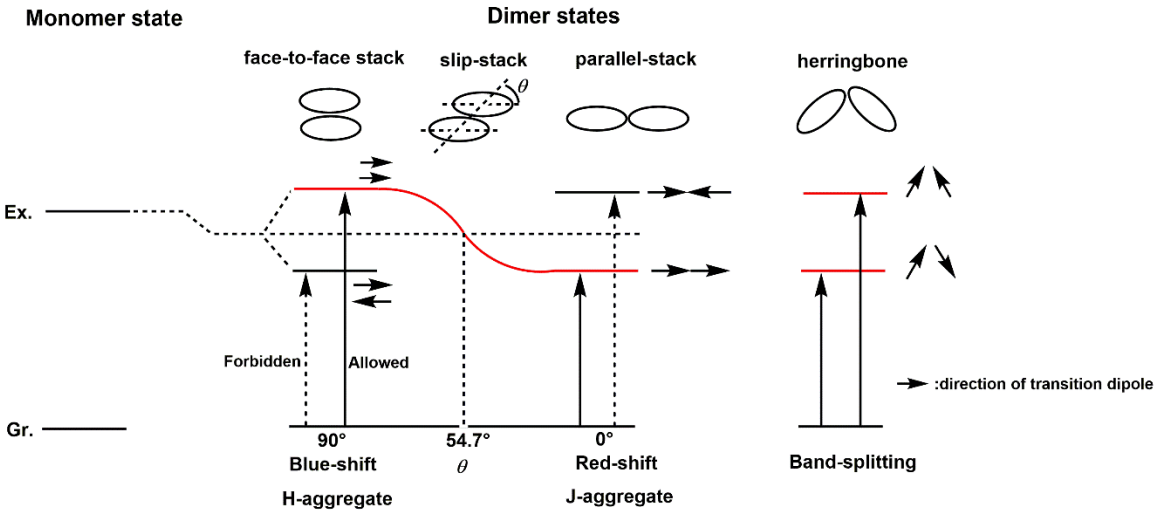

Figure 2-1. Exciton energy diagrams for four dimers.

2.1.4. Polarizing optical microscopy

Polarizing optical microscopic (POM) observations were carried out with polarizing optical microscope (NIKON ECLIPSE LV100ND) equipped with a hot stage (METTLER TOLEDO FP82HT). The technique probe the microscale ordering or homogenous isotropic nature of the samples. Neat samples sandwiched two glasses are observed directly under the microscope with/without temperature control. In liquid crystalline samples, birefringent textures are observed due to the presence of optically long-ranged ordered structure with anisotropy. The shape of textures is helpful to characterize structures of liquid crystalline phase (Figure 2-2). When anisotropic structure is present

in sample, birefringence is observed. In general, if the samples perfectly align on substrate, no birefringence is observed because the perfectly aligned sample is optically homogenous, i.e. not anisotropic. In liquid samples, no birefringence is observed due to the absence of optically long-ranged ordered structure.

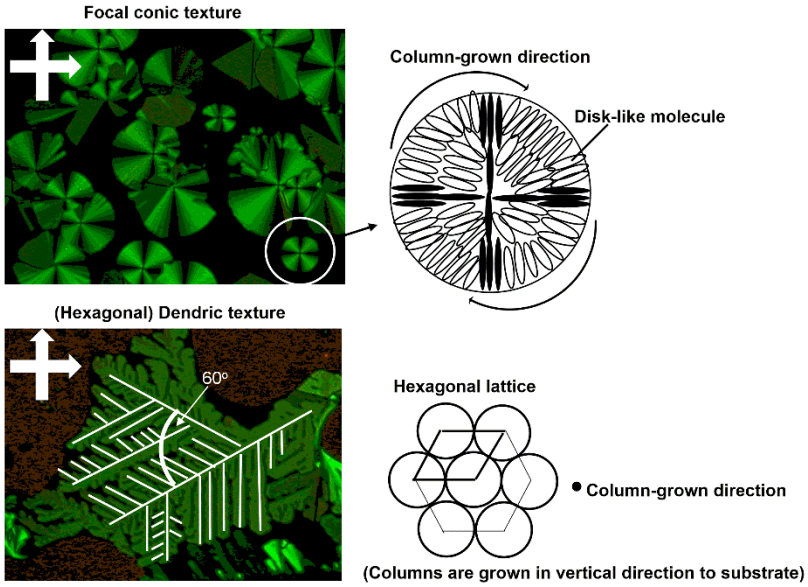

Figure 2-2. The relationship between textures and grown directions of column.

2.1.5. Thermogravimetric analysis

Thermogravimetric analysis (TGA) was carried out with Seiko Instruments EXSTAR TG/DTA6200 under nitrogen gas flow at san rate 10 °C /min. The decomposition temperature (T_d) of a sample can be determined by TGA. T_d has to been obtained in prior to differential scanning calorimetry to avoid decomposition of sample on thermal scan.

2.1.6. Differential scanning calorimetry

Differential scanning calorimetry (DSC) was carried out with Hitachi High-tech Science DSC7020 under liquid nitrogen cooling and nitrogen gas flow. The technique is important to define thermal phase transition behavior of samples. In a typical liquid crystalline sample, DSC thermogram shows two endothermic peak (Figure 2-3). The one at lower temperature can be assigned to crystal-liquid crystal transition (T_m). The other one at higher temperature can be assigned to liquid crystal-isotropic liquid transition (T_c). The area of peak correspond to enthalpy of phase transition. In a typical liquid sample, the thermogram shows only broad shift of baseline (T_g). External parameters like scan rate (°C /min) and hold time at a specific temperature can affect to the result in a few case such as supercooling behavior[2]. The difference of result by the external parameters providing us useful

information for characterizing phase transition behavior of the sample.

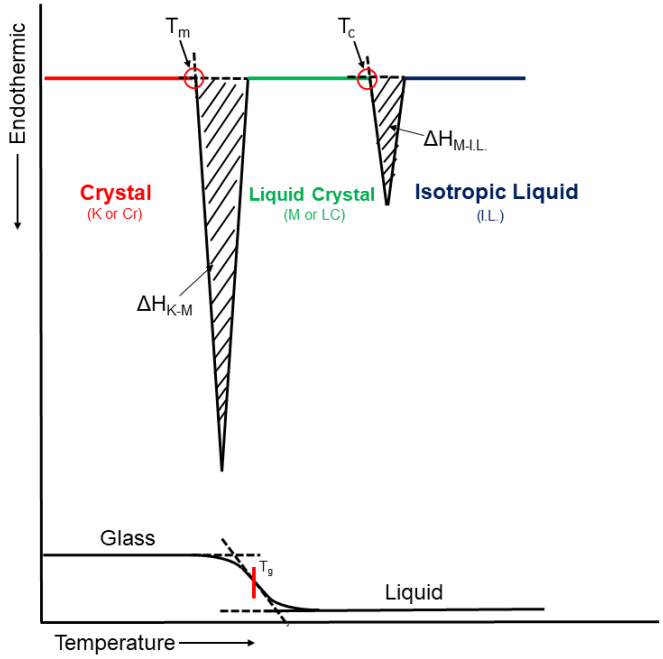

Figure 2-3. Typical DSC thermograms for liquid crystalline (upper) and liquid sample (lower).

2.1.7. Small-angle X-ray scattering/diffraction

Small angle X-ray scattering (SAXS) measurements were performed with Bruker Mac SAXS System (CuK_α source). Small angle X-ray diffraction (SAXD) measurements were performed with Rigaku RINT-ultima/S2K (CuK_α source). These techniques provide an information in distance between packing structures. In relatively ordered samples such as liquid crystals, the SAXS/SAXD peaks will be sharp and assignable. Peaks have an information on spacing distance. The spacing distance (d) can be obtained from Bragg's law:

$$\lambda = 2d \sin\theta \quad \text{(Bragg's law)}$$

where λ is wavelength of X-ray (1.5418 Å for CuK_α source), θ is glancing angle. The lattice structure can be determined from d-spacing, Miller indices, and structure factor (extinction rule) of the lattice.[3] In liquid samples, a broad peak and a halo appeared in small-angle region and wide-angle region, respectively. In general, the broad peak reflect average distance of π-conjugate units. The halo reflect average distance of disordered alkyl chains.

2.1.8. Rheology

Rheology measurements were carried out with Anton Parr Physica MCR301 rheometer, using the parallel plate geometry (10 mm diameter). Strain amplitude (γ) scans were firstly performed to determine the linear-viscoelastic region. For both samples strain amplitude (γ) of 0.1% and 50% were within this linear viscoelastic region. Rheology is one of the informative techniques for studies of fluids. The measurements give us an estimate of the storage modulus (G') and the loss modulus (G''). G' and G'' are defined as the functions of ω in following equations.[4]

$$G' = \frac{G\tau^2\omega^2}{1+\tau^2\omega^2} \quad , \quad G'' = \frac{G\tau\omega}{1+\tau^2\omega^2}$$

Where G and τ are relaxation modulus and relaxation time, respectively. **For liquids, the G'' should be greater than the G' ($G'' > G'$).** More importantly, rheology analysis give us the complex viscosity (η^*) of the liquid samples. The η^* vs. angular frequency (ω) plot helps us to categorize where the liquid has Newtonian or non-Newtonian behavior. **Newtonian liquids exhibit a constant η^* against to ω. On the other hand, for non-Newtonian liquids, η^* depends on ω.**

References

1. M. Kasha, H. R. Rawls, and M. A. El-Bayoumi, *Pure Appl. Chem.*, 1965, **11**, 371.
2. a) P. G. Debenedetti and F. H. Stillinger, *Nature*, 2001, **410**, 259. b) K. Chung, M. S. Kwon, B. M. Leung, A. G. Wong-Foy, M. S. Kim, J. Kim, S. Takayama, J. Gierschner, A. J. Matzger, and J. Kim, *ACS Cent. Sci*., 2015, **1**, 94. c) F. Lu, K. Jang, I. Osica, K. Hagiwara, M. Yoshizawa, M. Ishii, Y. Chino, K. Ohta, K. Ludwichowska, K. J. Kurzydłowski, S. Ishihara, and T. Nakanishi, *Chem. Sci.*, 2018, **9**, 6774.
3. a) K. Ohta, *Dimensionality and Hierarchy of Liquid Crystalline Phases: X-ray Structural Analysis of the Dimensional Assemblies*, Shinshu University Institutional Repository, submitted on 11 May, 2013; http://hdl.handle.net/10091/17016. b) K. Ohta, In *Identification of discotic mesophases by X-ray structure analysis, Introduction to Experiments in Liquid Crystal Science* (液晶実験科学入門 [in Japanese]), Japanese Liquid Crystal Society, Sigma Shuppan: Tokyo, 2007; Chap. 2-(3), pp. 11-21, ISBN-13:978-4915666490.
4. T. Shikata in *Polymer Chemistry* 5th edition (高分子化学 第 5 版 [in Japanese]), (Eds.: S. Murahashi, T. Kotaka, M. Kamachi, and T. Norisue), Kyoritu Syuppan, Tokyo, 2007, pp. 245-314, pp. 245-314, ISBN978-4-320-04380-0.

Chapetr 3

Synthesis and mesomorphism of phthalocyanines substituted by *m*-alkoxyphenylthio groups

Summary: We have successfully synthesized a series of novel octakis(*m*-alkoxyphenylthio)phthalocyaninato copper(II) complexes, (*m*-C_nOPhS)$_8$PcCu (*n* = 2, 4, 6, 8, 10, 12, 14, 16: **1b~i**), by our developed method to reveal their mesomorphism. The phase transition behavior and mesophase structures have been established by using a polarizing optical microscope, a differential scanning calorimeter, and a temperature-dependent small angle X-ray diffractometer. Interestingly, the very short chain-substituted derivatives, (*m*-C_1OPhS)$_8$PcCu (**1a**) and (*m*-C_2OPhS)$_8$PcCu (**1b**), show a hexagonal ordered columnar (Col_{ho}) mesophase, whereas each of the other longer-chain-substituted derivatives, (*m*-C_nOPhS)$_8$PcCu (*n*= 4~16: **1c~i**), shows only rectangular ordered columnar (Col_{ro}) mesophase(s). In contrast to the present longer-chain-substituted *phenylthio* derivatives, each of the previous longer-chain-substituted *phenoxy* derivatives, (*m*-C_nOPhO)$_8$PcCu (*n* = 10-20), shows a different columnar mesophase of Col_{ho}. We discuss this difference of mesomorphism from the viewpoint of the different steric hindrance originated by the peripheral substituents, PhO and PhS groups. Moreover, we could estimate the optical band gaps of (*m*-C_{10}OPhO)$_8$PcCu and (*m*-C_{10}OPhS)$_8$PcCu (**1f**) from a crossing point of their absorption edge of the Q-bands to be 1.79 eV and 1.70 eV, respectively. Therefore, the *phenylthio*-substituted derivative gave a narrower band gap by *ca.* 0.1 eV in comparison with the *phenoxy*-substituted derivative.

3.1. Introduction

Since the first discotic columnar liquid crystal was found by Chandrasekhar and co-workers in 1977 [1], various discogens have been synthesized up to date. In general, a columnar liquid crystal has a π-conjugated macrocyclic core such as triphenylene, hexabenzocoronene and phthalocyanine (Pc), together with more than six long alkyl chains in the periphery [2]. When these discogens are heated, the peripheral long alkyl chains firstly melt to form soft parts, but the central rigid cores maintain columnar stacking structure due to their strong π-π interaction. Accordingly, columnar liquid crystalline phases can be induced by this special situation. Therefore, pre-melting of the long alkyl chains by heating is driving force to induce liquid crystalline phases. In addition, since π orbitals of the π-conjugated macrocyclic cores are overlapped in one-dimensional columns formed by self-assembly, high charge carrier mobility along the columnar axis may be achieved. Therefore, the columnar liquid crystalline compounds exhibiting high charge carrier mobility have attracted a lot of our attention to apply to organic semiconducting devices such as organic photovoltaic cell, organic field effect transistor and so on [3]. In our previous works [4-6], we synthesized columnar liquid crystalline phthalocyanine compounds, $(C_{12}H_{25}O)_8PcH_2$ and $(C_{12}H_{25}S)_8PcH_2$, illustrated in Figure 3-1. The hexagonal ordered columnar (Col_{ho}) phases in $(C_{12}H_{25}O)_8PcH_2$ and $(C_{12}H_{25}S)_8PcH_2$ exhibited high charge carrier mobilities of 0.051 cm^2 /Vs and 0.28 cm^2 /Vs, respectively. Therefore, the *alkylthio*(RS)-substituted phthalocyanine derivative gives about 5 times higher charge carrier mobility than the *alkoxy*(RO)-substituted phthalocyanine derivative. In order to achieve much higher charge carrier mobility in columnar liquid crystalline Pc compounds, the following two points may be furthermore required:

(1) To show very short intracolumnar stacking distance,

(2) To exhibit highly ordered alignment (ideally, homeotropic alignment).

In our previous works [7, 8], we found that substitution of *m*-alkoxyphenoxy (*m*-C_nOPhO) groups at the β-positions of Pc gave columnar liquid crystalline derivatives, (*m*-C_nOPhO)$_8$PcCu (Figure 3-1), satisfying above two requirements. Therefore, if we can synthesise columnar liquid crystalline phthalocyanines substituted by *m*-alkoxyphenylthio(*m*-C_nOPhS) groups instead of *m*-alkoxyphenoxy(*m*-C_nOPhO) groups, higher charge carrier mobility may be realized. The *alkylthio*-substituted phthalocyanine derivative, $(C_nS)_8PcH_2$, exhibits 5 times higher charge carrier mobility than the *alkoxy*-substituted phthalocyanine derivative, $(C_nO)_8PcH_2$, as mentioned above [4-6]. Therefore, we can expect similarly that the *phenylthio*-substituted derivative, $(PhS)_8PcCu$, may exhibit higher charge carrier mobility than the *phenoxy*-substituted derivative, $(PhO)_8$Pc-Cu. Although the $(PhS)_8PcCu$ derivatives have been reported so far [9-19], no liquid crystalline $(PhS)_8PcCu$ derivatives have been reported.

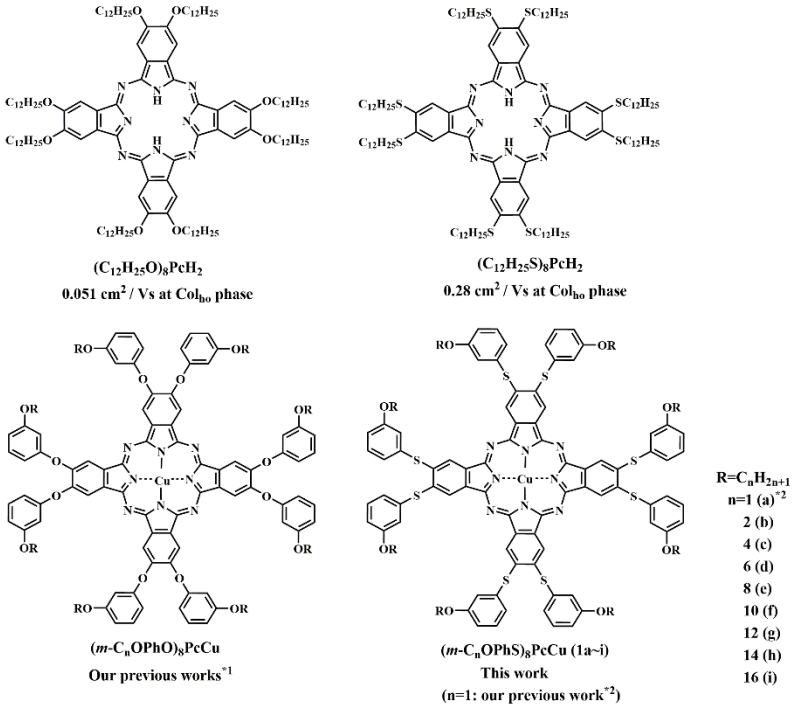

Figure 3-1. Molecular formulae of liquid crystals based on phthalocaynine.
*1: Ref. 8, 9, 21. *2: Ref. 20

Recently, we have synthesized $(PhS)_8PcCu$ complexes having very short methoxy groups at the *o-, m-, m- & p*-positions of the phenylthio group to induce mesomorphism in spite of the absence of long alkoxy chains [20]. The thermal fluctuation of the bulky substituents by heating makes soft parts to induce liquid crystalline phases. Hence, they are categorized to "flying-seed-like" liquid crystals [21-25]. However, these flying-seed-like liquid crystals (x-$C_1OPhS_{)8}PcCu$ substituted by very short alkoxy groups are not suitable for application to organic semiconductor, because they show mesomorphism only at extremely high temperatures and transform into isotropic liquid with accompanying decomposition. Therefore, we have planned to synthesize new long *n*-alkoxy-substituted (m-C_nOPhS)$_8$PcCu derivatives showing mesomorphism from room temperature and clearing into isotropic liquid without decomposition.

In this study, we have developed the synthetic route of the new *phenylthio*-substituted derivatives, (m-C_nOPhS)$_8$PcCu (n = 2-16: **1b-1i** in Figure 3-1), having long *n*-alkoxy groups at the *m*- position, in order to investigate their mesomorphism and mesomorphic structures. In comparison with the previous *phenoxy*-substituted Pc derivatives, (m-C_nOPhO)$_8$PcCu (n = 10-20), we discuss the difference of mesomorphism from the viewpoint of the different steric hindrance originated by the peripheral PhO and PhS groups.

3.2. Experimental

3.2.1. Materials

The chemical regents of 3-Hydroxybenzenethiol, tritylchloride, Et_3SiH, 3-iodophenol, *n*-alkylbromide, $NaBH_4$ and 4,5-dichlorophthalonitrile were purchased from Tokyo Chemical Industry and used without further purifications. Other reagents were purchased from Wako Pure Chemical Industries and used without further purifications. Thin layer chromatography sheet (TLC) and silica gel were purchased from Merck. All reaction solvents were purchased from Wako Pure Chemical Industries. DMF was pre-dried over KOH and distilled over CaH_2 under reduced pressure and stored in the presence of 4A molecular sieves. THF was pre-dried over $CaCl_2$ and distilled from Na wire / benzophenone kethyl. 1-Hexanol was used without further purifications. Deuterated chloroform and DMSO for NMR measurements were purchased from Merck and WAKO Pure Chemical Industries, respectively. Abbreviations of reagents and solvents were as follows:

DBU: 1,8-diazabicyclo[5.4.0]-7-undecene, DMF: *N,N*-dimethylformamide, THF: tetrahydrofuran, DMSO: dimethylsulfoxid and TFA: trifluoroacetic acid

3.2.2. Synthesis

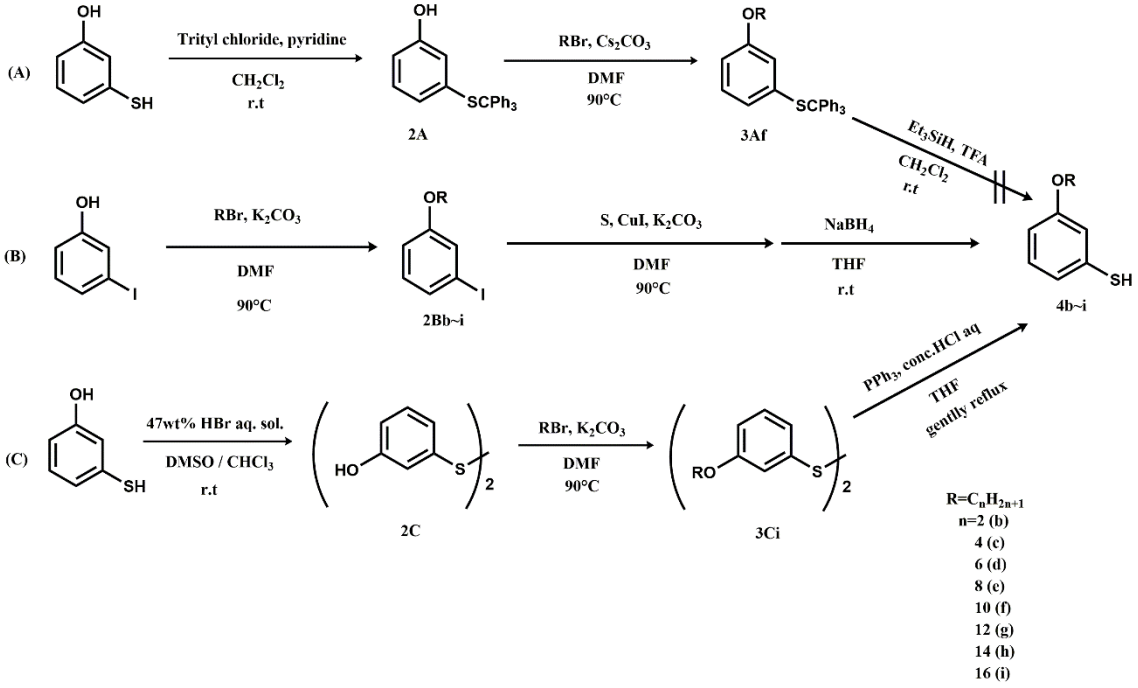

Scheme 3-1. Synthetic routes (a), (b), and (c) for 3-alkoxybenzenethiol: (a) by using the methods adopted Ref. 26 and 27; (b) Ref. 30; (c) Ref. 31.

Schemes 3-1 and 3-2 illustrate synthetic routes for the precursors of *m*-alkoxythiophenol (**4b~i**) and the corresponding liquid crystalline Pc derivatives (*m*-C_nOPhS)$_8$PcCu (**1b~i**), respectively. All reactions were carried out under nitrogen atmosphere.

[Route A]

3-Triphenylmethylsulfanylphenol (2A). (Scheme 3-1)

Synthetic method was adopted that of Ref. 26. A three necked flask dried was charged with 3-hydroxybenzenethiol (1.03 g, 8.15 mmol) and dry pyridine (0.679 g, 8.58 mmol). Trityl chloride (2.27 g, 8.14 mmol) was added to the reaction mixture and it was stirred at rt for 3.5 h. When TLC (SiO_2 / AcOEt: *n*-hexane = 1:1) confirmed disappearance of the spot of the starting reagent of 3-hydroxybenzenethiol (R_f= 0.50) and appearance of the target compound (R_f= 0.68), the reaction was terminated. The reaction mixture was diluted with water and extracted with dichloromethane. The organic layer was washed with water three times and saturated brine once. The organic layer was collected and dried over Na_2SO_4 overnight. Na_2SO_4 was filtrated off and dichloromethane and pyridine were evaporated *in vacuo*. The residue was dried *in vacuo* to obtain colorless oil (0.268 g).

Yield: 85.6%. ^{1}H-NMR (400 MHz, d_6-DMSO, TMS): δ, ppm 9.31 (brs, 1H, -OH), 7.33-7.20 (m, 15H, ArH), 6.83 (t, *J* = 8.0 Hz, 1H, ArH), 6.55-6.52 (m, 1H, ArH), 6.39-6.38 (m, 1H, ArH), 6.32-6.30 (m, 1H, ArH).

1-Decyloxy-3-triphenylmethylsulfanylbenzene (3Af). (Scheme 3-1)

Three necked flask dried was charged with 3-triphenylmethylsulfanylphenol (**2A**: 0.505 g, 1.37 mmol), Cs_2CO_3 (0.564 g, 1.73 mmol) and dry DMF (5 mL) at rt. 1-Bromodecane (0.315 g, 1.42 mmol) was added to the reaction mixture and stirred at r.t for 4.5 h. When TLC (SiO_2 / AcOEt: *n*-hexane = 1: 1) confirmed disappearance of the spot of starting reagent (R_f= 0.18) of **2A** and appearance of the target compound (**3Af**) (R_f= 0.63), the reaction was terminated. The reaction mixture was diluted with water and extracted with dichloromethane. The organic layer was washed with water three times and saturated brine once. The organic layer was collected and dried over Na_2SO_4 overnight. Na_2SO_4 was filtrated off and dichloromethane was evaporated *in vacuo* to obtain the crude product. It was purified by silica gel column chromatography (R_f = 0.55, CH_2Cl_2: *n*-hexane = 1:2). The solvents were evaporated *in vacuo* and resulting product was dried *in vacuo* to obtain colorless oil (0.598 g).

Yield: 85.8%. ^{1}H-NMR(400 MHz, d_6-DMSO, TMS): δ, ppm 7.35-7.21 (m, 15H, ArH), 6.98 (t, *J* = 7.9 Hz, 1H, ArH), 6.71, 6.70 (dd, *J* = 2.4, 6.0 Hz, 1H, ArH), 6.59 (d, *J* = 7.8Hz, 1H, ArH), 6.32-6.31 (m, 1H, ArH), 3.58 (t, *J* = 6.6 Hz, 2H, -OCH_2-), 1.53 (quin, *J* = 6.4 Hz, 2H, -$OCCH_2$-), 1.32-1.20 (m, 14H, -$(CH_2)_7$-), 0.857 (t, *J* = 6.7 Hz, 3H, -CH_3).

3-Decyloxybenzenethiol (4f). (Scheme 3-1)

Synthetic method was adopted that of Ref. 27. A three necked flask was charged with trifluoroacetic acid (3 mL), 1-decyloxy-3-triphenylmethylsulfanylbenzene (**3Af**: 0.598 g, 1.18 mmol), CH_2Cl_2 (1.1 mL) and Et_3SiH (0.487 g, 4.19 mmol). It was stirred at rt for 30 min. The reaction mixture was concentrated *in vacuo* and diluted with water and extracted with dichloromethane. The organic layer was washed with water three times and saturated brine once. The organic layer was collected and dried over Na_2SO_4 overnight. Na_2SO_4 was filtrated off and dichloromethane was evaporated *in vacuo*. Even by using any purification techniques, it was not possible to separate the target compound and the by-compound containing deprotection trityl group. Therefore, the synthesis of **4f** by Route A was abandoned. Next, synthesis of **4b**~**i** by Route B in Scheme 1 was carried out.

[*Route* (*b*)]

3-Ethoxyiodobenzene (2Bb). (Scheme 3-1)

A three necked flask dried was charged with K_2CO_3 (1.89 g, 13.7 mmol), 3-iodophenol (1.00 g, 4.55 mmol) and dry DMF (5 mL). Ethylbromide (0.595 g, 5.46 mmol) was then added to the reaction mixture and it was stirred at 90 °C. Proceeding of the reaction was monitored by TLC (SiO_2 / *n*-hexane). After 1 h, disappearance of the spot of 3-iodophenol (R_f = 0.0) was confirmed, so that the reaction was quenched with water and cooled to rt. The product was extracted with ethyl acetate and the organic layer was washed with water three times and saturated brine once. The organic layer was collected and dried over Na_2SO_4 overnight. Na_2SO_4 was filtrated off and the solvent was evaporated *in vacuo* to obtain yellowish liquid (1.06 g). Yield: 93.8%. The product was used for next reaction without further purification. ^{1}H-NMR (400 MHz, $CDCl_3$, TMS): δ, ppm 7.27-7.24 (m, 2H, ArH), 6.98 (t, J = 8.0 Hz, 1H, ArH), 6.86-6.84 (m, J = 2.4 Hz, 8.4 Hz, 1H, ArH), 4.00 (quart, J = 6.9 Hz, 2H, -OCH_2-), 1.40 (t, J = 7.0 Hz, 3H, -CH_3).

3-Hexyloxyiodobenzene (2Bd). (Scheme 3-1)

Yield: 91.6%. This synthesis was carried out as the same method of **2Bb**. The crude product was purification by silica gel column chromatography (*n*-hexane / R_f = 0.30) to obtain colorless liquid (1.29 g). ^{1}H-NMR (400 MHz, $CDCl_3$, TMS): δ, ppm 7.20-7.18 (m, 2H, ArH), 6.90 (t, J = 7.8 Hz, 1H, ArH), 6.79-6.77 (m, 1H, ArH), 3.84 (t, J = 6.6 Hz, 2H, -OCH_2-), 1.69 (quin, J = 7.0 Hz, 2H, -$OCCH_2$-), 1.41-1.22 (m, 6H, -$(CH_2)_3$-), 0.835 (t, J = 7.0 Hz, 3H, -CH_3).

^{1}H-NMR datum was in accordance with that of Ref. 28. Other homologues **2Bc**~**i** were synthesized by the same method for **2Bd**. Only the yield and 1H-NMR data were shown below. All compounds were obtained as liquid except for **2Bi**.

3-Butoxyiodobenzene (2Bc). (Scheme 3-1)

Yield: 42.7%. ^{1}H-NMR (400 MHz, $CDCl_3$, TMS): δ, ppm 7.27-7.25 (m, 2H, ArH), 6.98 (t, J = 8.0 Hz, 1H, ArH), 6.87-6.84 (m, 1H, ArH), 3.92 (t, J = 6.4 Hz, 2H, -OCH_2-), 1.75 (quin, J = 7.0 Hz, 2H, -$OCCH_2$-), 1.48 (sext, J = 7.4 Hz, 2H, -$OCCCH_2$-), 0.969 (t, J = 7.2 Hz, 3H, -CH_3).

3-Octyloxyiodobenzene (2Be). (Scheme 3-1)

Yield: 92.2%. ^{1}H-NMR (400 MHz, $CDCl_3$, TMS): δ, ppm 7.20-7.17 (m, 2H, ArH), 6.91 (t, J = 7.8 Hz, 1H, ArH), 6.79-6.77 (m, 1H, ArH), 3.84 (t, J = 6.6 Hz, 2H, -OCH_2-), 1.69 (quin, J = 7.2 Hz, 2H, -$OCCH_2$-), 1.40-1.20 (m, 10H, -$(CH_2)_5$-), 0.818 (t, J = 7.0 Hz, 3H, -CH_3). The ^{1}H-NMR datum was in accordance with that of Ref. 29.

3-Decyloxyiodobenzene (2Bf). (Scheme 3-1)

Yield: 93.9%. ^{1}H-NMR (400 MHz, $CDCl_3$, TMS): δ, ppm 7.30-7.27 (m, 2H, ArH), 7.04 (t, J = 8.2 Hz, 1H, ArH), 6.89-6.87 (m, 1H, ArH), 3.97 (t, J = 6.4Hz, 2H, -OCH_2-), 1.85 (quin, J = 6.6 Hz, 2H, -$OCCH_2$-), 1.50-1.30 (m, 14H, -$(CH_2)_7$-), 0.946 (t, J = 7.0 Hz, 3H, -CH_3).

3-Dodecyloxyiodobenzene (2Bg). (Scheme 3-1)

Yield: 85.2%. ^{1}H-NMR (400 MHz, $CDCl_3$, TMS): δ, ppm 7.26-7.24 (m, 2H, ArH), 6.97 (t, J = 7.8 Hz, 1H, ArH), 6.86-6.83 (m, 1H, ArH), 3.91 (t, J = 6.6 Hz, 2H, -OCH_2-), 1.75 (quin, J = 7.0 Hz, 2H, -$OCCH_2$-), 1.45-1.27 (m, 18H, -$(CH_2)_9$-), 0.881 (t, J = 7.0 Hz, 3H, -CH_3).

3-Tetradecyloxyiodobenzene (2Bh). (Scheme 3-1)

Yield: 84.1%. ^{1}H-NMR (400 MHz, $CDCl_3$, TMS): δ, ppm 7.27-7.24 (m, 2H, ArH), 6.97 (t, J = 8.0 Hz, 1H, ArH), 6.86-6.84 (m, 1H, ArH), 3.91 (t, J = 6.4 Hz, 2H, -OCH_2-), 1.75 (quin, J = 6.6 Hz, 2H, -$OCCH_2$-), 1.47-1.26 (m, 22H, -$(CH_2)_{11}$-), 0.88 (t, J = 7.0 Hz, 3H, -CH_3).

3-Hexadecyloxyiodobenzene (2Bi). (Scheme 3-1)

Yield: 83.3%. mp 32.4 ^{o}C. ^{1}H-NMR (400 MHz, $CDCl_3$, TMS): δ, ppm 7.27-7.23 (m, 2H, ArH)), 6.98 (t, J = 8.0 Hz, 1H, ArH), 6.86-6.83 (m,1H, ArH), 3.91 (t, J = 6.6 Hz, 2H, -OCH_2-), 1.76 (quin, J = 7.0 Hz, 2H, -$OCCH_2$-), 1.43 (quin, J = 7.3 Hz, 2H, -$OCCCH_2$-), 1.33-1.26 (m,24H, -CH_2-×12), 0.88 (t, J = 6.8 Hz, 3H,-CH_3).

3-Ethoxybenzenthiol (4b). (Scheme 3-1)

Synthetic method was adopted that of Ref. 30. A three necked flask dried was charged with K_2CO_3 (1.00 g, 7.26 mmol), powdered sulfur (0.358 g, 11.2 mmol), CuI (72.3 mg, 0.380 mmol), 3-ethoxyiodebenzene (**2Bb**) (0.897 g, 3.62 mmol) and dry DMF (4 mL). The reaction was carried out at

90 °C with stirring for 12 h. TLC (SiO_2 / *n*-hexane) confirmed disappearance of the spot of starting reagent of **2Bb** (R_f = 0.30) and appearance of the new spot (R_f = 0.0) were confirmed by TLC. The reaction mixture was cooled to rt and diluted with water. The product was extracted with ethyl acetate and the organic layer was washed with water three times and saturated brine once. The organic layer was collected and dried over Na_2SO_4 overnight. Na_2SO_4 was filtrated off and the solvent was evaporated *in vacuo* to obtain the crude product, which was used for next reaction without further purification. The three necked flask containing the crude product was charged with $NaBH_4$ (4.24 g, 112 mmol) and dry THF (10 mL) and it was stirred for 32 h. The reaction was quenched with slowly dropwise adding conc. HCl in an ice bath. The product was extracted with ethyl acetate and the organic layer was washed with water three times and saturated brine once. The organic layer was collected and dried over Na_2SO_4 overnight. Na_2SO_4 was filtrated off and the solvent was evaporated *in vacuo* to obtain colorless liquid (0.382 g). The product was used for next reaction without further purifications. Yield: 68.5%. ^{1}H-NMR (400 MHz, $CDCl_3$, TMS): δ, ppm 7.12 (t, *J* = 8.0 Hz, 1H, ArH), 6.84-6.81 (m, 2H, ArH), 6.68 (dd, *J*= 2.0 Hz, 6.0Hz, 1H, ArH), 4.00 (quart, *J* = 7.1 Hz, 2H, -OCH_2-), 3.44 (s, 1H, -SH), 1.39 (t, *J* = 7.0 Hz, 3H, -CH_3).

Other homologues **4c**~**i** were synthesized by the same method for **4b**. Only the yield and ^{1}H-NMR data were shown below. All compounds **4c**~**i** were obtained as liquid.

3-Butoxybenzenethiol (4c). (Scheme 3-1)

Yield: 77.9%. ^{1}H-NMR (400 MHz, $CDCl_3$, TMS): δ, ppm 7.12 (t, *J* = 8.0 Hz, 1H, ArH), 6.84-6.81 (m, 2H, ArH), 6.68 (dd, *J* = 3.2 Hz, 7.6 Hz, 1H, ArH), 3.93 (t, *J* = 6.4 Hz, 2H, -OCH_2-), 3.43 (s, 1H, -SH), 1.75 (quin, *J* = 7.0 Hz, 2H, -$OCCH_2$-), 1.48 (sext, *J* = 7.4 Hz, 2H, -$OCCCH_2$-), 0.969 (t, *J* = 7.4 Hz, 3H, -CH_3).

3-Hexyloxybenzenethiol (4d). (Scheme 3-1)

Yield: 65.9%. ^{1}H-NMR (400 MHz, $CDCl_3$, TMS): δ, ppm 7.05 (t, *J* = 7.8 Hz, 1H, ArH), 6.76-6.75 (m, 2H, ArH), 6.62-6.60 (m, 1H, ArH), 3.86 (t, *J* = 6.6Hz, 2H, -OCH_2-), 3.36 (s, 1H, -SH), 1.68 (quin, *J* = 7.1 Hz, 2H, -$OCCH_2$-), 1.41-1.27 (m, 6H, -$OCCCH_2$-), 0.832 (t, *J* = 6.8Hz, 3H, -CH_3).

3-Octyloxybenzenethiol (4e). (Scheme 3-1)

Yield: 91.6%. ^{1}H-NMR (400 MHz, $CDCl_3$, TMS): δ, ppm 7.05 (t, *J* = 8.0 Hz, 1H, ArH), 6.76-6.74 (m, 2H, ArH), 6.63-6.60 (m, 1H, ArH), 3.84 (t, *J* = 6.6 Hz, 2H, -OCH_2-), 3.36 (s, 1H, -SH), 1.69 (quin, *J* = 7.2 Hz, 2H, -$OCCH_2$-), 1.40-1.22 (m, 10H, CH_2×5), 0.816 (t, *J* = 7.0 Hz, 3H, -CH_3).

3-Decyloxybenzenethiol (4f). (Scheme 3-1)

Yield: 80.5%. ^{1}H-NMR (400 MHz, $CDCl_3$, TMS): δ, ppm 7.04 (t, *J* = 8.0 Hz, 1H, ArH), 6.79-6.73 (m, 2H, ArH), 6.63-6.59 (m, 1H, ArH), 3.84 (t, *J* = 6.6 Hz, 2H, -OCH_2-), 3.36 (s, 1H, -SH), 1.75 (quin, *J* = 7.0 Hz, 2H, -$OCCH_2$-), 1.41-1.20 (m, 14H, CH_2×7), 0.811 (t, *J* = 6.8 Hz, 3H, -CH_3).

3-Dodecyloxybenzenethiol (4g). (Scheme 3-1)

Yield: 62.3%. ^{1}H-NMR (400 MHz, $CDCl_3$, TMS): δ, ppm 7.12 (t, *J* = 8.2 Hz, 1H, ArH), 6.84-6.81 (m, 2H, ArH), 6.70-6.67 (m, 1H, ArH), 3.91 (t, *J* = 6.6 Hz, 2H, -OCH_2-), 3.43 (s, 1H, -SH), 1.76 (quin, *J* = 7.0 Hz, 2H, -$OCCH_2$-), 1.45-1.27 (m, 18H, CH_2×9), 0.881 (t, *J* = 7.0 Hz, 3H, -CH_3).

3-Tetradecyloxybenzenethiol (4h). (Scheme 3-1)

Yield: 92.7%. ^{1}H-NMR (400 MHz, $CDCl_3$, TMS): δ, ppm 7.12 (t, *J* = 7.8 Hz, 1H, ArH), 6.84-6.81 (m, 2H, ArH), 6.70-6.67 (m, 1H, ArH), 3.92 (t, *J* = 6.6 Hz, 2H, -OCH_2-), 3.43 (s, 1H, -SH), 1.76 (quin, *J* = 7.0 Hz, 2H, -$OCCH_2$-), 1.47-1.26 (m, 22H, CH_2×11), 0.88 (t, *J* = 6.8 Hz, 3H, -CH_3).

3-Hexadecyloxybenzenethiol (4i). (Scheme 3-1)

Yield: 51.8%. ^{1}H-NMR (400 MHz, $CDCl_3$, TMS): δ, ppm 7.12 (t, *J* = 8.2 Hz, 1H, ArH), 6.84-6.81 (m, 2H, ArH), 6.69, 6.68 (dd, *J* = 2.0 Hz, 6.0 Hz, 1H, ArH), 3.92 (t, *J* = 6.6 Hz, 2H, -OCH_2-), 3.44 (s, 1H, -SH), 1.76 (quin, *J* = 7.0 Hz, 2H, -$OCCH_2$-), 1.47-1.26 (m, 26H, -$(CH_2)_{13}$-), 0.88 (t, *J* = 6.4 Hz, 3H, -CH_3).

[*Route (c)*]

Derivative **4i** was also synthesized by another method of Refs. 31 and 32.

Bis(3-hydroxyphenyl)disulfide (2C). (Scheme 3-1)

In a three neck flask 3-hydroxybenezenthiol (0.247 g, 1.96 mmol) was dissolved in 10 mL of DMSO-$CHCl_3$ mixed solvent (1:1, v/v). To the reaction mixture, 47wt% HBr aq. sol. (72.9 mg, 0.423 mmol) was added and it was stirred at rt for 12.5 h. When TLC (SiO_2/$CHCl_3$) confirmed disappearance of the spot of starting reagent of 3-hydroxybenzenethiol (R_f = 0.10) and appearance of a new spot of target compound **2C** (R_f = 0. 0), the reaction was terminated. The solvents were evaporated *in vacuo* to concentrate the reaction mixture. The product was extracted with ethyl acetate and washed with water three times and saturated brine once. The organic layer was collected and dried over Na_2SO_4 overnight. Na_2SO_4 was filtrated off and the solvent was evaporated *in vacuo*. The residue was dried *in* vacuo to obtain the target compound **2C** as white powder (0.242 g). Yield: 98.5%. mp 80-90 °C (broad).

^{1}H-NMR (400 MHz, d_6-DMSO, TMS): δ, ppm 9.75 (s, 2H, -OH), 7.17 (t, *J* = 8.0 Hz, 2H, ArH), 6.93-6.90 (m, 4H, ArH), 6.68-6.60 (m, 2H, ArH).

Bis(3-hexadecyloxypheny)disulfide (3Ci). (Scheme 3-1)

A three necked flask was charged with bis(3-hydroxyphenyl)disulfide (**2C**) (0.263 g, 1.05 mmol), K_2CO_3 (0.744 g, 5.38 mmol) and dry DMF (4 mL). 1-Bromohexadecane (0.808 g, 2.64 mmol) was then added to the reaction mixture and it was stirred at 90 ^oC for 3.5 h. The reaction was terminated when TLC (SiO_2/CH_2Cl_2) confirmed disappearance of both the spots of starting reagent of **2C** (R_f = 0.0) and monoalkylated compound (R_f = 0.55), and appearance of only one spot of dialkylated compound (SiO_2/CH_2Cl_2, R_f= 0.95). The reaction mixture was diluted with water and the product was extracted with dichloromethane. The organic layer was washed with water three times and saturated brine once. The organic layer was collected and dried over Na_2SO_4 overnight. Na_2SO_4 was filtrated off and the solvent was evaporated *in vacuo*. The crude product was recrystallized from acetone and then *n*-hexane at 25 ^oC to obtain white powder (0.330 g). Yield: 44.9% mp: 62.5 ^oC (mp1), 64.8 ^oC (mp2). (This compound showed double melting behavior.). ^{1}H-NMR (400 MHz, $CDCl_3$, TMS): δ, ppm 7.18(t, *J* = 8.2 Hz, ArH, 2H), 7.06-7.04(m, ArH, 4H), 6.75, 6.74(dd, *J* = 2.2 Hz, 6.6 Hz, ArH, 2H), 3.90(t, *J* = 6.6 Hz, -(OCH_2)-×2, 4H), 1.74(quin, *J* = 7.1 Hz, -($OCCH_2$)-×2, 4H), 1.45-1.26(m, -(CH_2)-×26, 52H), 0.879(t, *J* = 6.8 Hz, -CH_3×2, 6H).

3-Hexadecyloxybenzenthiol (4i). (Scheme 3-1)

Compound **4i** was synthesized from Compound **3Ci** according to the method of Ref. 32. A three necked flask was charged with bis(3-hexadecyloxypheny)disulfide (**3Ci**: 0.324 g, 0.464 mmol), PPh_3 (0.299 g, 1.14 mmol) and THF (12 mL) and then conc. HCl aq. sol. (0.4 mL) and H_2O (2mL). It was gently refluxed with stirring for 5 h. After cooled to r.t, large excessive amounts of iodomethane was added to the reaction mixture and stirred at r.t for 9 h. The reaction mixture was diluted with water and extracted with toluene. The organic layer was washed with water three times and saturated brine once. The organic layer was collected and dried over Na_2SO_4 overnight. Na_2SO_4 was filtrated off and the solvent was concentrated *in vacuo*. *n*-Hexane was added to the solution until precipitation was occurred. It was heated until the precipitates were completely dissolved and then cooled to r.t. The resulted precipitates were removed by filtration. To the filtrate *n*-hexane was furthermore added to occur precipitation completely. The precipitates were removed again by filtration, and then the filtrate was evaporated *in vacuo* to remove the solvent to afford colorless oil (0.151 g).

Yield: 46.5%. ^{1}H-NMR (400 MHz, $CDCl_3$, TMS): δ, ppm 7.12 (t, *J* = 8.2 Hz, 1H, ArH), 6.84-6.81 (m, 2H, ArH), 6.69, 6.68 (dd, *J* = 2.0 Hz, 6.0 Hz, 1H, ArH), 3.92 (t, *J* = 6.6 Hz, 2H, -OCH_2-), 3.44 (s, 1H, -SH), 1.76 (quin, *J* = 7.0 Hz, 2H, -$OCCH_2$-), 1.47-1.26 (m, 26H, -$(CH_2)_{13}$-), 0.88 (t, *J* = 6.4 Hz, 3H, -CH_3).

4,5-Bis(*m*-ethoxyphenylthio)phthalonitrile (5b). (Scheme 3-2)

Synthetic method was adopted that of [33]. A three necked flask was charged with K_2CO_3 (0.653 g, 4.73 mmol), 3-ethoxybenzenethiol (**3a**) (0.234 g, 1.52 mmol) and DMF (5mL) and it was heated up to 90 °C. To the reaction mixture, 4, 5-dichlorophthalonitrile (0.102 g, 0.517 mmol) was added and stirred at 90 °C for 7 h with occasionally monitoring by TLC. When the reaction was completed, it was quenched with water. The product was extracted with ethyl acetate and the organic layer was washed with water three times and saturated brine once. The organic layer was collected and dried over Na_2SO_4 overnight. Na_2SO_4 was filtrated off and the solvent was evaporated *in vacuo*. The crude product was purified by column chromatography (SiO_2, CH_2Cl_2, R_f = 0.50) to obtain white crystals (0.112 g). Yield: 50.2%. mp: 139.8 °C. ^{1}H-NMR (400 MHz, $CDCl_3$, TMS): δ, ppm 7.41 (t, J = 8.2 Hz, 2H, ArH), 7.12-7.03 (m, 8H, ArH), 4.07 (quart, J = 7.1 Hz, 4H, -OCH_2-), 1.45 (t, J = 7.0 Hz, 6H, -CH_3).

Other homologues **5c**~**i** were synthesized by the same method for **5b**. The eluents for the column chromatography, yields, melting points and ^{1}H-NMR data were described below for these homologues.

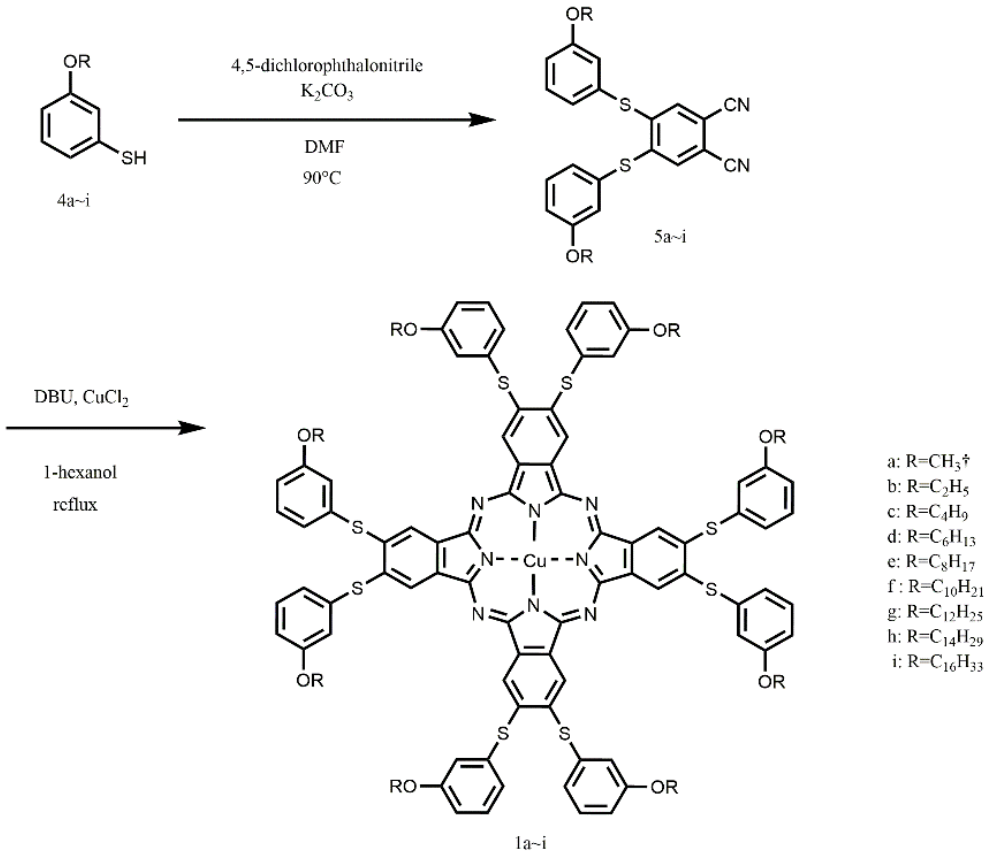

Scheme 3-2. Synthetic route for (*m*-C$_n$OPhS)$_8$PcCu (**1a**~**1i**). **1a**: previous work Ref. 20.

4,5-Bis(*m*-butoxyphenylthio)phthalonitrile (5c). (Scheme 3-2)

SiO_2, CH_2Cl_2: *n*-hexane = 4:1, R_f = 0.30. Yield: 68.9%. mp: 96.1 °C. ^{1}H-NMR (400 MHz, $CDCl_3$, TMS): δ, ppm 7.41 (t, *J* = 7.4 Hz, 2H, ArH), 7.11-7.04 (m, 8H, ArH), 3.99 (t, *J* = 6.6 Hz, 4H, -OCH_2-), 1.80 (quin, *J* = 7.0 Hz, 4H, -$OCCH_2$-), 1.51 (sext, *J* = 7.5 Hz, 4H, -$OCCCH_2$-), 0.993 (t, *J* = 7.4 Hz, 6H, -CH_3).

4,5-Bis(*m*-hexyloxyphenylthio)phthalonitrile (5d). (Scheme 3-2)

SiO_2, CH_2Cl_2: *n*-hexane = 4:1, R_f = 0.48. Yield: 86.0%. mp: 64.1 °C. ^{1}H-NMR (400 MHz, $CDCl_3$, TMS): δ, ppm 7.41 (t, *J* = 7.9 Hz, 2H, ArH), 7.11-7.03 (m, 8H, ArH), 3.98 (t, *J* = 6.4 Hz, 4H, -OCH_2-), 1.81 (quin, *J* = 7.0 Hz, 4H, -$OCCH_2$-), 1.49-1.33 (m, 12H, (-CH_2-)$_3$×2), 0.914 (t, *J* = 7.0 Hz, 6H, -CH_3).

4,5-Bis(*m*-octyloxyphenylthio)phthalonitrile (5e). (Scheme 3-2)

SiO_2, CH_2Cl_2: *n*-hexane = 4:1, R_f = 0.58. Yield: 95.1%. mp: 72.1 °C. ^{1}H-NMR (400 MHz, $CDCl_3$, TMS): δ, ppm 7.41 (t, *J* = 8.0 Hz, 2H, ArH), 7.11-7.03 (m, 8H, ArH), 3.98 (t, *J* = 6.6 Hz, 4H, -OCH_2-), 1.81 (quin, *J* = 7.1 Hz, 4H, -$OCCH_2$-), 1.49-1.24 (m, 20H, (-CH_2-)$_5$×2), 0.889 (t, *J* = 6.8 Hz, 6H, -CH_3).

4,5-Bis(*m*-decyloxyphenylthio)phthalonitrile (5f). (Scheme 3-2)

SiO_2, CH_2Cl_2, R_f = 0.80. Yield: 78.1%. mp: 76.5 °C. ^{1}H-NMR (400 MHz, $CDCl_3$, TMS): δ, ppm 7.43 (t, *J* = 7.6 Hz, 2H, ArH), 7.13-7.08 (m, 8H, ArH), 4.00 (t, *J* = 6.6 Hz, 4H, -OCH_2-), 1.83 (quin, *J* = 7.4 Hz, 4H, -$OCCH_2$-), 1.53-1.31 (m, 28H, (-CH_2-)$_7$×2), 0.904 (t, *J* = 6.6 Hz, 6H, -CH_3).

4,5-Bis(*m*-dodecyloxyphenylthio)phthalonitrile (5g). (Scheme 3-2)

SiO_2, CH_2Cl_2: *n*-hexane = 4:1, R_f = 0.58. Yield: 29.3%. mp: 76.2 °C. ^{1}H-NMR (400 MHz, $CDCl_3$, TMS): δ, ppm 7.41 (t, *J* = 8.2 Hz, 2H, ArH), 7.11-7.03 (m, 8H, ArH), 3.98 (t, *J* = 6.6 Hz, 4H, -OCH_2-), 1.81 (quin, *J* = 7.1 Hz, 4H, -$OCCH_2$-), 1.50-1.21 (m, 36H, (-CH_2-)$_9$×2), 0.88 (t, *J* = 6.8 Hz, 6H, -CH_3).

4,5-Bis(*m*-tetradecyloxyphenylthio)phthalonitrile (5h). (Scheme 3-2)

SiO_2, CH_2Cl_2: *n*-hexane = 4:1, R_f = 0.38. Yield: 75.0%. mp: 50.0 °C(mp1), 83.3 °C(mp2) (This compound showed double melting behavior). ^{1}H-NMR (400 MHz, $CDCl_3$, TMS): δ, ppm 7.41 (t, *J* = 7.8 Hz, 2H, ArH), 7.11-7.04 (m, 8H, ArH), 3.98 (t, *J* = 6.4 Hz, 4H, -OCH_2-), 1.81 (quin, *J* = 7.0 Hz, 4H, -$OCCH_2$-), 1.49-1.26 (m, 44H, (-CH_2-)$_{11}$×2), 0.879 (t, *J* = 6.8 Hz, 6H, -CH_3).

4,5-Bis(*m*-hexadecyloxyphenylthio)phthalonitrile (5i). (Scheme 3-2)

SiO_2, CH_2Cl_2: *n*-hexane = 5:2, R_f = 0.70. Yield: 73.9%. mp: 58.3 °C(mp1), 70.2 °C(mp2) (This compound showed double melting behavior.). ^{1}H-NMR (400 MHz, $CDCl_3$, TMS): δ, ppm 7.41 (t, *J* = 8.2 Hz, 2H, ArH), 7.11-7.03 (m, 8H, ArH), 3.98 (t, *J* = 6.4 Hz, 4H, -OCH_2-), 1.81 (quin, *J* = 7.0 Hz, -$OCCH_2$-), 1.47 (quin, *J* = 7.2 Hz, -$OCCCH_2$-), 1.38-1.26 (m, 48H, -$(CH_2)_{12}$-,), 0.878 (t, *J* = 6.8 Hz, 6H, -CH_3).

Octakis(*m*-ethoxyphenylthio)phthalocyaninato copper(II) (1b). (Scheme 3-2)

A three necked flask was charged with anhydrous $CuCl_2$ (15.5 mg, 0.115 mmol), 4,5-bis(3-ethoxyphenylthio)phthalonitrile (94.1 mg, 0.218mmol) and 1-hexanol (5mL). To the reaction mixture 5 drops of DBU was added and refluxed for 1.5 h. It was cooled to rt and poured into methanol to precipitate. The precipitates were collected by filtration and washed with methanol, ethanol and ethyl acetate successively. The precipitates were purified by Soxhlet extraction (toluene) two times. The obtained toluene solution was concentrated *in vacuo* and the residue was reprecipitated from acetone to obtain green solid (43.1 mg).

The homologues **1c**, **1h** and **1i** were also synthesised and purified by the same procedure for **1b**.

Octakis(*m*-ethoxyphenylthio)phthalocyaninato copper(II) (1d). (Scheme 3-2)

A three necked flask was charged with anhydrous $CuCl_2$ (9.2 mg, 0.068 mmol), 4,5-bis(3-hexyloxyphenylthio)phthalonitrile (**5d**: 48.2 mg, 0.0885mmol) and 1-hexanol (5mL). To the reaction mixture 5 drops of DBU was added and it was refluxed with stirring for 1.5 h. It was cooled to rt and poured into methanol to precipitate. The precipitates were collected by filtration and washed with methanol, ethanol and ethyl acetate successively. The residue was dissolved in chloroform and the solution was concentrated *in vacuo*. Subsequently, the crude product was purified by column chromatography (SiO_2, $CHCl_3$, R_f = 1.0) to obtain green solid (27.6 mg).

The homologues **1e~g** were also synthesized and purified by the same procedure for **1d**. Table 1 lists the yields, MALDI-TOF-MASS and elemental analysis data of all the homologues **1b~i**. The UV-vis spectral data were summarized in Table 2.

Decomposition temperatures of 1b~1i

Decomposition temperatures (T_d) obtained from TGA are listed below.

1b. T_d > 400 °C, **1c**. T_d = 389 °C, **1d**. T_d = 397 °C, **1e**. T_d = 359 °C, **1f**. T_d = 386 °C, **1g**. T_d = 399 °C, **1h**. T_d = 371 °C, **1i**. T_d = 360 °C.

Table 3-1. Yields and elemental analysis data of (*m*-C$_n$OPhS)$_8$PcCu (**1a**~**1i**).

Compound	Mol. formula (Mol. wt)	Exact Mass	Mass observed	Elemental analysis: Found(Calcd.)(%)			Yield(%)
				C	H	N	
1b : (*m*-C$_2$OPhS)$_8$PcCu	$C_{96}H_{80}N_8O_8S_8Cu$ (1793.77)	1791.32	1791.32	64.60 (64.28)	4.91 (4.50)	5.92 (6.25)	44.1
1c : (*m*-C$_4$OPhS)$_8$PcCu	$C_{112}H_{112}N_8O_8S_8Cu$ (2018.21)	2015.58	2015.50	66.30 (66.65)	5.74 (5.59)	5.47 (5.55)	65.9
1d : (*m*-C$_6$OPhS)$_8$PcCu	$C_{128}H_{144}N_8O_8S_8Cu$ (2242.64)	2239.83	2239.80	68.69 (68.55)	6.57 (6.47)	5.05 (5.00)	55.7
1e : (*m*-C$_8$OPhS)$_8$PcCu	$C_{144}H_{176}N_8O_8S_8Cu$ (2467.06)	2467.06	2464.14	69.97 (70.11)	7.31 (7.19)	4.81 (4.54)	60.4
1f : (*m*-C$_{10}$OPhS)$_8$PcCu	$C_{160}H_{208}N_8O_8S_8Cu$ (2691.49)	2688.33	2688.31	71.76 (71.40)	8.10 (7.79)	4.22 (4.16)	65.6
1g : (*m*-C$_{12}$OPhS)$_8$PcCu	$C_{176}H_{240}N_8O_8S_8Cu$ (2915.91)	2912.58	2913.61	72.47 (72.49)	8.53 (8.30)	3.59 (3.84)	68.1
1h : (*m*-C$_{14}$OPhS)$_8$PcCu	$C_{192}H_{272}N_8O_8S_8Cu$ (3140.34)	3136.83	3138.02	73.34 (73.43)	8.92 (8.73)	3.55 (3.57)	47.4
1i : (*m*-C$_{16}$OPhS)$_8$PcCu	$C_{208}H_{304}N_8O_8S_8Cu$ (3364.79)	3361.07	3362.24	74.07 (74.25)	9.42 (9.11)	3.23 (3.33)	66.1

Table 3-2. UV-vis spectral data in $CHCl_3$ solution of (*m*-C$_n$OPhS)$_8$PcCu (**1b~1i).**

Compound	Concentration ($X10^{-6}$mol L^{-1})	λ / nm (loge)		
		Soret band	Q-band	
			$Q_{0\text{-}1}$-band	$Q_{0\text{-}0}$-band
1b : (*m*-C$_2$OPhS)$_8$PcCu	2.32	344.0(4.91)	642.0(4.68)	718.0(5.42)
1c : (*m*-C$_4$OPhS)$_8$PcCu	2.39	344.0(4.92)	642.0(4.69)	716.0(5.42)
1d : (*m*-C$_6$OPhS)$_8$PcCu	2.26	344.0(4.93)	642.0(4.69)	718.0(5.43)
1e : (*m*-C$_8$OPhS)$_8$PcCu	2.26	344.0(4.93)	642.0(4.70)	718.0(5.44)
1f : (*m*-C$_{10}$OPhS)$_8$PcCu	2.29	345.5(4.90)	643.0(4.65)	718.9(5.42)
1g: (*m*-C$_{12}$OPhS)$_8$PcCu	2.42	342.0(4.88)	642.0(4.66)	718.0(5.40)
1h: (*m*-C$_{14}$OPhS)$_8$PcCu	2.34	344.0(4.88)	642.0(4.65)	718.0(5.38)
1i: (*m*-C$_{16}$OPhS)$_8$PcCu	2.37	344.0(4.89)	6420(4.65)	718.0(5.38)

3.3. Results and discussion

3.3.1. Synthesis

Phenylthio substituted phthalocyanine derivatives $(PhS)_8PcM$ (M = H_2, metal) reported up to date were prepared from commercially available benzenthiol derivatives as the starting reagents [10-20]. However, each of these benzenethiol derivatives doesn't have long alkyl chains. Therefore, at first we have developed the synthetic route for the long alkoxy chain-substituted benzenethiols **4b~i** in this study. Although many synthetic methods for benzenethiol derivatives have been reported so far [34-39], we have tried in this study the following three relatively simple methods (Routes A, B and C in Scheme 3-1) for the long alkoxy chain-substituted benzenethiol precursors **4b-i**.

Route A in Scheme 3-1 was followed those of Refs. 26 and 27. The starting material, 3-hydroxybenzenethiol, was commercially available. The thiol group in 3-hydroxybenzenethiol was protected with trityl group to obtain derivative **2A**. Subsequently, the OH group in the phenol derivative **2A** was substituted by an alkoxy group using Williamson reaction to obtain derivative **3Af**. The trityl group in **3Af** was deprotected by triethylsilane in acidic condition. Although the reaction proceeded, it was not possible to separate the target compound **4f** and the by-product containing trityl group. It is attributable to the nonpolarity of both the target compound and the by-product having non-polar decyl groups. If they would have big difference of the polarities, they could separate them like as the derivatives reported in Refs. 26 and 27.

Route B in Scheme 3-1 was followed that of Ref. 30. Firstly, the OH group in 3-iodophenol was substituted by long alkoxy group using Williamson reaction to obtain derivatives **2Bb~i**. Subsequently, these iodobenzene derivatives **2Bb~i** were successfully converted into benzenethiol derivatives **4b~i** in good yields (average total yield: 62.8%).

Derivative **4i** was also successfully synthesized by using another method [31] (Route C in Scheme 3-1). Firstly, commercially available 3-hydroxybenzenethiol was converted into corresponding disulfide derivative **2C** in the presence of HBr aq. sol. and DMSO. Subsequently, the OH groups in this disulfide derivative **2C** were substituted by long alkoxy groups using Williamson reaction to obtain disulfide derivative **3Ci**. Following the method of Ref. 32, derivative **3Ci** was converted into corresponding benzenethiol derivative **4i**. This method also successfully provided the key benzenethiol derivative **4i** in moderate yield (total yield: 20.1%).

Thus, the methods of Routes B and C in Scheme 3-1 successfully provided the long alkoxy-substituted benzenethiol derivatives **4b~i**.

As shown in Scheme 3-2, the synthetic method of target phthalocyanine derivatives (m-C_nOPhS)$_8$PcCu (**1a~i**) was followed the method of Ref. 33. Firstly, each of the long alkoxy-substituted benzenethiol derivatives **4a~i** was reacted with 4,5-dichlorophthalonitrile to obtain the phthalonitrile derivatives **5a~i**. These phenylthio-substituted phthalonitriles **5a~i** were tetracyclised to afford the target phenylthio-substituted phthalocyanines, (m-C_nOPhS)$_8$PcCu (**1a~i**), in relatively good yields

(average yield: 59%). Each of the phthalocyanines could be satisfactorily identified by the MALDI-TOF MASS, elemental analysis and UV-vis spectrum (Tables 3-1 and 3-2).

Table 3-3. Phase transition temperatures and enthalpy changes of **1b**~**1i**.

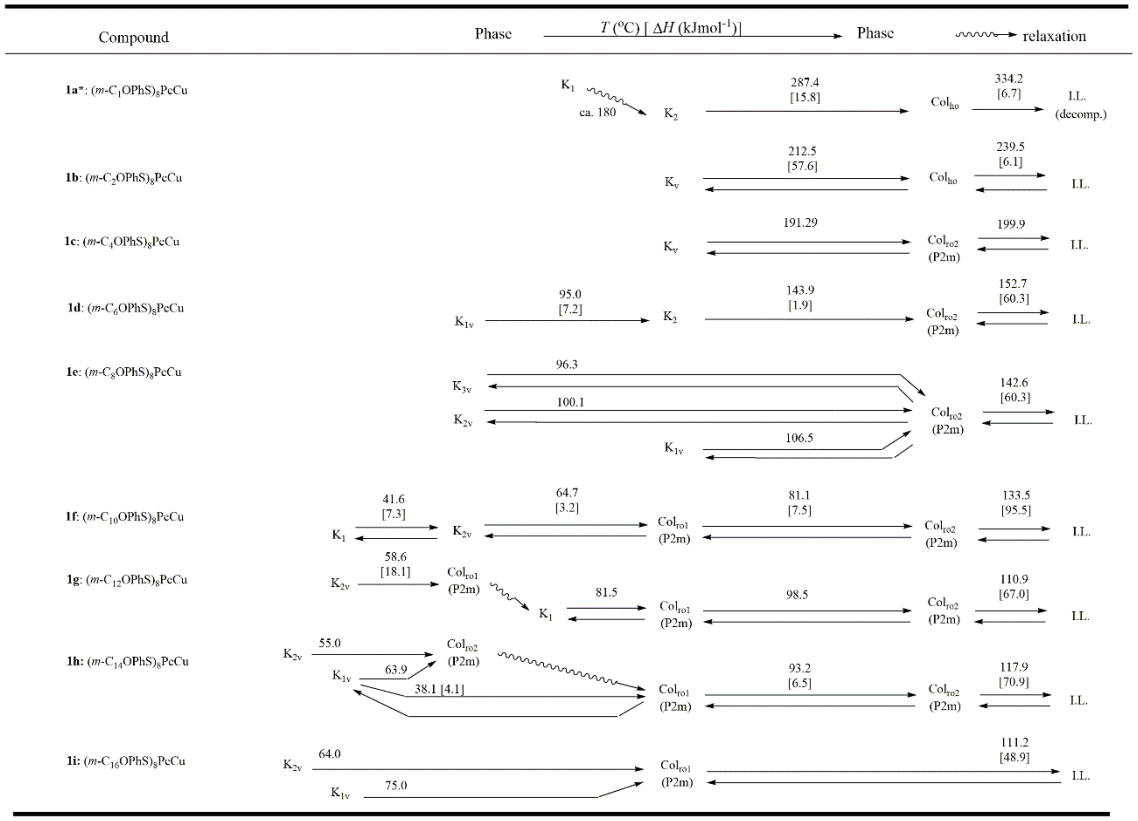

Phase nomenclature : K= crystal, Col_{ro} = rectangular ordered columnar, I.I. = isotropic liquid and v = virgin state.
Col_{ro1}~Col_{ro2} : See Figure 2. * Ref [20]

3.3.2. Phase transition behavior

Table 3-3 summarizes phase transition behavior of all the phenylthio-substituted PcCu complexes: the shortest-alkoxy-substituted derivative (*m*-C_1OPhS)$_8$PcCu (**1a**) synthesized in our previous work, and the other longer-alkoxy-substituted derivatives, (*m*-C_nOPhS)$_8$PcCu (*n* = 2~16; **1b**~**i**), synthesized in this work.

In Figure 3-2, the phase transition temperatures of all the derivatives (*m*-C_nOPhS)$_8$PcCu (*n* = 1~16: **1a**~**i**) were plotted against the alkyl chain length (n). As can see this figure, each of the lines for the clearing points (○), the highest melting points (●), and the liquid crystal - liquid crystal transition points (▲) is very smoothly connected. However, there is only a gap between *n*=2 and 4 for the melting points. It may correspond to the difference of mesomorphism driving forces between the hexagonal ordered columnar (Col_{ho}) phases for **1a**-**b** (*n* = 1, 2) and the rectangular ordered columnar (Col_{ro} (P2m)) phases for **1c**~**i** (*n* = 4~16). Furthermore, each of the derivatives **1f**~**i** (*n* = 10~16) shows two rectangular ordered columnar phases of Col_{ro1} (P2m) and Col_{ro2} (P2m).

Interestingly, the Col_{ho} phases appear only for the extremely short alkoxy-substituted derivatives **1a-b** (*n* = 1, 2), so that these discogens can be considered as flying-seed-like liquid crystals induced by thermal fluctuation of the bulky peripheral substituents [20-25]. On the other hand, the Col_{ro} (P2m) phase(s) appear only for the longer alkoxy- substituted derivatives **1c~i** (*n* = 4~16), so that these discogens can be considered as conventional liquid crystals induced by melting of the peripheral long alkoxy chains. To the best of our knowledge, this is the first example changing from flying-seed-like liquid crystals to long alkyl chain type of liquid crystals in a series of liquid crystalline homologues.

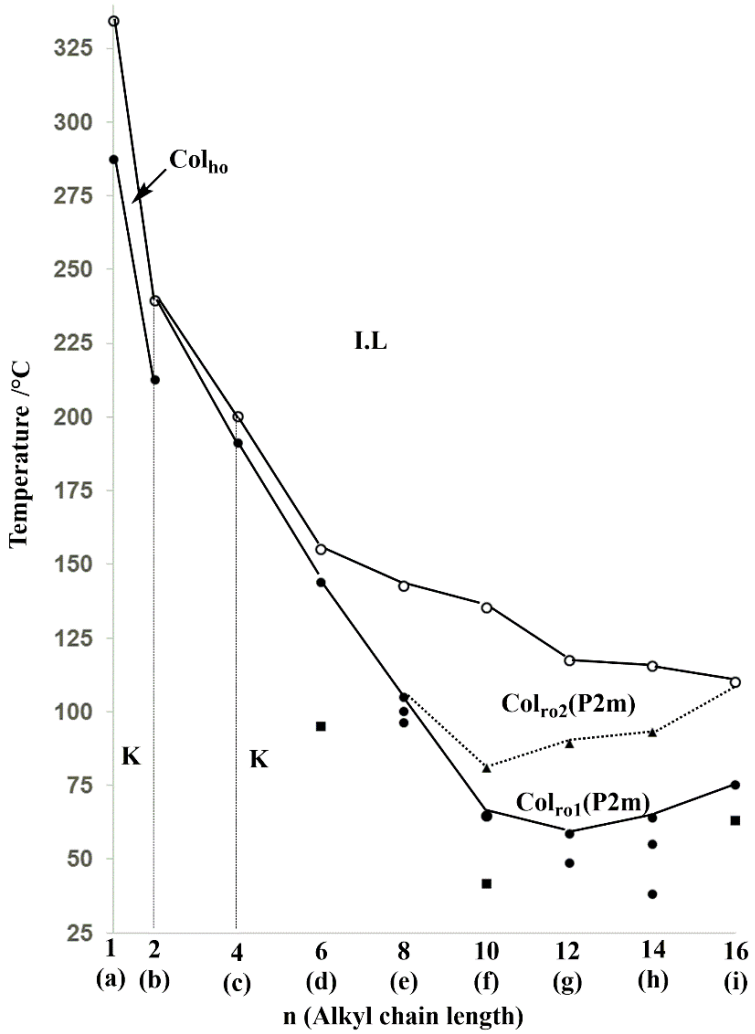

Figure 3-2. Phase transition temperature vs. the number of carbon atom in the alkoxy chains for (*m*-C_nOPhS)$_8$PcCu (**1a-1i**). ○: clearing point, ●: melting point, ▲: mesophase-mesophase transition.

3.3.3. Polarizing optical microscopic observation

Figure 3-3 shows the polarizing optical photomicrographs of liquid crystalline phases in the representative derivatives, **1b** (n = 2), **1f** (n = 10) and **1i** (n = 16). Both (a) and (b) are the photomicrographs of the liquid crystalline phase in the shortest alkoxy-substituted derivative (m-C_2OPhS)$_8$PcCu (**1b**) at 220 °C. As can see from these photos, photo (a) shows a focal conic texture typical of liquid crystalline phases and photo (b) shows a dendritic texture typical of a hexagonal columnar (Col_h) phase. Therefore, this liquid crystalline phase of **1b** could be identified as a Col_h phase. Photo (c) is a Col_{ro2} (P2m) phase in the moderately long alkyl-substituted derivative (m-C_{10}OPhS)$_8$PcCu (**1f**) at 115 °C. Both (d) and (e) are a Col_{ro1} (P2m) phase in the same derivative **1f** at 90 °C. As can see from these photos, both $Col_{ro1, 2}$ phases did not give any typical textures of mesophases. However, when the phase in photo (d) was pressed and sheared, it showed both stickiness and birefringence as shown in photo (e). Therefore, the Col_{ro1} (P2m) phase in **1f** could be identified as a liquid crystalline phase. Photo (f) shows a Col_{ro1} (P2m) phase in the longest alkoxy-substituted derivative (m-C_{16}OPhS)$_8$PcCu (**1i**) at 100 °C. This photo exhibits a focal conic texture typical of liquid crystalline phases. In addition, when this sample was pressed and sheared, it showed both stickiness and birefringence as shown in photo (g). Therefore, this phase could be also identified as a liquid crystalline phase.

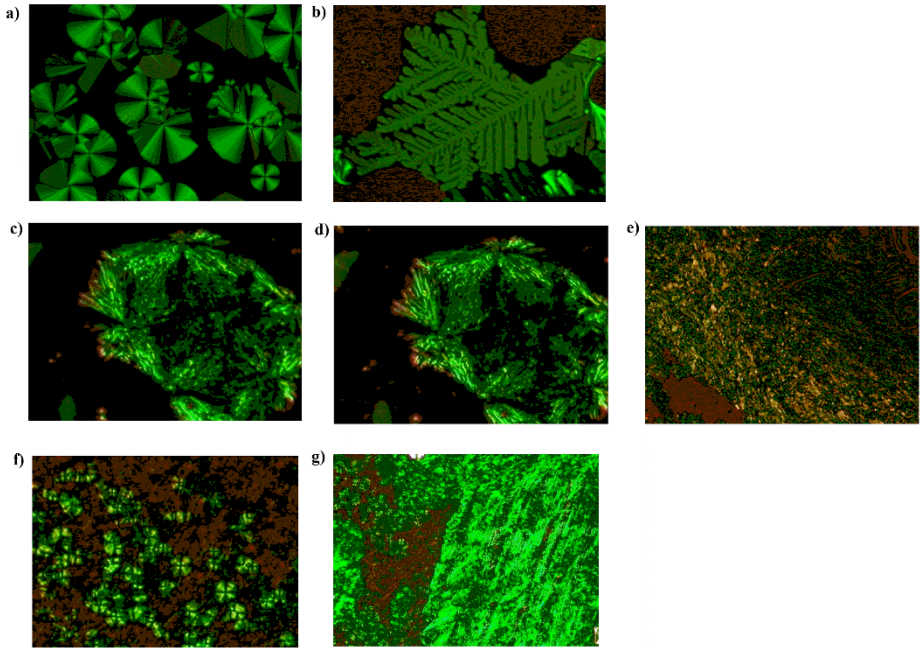

Figure 3-3. Photomicrographs of (a) and (b): Col_{ho} of (m-C_2OPhS)$_8$PcCu (**1b**) at 220 °C; (c) Col_{ro2} (P2m) of (m-C_{10}OPhS)$_8$PcCu (**1f**) at 115 °C; (d) Col_{ro1} (P2m) of (m-C_{10}OPhS)$_8$Pc-Cu (**1f**) at 90 °C; (e) sheared sample of the photo (d) of **1f** at 90 °C; (f) Col_{ro1} (P2m) of (m-C_{16}OPhS)$_8$PcCu (**1i**) at 100 °C; (g) sheared sample oh the photo (f) of **1i** at 100 °C.

3.3.4. Temperature-dependent small angle X-ray diffraction (TD-SAXS) measurements

Table 3-4 summarizes temperature-dependent small angle X-ray diffraction (TD-SAXS) data of the liquid crystalline phases in (*m*-C_nOPhS)$_8$PcCu (**1a~i**). Figures 3-4, 3-5 and 3-6 show the representative SAXS patterns of (*m*-C_2OPhS)$_8$PcCu (**1b**), (*m*-C_{10}OPhS)$_8$PcCu (**1f**) and (*m*-C_{16}OPhS)$_8$PcCu (**1i**), respectively. In these figures, the enlarged diffractgrams are shown as the insets. These SAXS patterns were measured for the samples obtained by cooling from isotropic liquid.

The SAXS pattern of (*m*-C_2OPhS)$_8$PcCu (**1b**) at 220 °C is shown in Figure 3-4. As can see from this figure, a very broad halo (#1) due to thermal fluctuation of phenylthio groups was observed in 2θ = 13~23°. This broad halo #1 was also observed for the previous flying-seed-like liquid crystalline derivative, (*m*-C_1OPhS)$_8$PcCu (**1a**) [20]. The *d*-spacings in the low angle region are in a ratio of 1: 1/√3: 1/√7: 1/3, which is typical of a Col_h phase. Therefore, the mesophase could be identified as a Col_h phase. This identification is consistent with the dendritic texture typical of a Col_h mesophase mentioned above. In addition, two peaks at around 2θ = 6° and 13° could be assigned to the interdimer stacking d_{001} (2h = 14.3 Å) and the intermonomer stacking d_{001} (h = 7.12 Å), respectively. This means that an equilibrium between the dimers and monomers exists in the Col_{ho} mesophase as the same case as the [*m*,*p*-(C_nO)$_2$PhO]$_8$PcCu derivatives reported in 2001 [7]. From the Z value calculation [40], the Z value of this Col_{ho} mesophase in **1b** could be obtained as Z = 1.0 assuming the intermonomer stacking distance as h = 7.12 Å and the density of the mesophase as ρ = 1.0 g/cm^3. Although the intracolumnar stacking distance h (7.12 Å) is much larger than that of conventional Col_{ho} phases. However, the value Z = 1.0 is consistent with the theoretical value (Z = 1.0) for a Col_{ho} mesophase. Moreover, the large stacking distance h = 7.12 Å is comparable as that of flying-seed-like liquid crystals reported in our previous works [20, 24]. Thus, the present derivative **1b** could be classified as a flying-seed-like liquid crystal similar to the previously reported derivative **1a**. In our previous work, this liquid crystalline phase of **1a** was identified as a Col_{ro} (P2m) phase [20]. However, the d spacings of **1a** are also in a ratio of 1: 1/√3: 1/√7: 1/3 as the same as that of **1b**. From the Z value calculation, the result (Z = 0.95 ≒ 1.0) is consistent with a Col_{ho} phase. Moreover, the equilibrium between the dimers and monomers in the Col_{ho} mesophase could be also observed as the same case as the (*m*-C_2OPhS)$_8$PcCu (**1b**) homologue. Therefore, the liquid crystalline phase of **1a** could be also identified as Col_{ho} phase, so that we correct the identification of this mesophase from Col_{ro} (P2m) to Col_{ho} in this study.

Figure 3-5 shows a SAXS pattern of the moderately long alkoxy-substituted derivative (*m*-C_{10}OPhS)$_8$PcCu (**1f**) at 115 °C. As can see from this figure, a broad halo (#2) due to the molten long alkyl chains was observed. From the reciprocal lattice calculation [40], the liquid crystalline phase was identified as Col_{ro2} (P2m) (a = 37.0 Å, b = 27.6 Å, h = 4.06 Å). Figure 3-6 shows the SAXS pattern of the longest alkoxy-substituted derivative (*m*-C_{16}OPhS)$_8$PcCu (**1i**) at 100°C. The liquid crystalline phase was also identified as Col_{ro1} (P2m) (a = 49.9 Å, b = 28.6 Å, h = 4.07 Å). It is very interesting that each of the present longer alkoxy-substituted *phenylthio* derivatives (*m*-C_nOPhS)$_8$PcCu (*n* = 4~16)

Table 3-4. X-ray data of **1a~1i.**

Compound (mesophase)	Lattice constants/Å	Spacing/Å		Miller indices
		Observed	Calculated	(*hkl*)
1a* : (*m*-C_1OPhS)$_8$PcCu		18.1	18.2	(100)
Col_{ho} at 300°C	a = 20.9	13.6	13.6	$(001)^{2h}$
	h = 6.82	10.1	10.5	(110)
	Z = 0.95 for ρ = 1.1	9.16	9.05	(200)
		6.82	6.82	$(001)^{h}$
		*ca.*5.9	6.03	(300)+#1
		3.98	3.95	(410)
1b : (*m*-C_2OPhS)$_8$PcCu		19.0	19.0	(100)
Col_{ho} at 220°C	a = 22.0	14.3	14.4	$(001)^{2h}$
	h = 7.12	10.9	11.0	(110)
	Z = 1.0 for ρ = 1.1	7.12	7.19	$(210)+(001)^{h}$
		6.23	6.34	(300)
		*ca.*5.2	-	#1
		4.00	4.15	(410)
1c : (*m*-C_4OPhS)$_8$PcCu		22.7	22.7	(100)
Col_{ro2} (P2m) at 199°C	a = 22.7	10.8	10.8	(020)
	b = 21.7	7.17	7.17	$(001)^{h}$
	h = 7.17	5.26	5.27	(140)
	Z = 1.1 for ρ = 1.0	4.88	4.89	(240)+#1
		4.18	4.19	(520)
		3.71	3.73	(610)
1d: (*m*-C_6OPhS)$_8$PcCu		26.6	26.6	(010)
Col_{ro2} (P2m) at 148°C	a = 36.8	18.4	18.4	(200)
	b = 26.6	10.7	10.8	(220)
	h = 3.60	8.61	8.63	(130)
	Z = 1.0 for ρ = 1.1	7.92	8.00	(230)
		5.82	5.85	(340)
		5.02	5.04	(630)
		4.58	4.60	(800)+#2
		4.06	4.08	(830)
		3.60	3.60	$(001)^{h}$
1e: (*m*-C_8OPhS)$_8$PcCu		35.0	35.0	(100)
Col_{ro2} (P2m) at 115°C	a = 35.0	21.6	21.6	(110)
	b = 27.5	15.9	14.8	(210)
	h = 3.99	10.8	10.7	(310)
	Z = 1.0 for ρ = 1.1	7.06	7.00	(500)
		6.58	6.41	(240)
		5.14	5.25	(250)+#2
		4.69	4.70	(720)+#2
		3.99	3.99	$(001)^{h}$
1f : (*m*-C_{10}OPhS)$_8$PcCu		36.6	36.6	(100)
Col_{ro1}(P2m) at 80°C	a = 36.6	21.8	21.8	(110)
	b = 27.2	13.7	13.6	(020)
	h = 4.01	10.7	10.9	(220)
	Z = 0.98 for ρ = 1.1	6.93	7.07	(510)
		5.01	4.98	(540)+#2
		4.61	4.57	(800)+#2
		4.01	4.01	$(001)^{h}$
Col_{ro2}(P2m) at 115°C	a = 37.0	37.0	37.0	(100)
	b = 27.6	22.1	22.1	(110)
	h = 4.06	10.6	11.1	(220)
	Z = 1.0 for ρ = 1.1	7.06	7.15	(510)
		5.08	5.05	(540)+#2
		4.61	4.60	(060)+#2
		4.06	4.06	$(001)^{h}$

#1, #2 = Broad halo due to the thermal fluctuation of the phenylthio groups and molten alkyl chain, respectably.
h = Stacking distance. *p* = assumed density (g/cm^3). * Ref [20]

Table 3-4. (Continued)

Compound (mesophase)	Lattice constants/Å	Spacing/Å		Miller indices
		Observed	Calculated	(*hkl*)
1g : (*m*-C_{12}OPhS)$_8$PcCu				
Col_{ro2} (P2m) at 100°C	a = 39.5	39.5	39.5	(100)
	b = 21.3	21.3	21.3	(010)
	h = 5.09	10.7	10.7	(020)
	Z = 0.97 for ρ = 1.1	8.02	7.90	(500)
		6.98	7.00	(130)
		5.09	5.09	(001)^h
		4.63	-	#2
Col_{ro1} (P2m) at 90°C	a = 43.1	43.1	43.1	(100)
	b = 21.6	21.6	21.6	(010)
	h = 4.96	13.7	13.7	(300)
	Z = 1.1 for ρ = 1.1	10.8	10.8	(400)
		7.04	7.11	(130)
		4.96	4.96	(001)^h
		4.62	-	#2
1h : (*m*-C_{14}OPhS)$_8$PcCu				
Col_{ro2} (P2m) at 105°C	a = 43.7	43.7	43.7	(100)
	b = 21.5	21.5	21.5	(010)
	h = 5.08	14.4	14.6	(300)
	Z = 1.0 for ρ = 1.1	10.6	10.7	(020)
		7.14	7.15	(030)
		5.08	5.08	(001)^h
		*ca.*4.6	-	#2
Col_{ro1} (P2m) at 85°C	a = 50.1	50.1	50.1	(100)
	b = 22.6	22.6	22.6	(010)
	h = 4.59	14.3	13.4	(310)
	Z = 1.1 for ρ = 1.1	10.7	11.0	(410)
		7.09	7.16	(700)
		*ca.*4.9	-	#2
		4.59	4.59	(001)^h
1i : (*m*-C_{16}OPhS)$_8$PcCu				
Col_{ro1} (P2m) at 100°C	a = 49.9	49.9	49.9	(100)
	b = 28.6	24.8	24.8	(110)
	h = 4.07	17.0	16.6	(300)
	Z = 1.0 for ρ = 1.0	10.7	10.8	(320)
		7.07	7.07	(140)
		*ca.*5.1	-	#2
		*ca.*4.6	-	#2
		4.07	4.07	(001)^h

#1, #2 = Broad halo due to the thermal fluctuation of the phenylthio groups and molten alkyl chain, respectably.
h = Stacking distance. ρ = assumed density (g/cm^3).

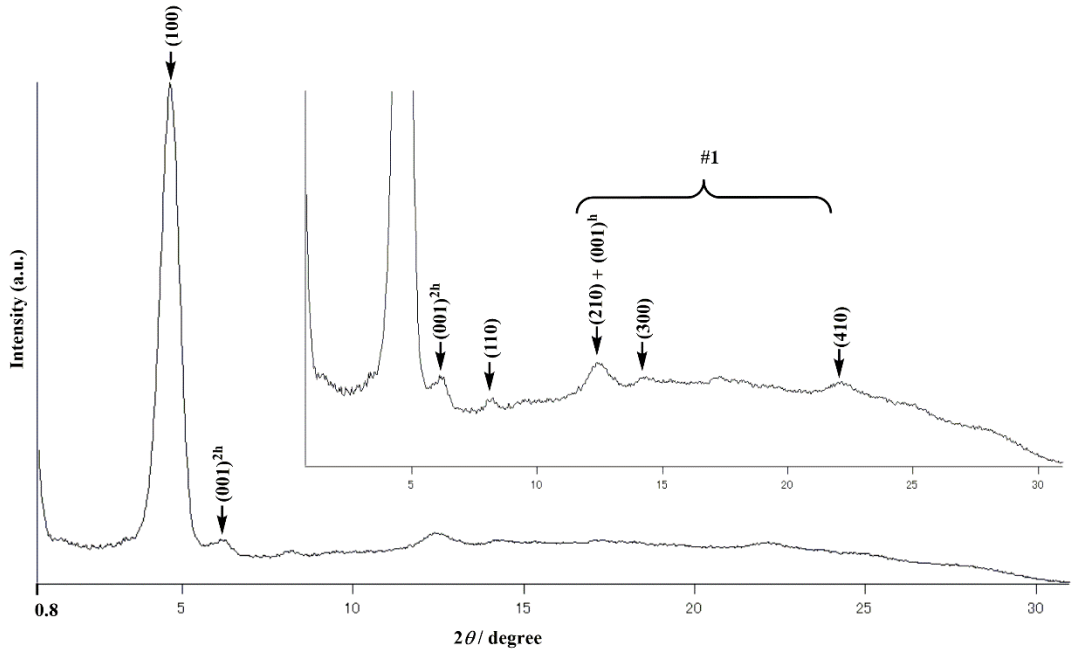

Figure 3-4. XRD pattern of (*m*-C_2OPhS)$_8$PcCu (**1b**) at 220 ºC (on cooling from I. L.). #1 = broad halo due to the thermal fluctuation of the phenylthio groups.

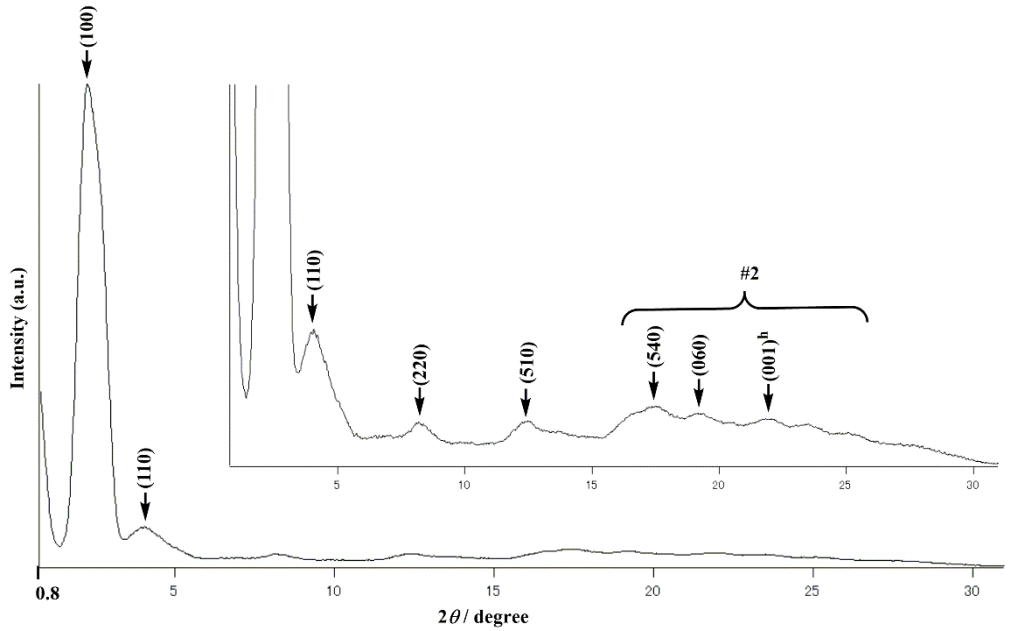

Figure 3-5. XRD pattern of (*m*-C_{10}OPhS)$_8$PcCu (**1f**) at 115 ºC. #2 = broad halo due to the molten alkyl chains.

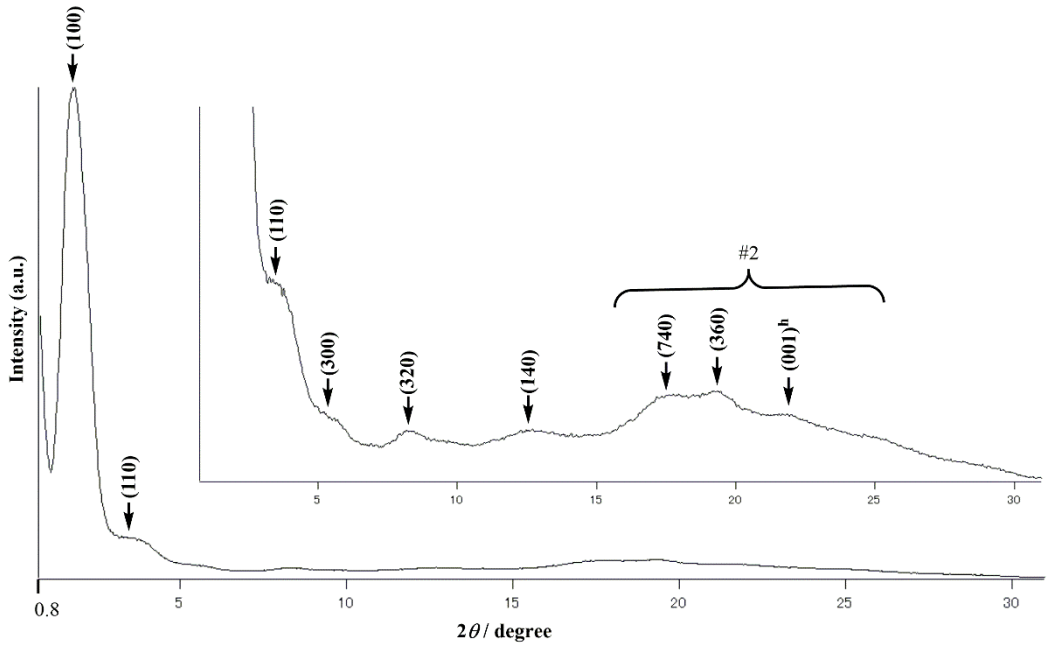

Figure 3-6. XRD pattern of (*m*-C_{16}OPhS)$_8$PcCu (**1i**) at 100 °C (on cooling from I. L.). #2 = broad halo due to the molten alkyl chains.

showed only *rectangular* columnar (Col_{ro} (P2m)) phase(s), whereas each of the previous longer alkoxy-substituted *phenoxy* derivatives (*m*-C_nOPhO)$_8$PcCu (*n* = 10~20) showed only a *hexagonal* columnar (Col_{ho}) phase[8, 9].

3.3.5. Columnar stacking structures of (*m*-C_nOPhO)$_8$PcCu (*n* = 10-20) and (*m*-C_nOPhS)$_8$PcCu (*n* = 1-16).

The different mesophase appearance mentioned above may be attributed to difference of interaction among the Pc cores having steric hindrance of the peripheral substituents (PhO and PhS).

It is well known that stronger interaction between cores is required to form a rectangular columnar (Col_r) phase in comparison with a hexagonal columnar (Col_h) phase [41-43]. As schematically shown in Figure 3-7, covalent bond radius of sulfur atom (1.04 Å) is larger than that of oxygen atom (0.66 Å). Hence, C-S bond length (1.81 Å) is longer than C-O bond length (1.43 Å) [44]. Accordingly, the interaction between Pc cores in the *phenoxy*-substituted derivatives (*m*-C_nOPhO)$_8$PcCu (*n* =10-20) is weakened by bigger steric hindrance of the *phenoxy* groups closer to the Pc core. As the result, the *phenoxy*-substituted derivatives (*m*-C_nOPhO)$_8$PcCu (*n* = 10-20) may form the hexagonal columnar phase (Col_h). On the other hand, the interaction between Pc cores in the *phenylthio*-substituted derivatives (*m*-C_nOPhS)$_8$PcCu (*n* = 4-16) is strengthened by smaller steric hindrance of phenylthio group farther from the Pc core. In this case, an additional coordination bonds may be formed between copper atoms and nitrogen atoms between the upper and lower Pc cores, as illustrated in Figure 3-7

(dotted lines). Thus, the *phenylthio*-substituted derivatives (*m*-C_nOPhS)$_8$PcCu (*n* = 4-16) may form the rectangular columnar (Col_r) phase.

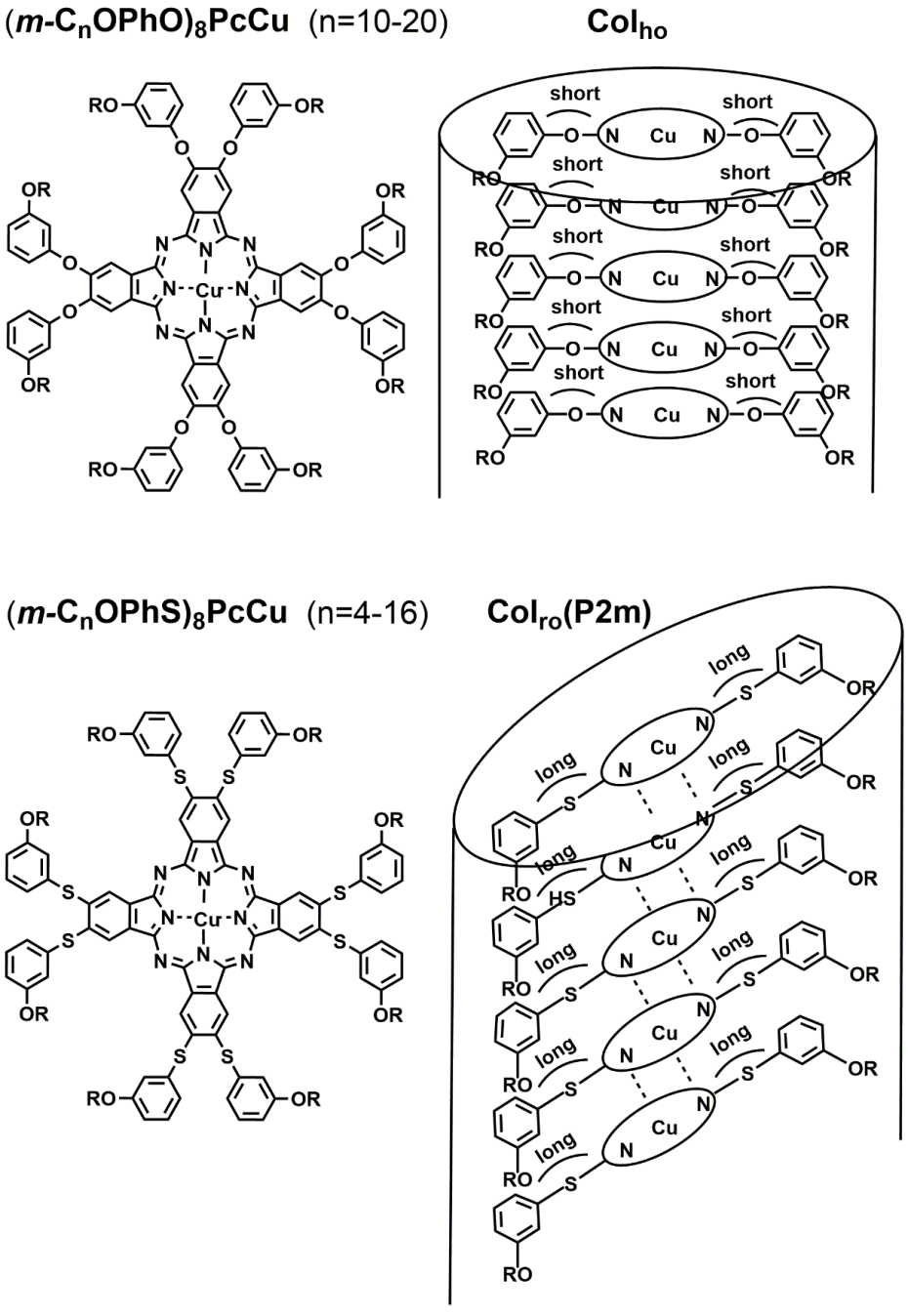

Figure 3-7. Columnar stacking structures of (*m*-C_nOPhO)$_8$PcCu (*n* = 10-20) and (*m*-C_nOPhS)$_8$PcCu (*n* = 4-16).

3.3.6. UV-vis absorption spectra

Figure 3-8 shows the UV-vis absorption spectra (dotted line) and the fluorescence spectra (solid line) of (*m*-C_{10}OPhO)$_8$PcCu (upper) and (*m*-C_{10}OPhS)$_8$PcCu (**1f**) (lower) in THF solution. Table 3-5 lists their spectral data. As can see from these figure and table, the Q-band of the *phenylthio*-substituted derivative (*m*-C_{10}OPhS)$_8$PcCu (**1f**) red-shifts by 35.7 nm into near infrared region compared with the *phenoxy*-substituted derivative (*m*-C_{10}OPhO)$_8$PcCu. This result is compatible with those of the *phenylthio*-substituted phthalocyanines reported so far[16-20].

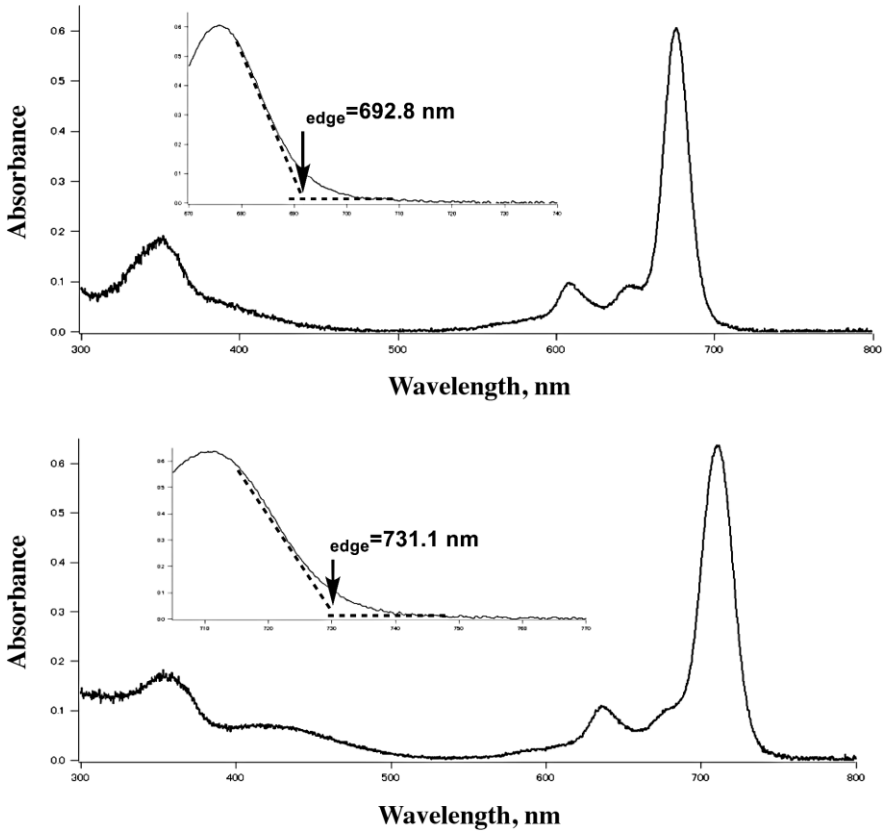

Figure 3-8. UV-vis absorption spectra of (*m*-C_{10}OPhO)$_8$PcCu (upper) and (*m*-C_{10}OPhS)$_8$PcCu (**1f**) (lower) in THF solution.

Moreover, we could estimate the optical band gaps of (*m*-C_{10}OPhO)$_8$PcCu and (*m*-C_{10}OPhS)$_8$PcCu (**1f**) from absorption edge of the Q-bands to be 1.79 eV and 1.70 eV, respectively. Hence, the *phenylthio*-substituted derivative gave a narrower band gap by *ca.* 0.1 eV in comparison with the *phenoxy*-substituted derivative.

Table 3-5. UV-vis spectral data of (*m*-C_{10}OPhO)$_8$PcCu and (*m*-C_{10}OPhS)$_8$PcCu in THF solution.

Compound	Concentration ($X10^{-6}$mol L^{-1})	λ_{abs} / nm (logε)			λ_{edge} / nm	E_{0-0} * / eV
		Soret band	Q-band			
			Q_{0-1}-band	Q_{0-0}-band		
(*m*-C_{10}OPhO)$_8$PcCu	2.27	351.9(4.93)	608.3(4.64)	675.9(5.43)	692.8	1.79
(*m*-C_{10}OPhS)$_8$PcCu (**1f**)	2.29	353.3(4.90)	635.7(4.69)	711.6(5.44)	731.1	1.70

* E_{0-0} was estimated from the crossing point of normalized absorption and fluorescence spectra.

3.4. Conclusion

In this study, we have successfully synthesized novel phenylthio-substituted phthalocyanine derivatives (*m*-C_nOPhS)$_8$PcCu (**1b**~**1i**) to reveal their mesomorphism. We found that the shortest alkoxy-substituted derivatives, (*m*-C_1OPhS)$_8$PcCu (**1a**) and (*m*-C_2OPhS)$_8$PCu (**1b**) could be classified as flying-seed-like liquid crystals. On the other hand, the other longer alkoxy-substituted derivatives (*m*-C_nOPhS)$_8$PcCu: n = 4~16 (**1c**~**1i**) could be classified as conventional long alkyl-chain-melting liquid crystals. It is very interesting that each of the present longer alkoxy-substituted *phenylthio* derivatives (*m*-C_nOPhS)$_8$PcCu (n = 4~16) showed only *rectangular* columnar (Col_{ro}- (P2m)) phase(s), whereas each of the previous longer alkoxy-substituted *phenoxy* derivatives (*m*-C_nOPhO)$_8$PcCu (n = 10~20) showed only a *hexagonal* columnar (Col_{ho}) phase. The different mesophase appearance may be originated from the difference of interaction among the Pc cores having steric hindrance of the peripheral substituents (PhO and PhS). The Q-band of the *phenylthio*-substituted derivative (*m*-C_{10}OPhS)$_8$PcCu (**1f**) red-shifts by 35.7 nm into near infrared region compared with the *phenoxy*-substituted derivative (*m*-C_{10}OPhO)$_8$PcCu. Thus, in this study, we successfully synthesized a novel series of liquid crystalline (*m*-C_nOPhS)$_8$PcCu (n = 1~16) derivatives showing the Q-bands in near infrared region. We intend to measure the charge carrier mobilities in the near future.

References

1. S.Chandrasekhar, B. K. Sadashira, and K. A. Suresh, *Pramana,* 1977, **9**, 471.
2. A. N. Cammidge and R. J. Bushby, Handbook *of Liquid Crystals*, Vol. 2B, Wiley-VCH, 1998, Chap. 7, pp. 693.
3. S. Sergeyev, W. Pisula, and Y. H. Geerts, *Chem. Soc. Rev*., 2007, **36**, 1902.
4. K. Ban, K. Nishizawa, K. Ohta, and H. Shirai, *J. Mater. Chem.,* 2000, **10**, 1083.
5. A. M. van de Craats, P. G. Shouten, and J. M. Warman, *Ekisho*, 1998, Vol. 2, no. 1.
6. J. M. Warman, J. E. Kroeze, P. G. Schouten, and A. M. van de Craats, *J. Porphyrins Phthalocyanines,* 2003, **7**, 342.
7. K. Hatsusaka, K. Ohta, I. Yamamoto, and H. Shirai, *J. Mater. Chem.,* 2001, **11**, 423.
8. M. Ichihara, A. Suzuki, K. Hatsusaka, and K. Ohta, *J. Porphyrins Phthalocyanines,* 2007, **11**, 503.
9. H. Sato, K. Igarashi, Y. Yama, M. Ichihara, E. Itoh, and K. Ohta, *J. Porphyrins Phthalocyanines,* 2012, **16**, 1148.
10. M. Kandaz, İ.Yılmaz, and Ö. Bekaroğlu, *Polyhedron,* 2000, **19**, 115.
11. O. V. Balakireva, V. E. Maizlish, and G. P. Shaposhnikov, *Russ. J. Gen. Chem*., 2003, **73**, 292.
12. N. Kobayashi, H. Ogata, N. Nonaka, and E. A. Luk'yanets, *Chem. -Eur. J.,* 2003, **9**, 5123.
13. G. Lu, M. Bai, R. Li, X. Zhang, C. Ma, P-C. Lo, D. K. P. Ng, and J. Jiang, *Eur. J. Inorg. Chem.* 2006, 3703.
14. D. Arican, M. Arici, A. L. Uğur, A. Erdoğmus, and A. Koca, *Electrochimica Acta,* 2013, **106**, 541.
15. M. Mayukh, C-W. Lu, E. Hernandez, and D. V. McGrath, *Chem. -Eur. J*., 2011, **17**, 8427.
16. N. W. Polaske, H-C. Lin, A. Tang, M. Mayukh, L. E. Oquendo, J. Green, E. L. Ratcliff, N. R. Armstrong, S. S. Saavedra, and D. V. McGrath, *Langmuir,* 2011, **27**, 14900.
17. L. Yu, W. Shi, L. Lin, Y. Guo, R. Li, and T. Peng, *Dyes Pigm.,* 2015, **114**, 231.
18. W. Shi, B. Peng, Y. Guo, L. Lin, T. Peng, and R. Li, *J. Photochem. Photobiol. A,* 2016, **321**, 248.
19. P. Zimcik, A. Malkova, L. Hruba, M. Miletin, and V. Novakova, *Dyes Pigm.,* 2017, **136**, 715.
20. A. Ishikawa, K. Ohta, and M. Yasutake, *J. Porphyrins Phthalocyanines,* 2015, **19**, 639.
21. K. Ohta, T. Shibuya, and M. Ando, *J. Mater. Chem.,* 2006, **16**, 3635.
22. Y. Takagi, K. Ohta, S. Shimosugi, T. Fujii, and E. Itoh, *J. Mater. Chem*., 2012, **22**, 14418.
23. A. Hachisuga, M. Yoshioka, K. Ohta and T. Itaya, *J. Mater. Chem. C,* 2013, **1**, 5315.
24. M. Yoshioka, K. Ohta, and M. Yasutake, *RSC Adv.,* 2015, **5**, 13828.
25. A. Watarai, K. Ohta, and M. Yasutake, *J. Porphyrins Phthalocyanines,* 2016, **20**, 822.
26. S. Barluenga, P-Y. Dakas, Y. Ferandin, L. Meijer, and N. Winssinger, *Angew. Chem. Int. Ed*., 2006, **45**, 3951.
27. Patent PCT/US2006/041501.
28. J. Y. Hwang, L. A. Arnold, F. Zhu, A. Kosinski, T. J. Mangano, V. Setola, B. L. Roth, and R. K. Guy, *J. Med. Chem.,* 2009, **52**, 3892.

29. M. Wakioka, M. Ikegami, and F. Ozawa, *Macromolecules,* 2010, **43**, 6980.
30. Y. Jiang, Y. Qin, S. Xie, X. Zhang, J. Dong, and D. Ma, *Org. Lett.,* 2009, **11**, 5250.
31. P. Natarajan, H. Sharma, M. Kaur, and P. Sharma , *Tetrahedron Lett.,* 2015, **56**, 5578.
32. S. K. Patel and T. E. Long, *Tetrahedron Lett.,* 2009, **50**, 5067.
33. D. Wöhrle, M. Eskes, K. Shigehara, and A. Yamada, *Synthesis,* 1993, 194.
34. T. Kamiyama, S. Enomoto and M. Inoue, *Chem. Pharm. Bull.,* 1985, **33**, 5184.
35. M. S. Newman and H. A. Karnes, *J. Org. Chem.,* 1996, **31**, 3980.
36. T. Itoh and T. Mase, *Org. Lett.,* 2004, **6**, 4587.
37. T. Itoh and T. Mase, *J. Org. Chem.,* 2006, **71**, 2203.
38. K. A. Mazzio, K. Okamoto, Z. Li, S. Gutmann, E. Strein, D. S. Glinger, R. Sclaf, and C. K. Luscombe, *Chem. Commun.,* 2013, **49**, 1321.
39. N. B. Heine and A. Studer, *Macromol. Rapid. Commun.,* 2016, **37**, 1494.
40. (a) K. Ohta, *Dimensionality and Hierarchy of Liquid Crystalline Phases: X-ray Structural Analysis of the Dimensional Assemblies*, Shinshu University Institutional Repository, submitted on 11 May, 2013; http://hdl.handle.net/10091/17016. (b) K. Ohta, In *Identification of discotic mesophases by X-ray structure analysis*, *Introduction to Experiments in Liquid Crystal Science* (*Ekisho Kagaku Jikken Nyumon* [*in Japanese*]), Japanese Liquid Crystal Society, Sigma Shuppan: Tokyo, 2007; Chap. 2-(3), pp. 11–21, ISBN-13:978-4915666490.
41. S. Laschat, A. Baro, N. Steinke, F. Giesselmann, C. Hägele, G. Scalia, R. Judele, E. Kapatsina, S. Sauer, A. Schreivogel, and M. Tosoni, *Angew. Chem. Int. Ed.,* 2007, **46**, 4832.
42. H. Zheng, C. K. Lai, and T. M. Swager, *Chem. Mater.,* 1995, **7**, 2067.
43. F. Morale, R. W. Date, D. Gullion, D. W. Bruce, R. L. Finn, C. Wilson, A. J. Blake, M. Schröder, and B. Donnio, *Chem. -Eur. J.*, 2003, **9**, 2484.
44. P. W. Atkin and J. de Paula, *Physical Chemistry,* 8th edition, 2006.

Chapetr 4

Stimuli-responsive rheological properties for liquid phthalocyanines

Summary: Highly viscous phthalocyanine-based molecular liquids **1** and **2** were synthesized, and detailed analyses of their liquid property were conducted. **1** and **2** formed face-to-face aggregates in solvent-free liquid state. They exhibited stimuli-responsive rheological properties in response to the changes of temperature and shear force due to collapse of the rod-like aggregates.

4.1. Introduction

Combination of functional π-molecules with flexible alkyl chains has received great attention because of the possible applications to optoelectronic devices.[1] This method can not only enhance solubility but also offer formation of well-ordered self-assembled structures such as liquid crystalline (LC) phases.[2] These states are induced by the phase segregation between a rigid π-conjugated unit and molten alkyl chains as well as noncovalent interactions among molecular components. Functional molecular liquids (FMLs) are being intensively developed by the precise tuning of intermolecular interactions among π-molecules.[3]

Phthalocyanines (Pcs) and their metal complexes (MPcs) have been used as blue or green dyes and pigments because of their intense absorption bands positioning at red or near-infrared light regions and their excellent photo and chemical stability.[4] The control of their organized states and structures is crucial for enhancing the performance in applications.[5] Pcs form various states in their condensed phases such as LC, glassy, and crystalline states.[6] To date, a handful of Pc-based liquid-like compounds have been reported.[7] Ohta *et al*. investigated the systematic reduction of intermolecular π-π interactions among CuPc rings by changing the position of linear long-alkyl chains at the peripheral phenoxy units.[7f] Among them, orthosubstituted CuPc **1** did not exhibit typical LC behavior, and its state was assigned as an amorphous liquid by polarized microscope (POM) analyses. However, no detailed investigation for **1** has been reported so far. Liquid-like Pcs are still limited in examples and leave open questions about the origin of their high viscosity. In this paper, we investigated the rheological properties of viscous Pc-based molecular liquids **1** and **2**, and found their unique stimuli-responsive rheological properties. We also examined the organized structures in nanometer length scale of **1** and **2** in the condensed state by spectroscopic, thermal, and X-ray scattering analyses.

4.2. Experimental

4.2.1. Materials

All commercial available chemicals were used without further purification unless otherwise noted. 4, 5-dichlorophthalonitrile and 1-bromododecane were purchased from Tokyo Chemical Industry. Others were purchased from Wako pure chemical. Molecular sieves and K_2CO_3 were dried at 200 ^oC in vacuo in prior to use to activate them. All solvents were purchased from Wako Pure Chemical and solvents for synthesis were dried over drying agents in prior to use (3A molecular sieves for DMF and 1-butanol).

4.2.2. Synthesis

2-Dodecyloxyphenol and 4,5-bis(2′-dodecyloxyphenoxy)phthalonitrile were synthesized according to literature methods.[7f]

1: 2,3,9,10,16,17,23,24-octa(2′ -dodecyloxyphenoxy)phthalocyanine

A test tube was filled with dry 1-butanol (3.0 mL) and lithium metal (11.6 mg, 1.67 mmol). The mixture was slowly heated up to 70 °C to dissolve all lithium metal. After perfectly dissolved, the mixture was cooled to r. t. 4,5-bis(2′-dodecyloxyphenoxy) phthalonitrile (416 mg, 0.611 mmol) was added to this solution at r. t., and the resulting mixture was refluxed under Ar for 2 h. After cooling to r. t., one portion of acetic acid and water were added to this mixture, and extracted with n-hexane. The organic layer was washed with water and brine, and dried over Na_2SO_4. After removing Na_2SO_4, the filtrate was evaporated *in vacuo*. Subsequently, the crude product was purified with silica gel column chromatography (CH_2Cl_2: *n*-hexane = 5:1, R_f = 0.50) and recycling preparative HPLC ($CHCl_3$) to obtain dark colored viscous liquid (103 mg, 25%).

High resolution HR-APCI-TOF-Mass (negative): *m/z* 2723.8638 [M]; calcd for $C_{176}H_{242}O_{16}N_8$: *m/z* 2723.8363.

^{1}H-NMR (400.13 MHz, $CDCl_3$, TMS): δ (ppm) = 8.69 (s, 8H, ArH), 7.37-7.28 (m, 16H, ArH), 7.19 (d, *J* = 7.2Hz, 8H, ArH), 7.12 (m, 8H, ArH), 4.11 (t, *J* = 6.8 Hz, 16H, -OCH_2-), 1.71 (quin, *J* = 7.1 Hz, 16H, -$OCCH_2$-), 1.24 (quin, *J* = 7.5 Hz, 16H, -$OCCCH_2$-), 1.07 (quin, *J* = 7.2 Hz, 32H, -$OCCCCH_2CH_2$-), 0.945-0.580 (m,120H, -$(CH_2)_6CH_3$), -0.542 (s, 2H, -NH).

^{13}C-NMR (100.61 MHz, $CDCl_3$, TMS): δ(ppm) = 151.3, 151.2, 145.9, 125.6, 121.9, 121.6, 115.0, 111.6, 69.5, 32.1, 29.8, 29.7, 29.4, 26.3, 22.9.

UV-visible (THF) λ_{max} /nm (log ε): 704 (5.14), 668 (5.13), 349 (4.88).

2: 2,3,9,10,16,17,23,24-octa(2′-dodecyloxyphenoxy)phthalocyaninato copper(II)

A three necked flask was filled with anhydrous $CuCl_2$ (36.8 mg, 0.274 mmol), 4,5-bis(2′ dodecyloxy)phthalonitrile (492 mg, 0.722 mmol), 1-pentanol (6.0 mL), and DBU (1,8-diazabicyclo[5.4.0]-7-undecene) (121 mg, 0.795 mmol). The reaction mixture was refluxed for 24 h with stirring under Ar. After cooling down to r. t., methanol was added to precipitate the target compound. The precipitates were collected by filtration and washed with methanol to remove residual Cu ion. The crude product was purified with silica gel column chromatography ($CHCl_3$, R_f = 1.0) and recycling preparative HPLC ($CHCl_3$) to obtain dark colored viscous liquid (339 mg, 67%).

HR-APCI-TOF-Mass (negative): *m/z* 2784.7455 $[M]^+$; calcd for $C_{176}H_{240}O_{16}N_8Cu$: m/z 2784.7503.

UV-visible (THF) λ_{max} /nm (log ε): 681 (5.48), 347(4.93).

4.3. Results and discussion

4.3.1. Synthesis

We synthesized compounds **1** and **2**, in which eight 2-dodecyloxypheoxy units were attached at the peripheral positions of a Pc ring (Figure 4-1a).[7f] After tetramerization of 4,5-bis(2-dodecyloxy-pheoxy)phthalonitrile **3** in the presence or absence of $CuCl_2$, **1** and **2** were purified by silica gel column chromatography and recycling preparative HPLC to obtain dark colored highly viscous oils (Figure 4-1b). The obtained **1** and **2** exhibited good solubility in various organic solvents except for polar ones, e.g. methanol, ethanol, and water. The mass spectra of **1** and **2** showed $[M]^-$ peaks at *m/z* 2784.7455 and 2723.8638 g mol^{-1}, respectively which exactly agreed with their calculated molecular weights. All peaks of the ^{1}HNMR spectrum of **2** in $CDCl_3$ were well resolved and sharp (Figure 4-2). In particular, the six protons of the Pc ring can be found as a sharp singlet at 8.69 ppm, indicating no formation of aggregates among the Pc rings in $CDCl_3$. Thermogravimetric analysis (TGA) was performed for **1** and **2** to confirm the absence of impurities such as solvents or unreacted precursors (Figure 4-3). In both TGA data, only decomposition-triggered weight losses were observed at around 390 °C. Therefore, the highly viscous fluid states of pure **1** and **2** as shown in Figure 4-1b are their intrinsic properties without contamination of residual solvents and impurities.

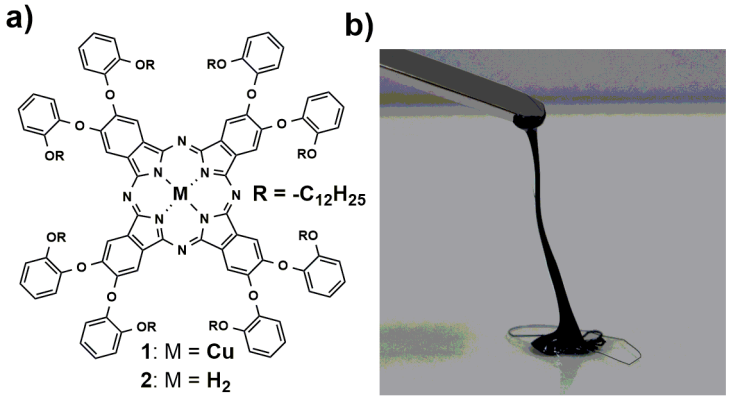

Figure 4-1. a) Molecular structure of **1** and **2**. b) A photograph of **2** as a sticky compound on glass plate at r. t.

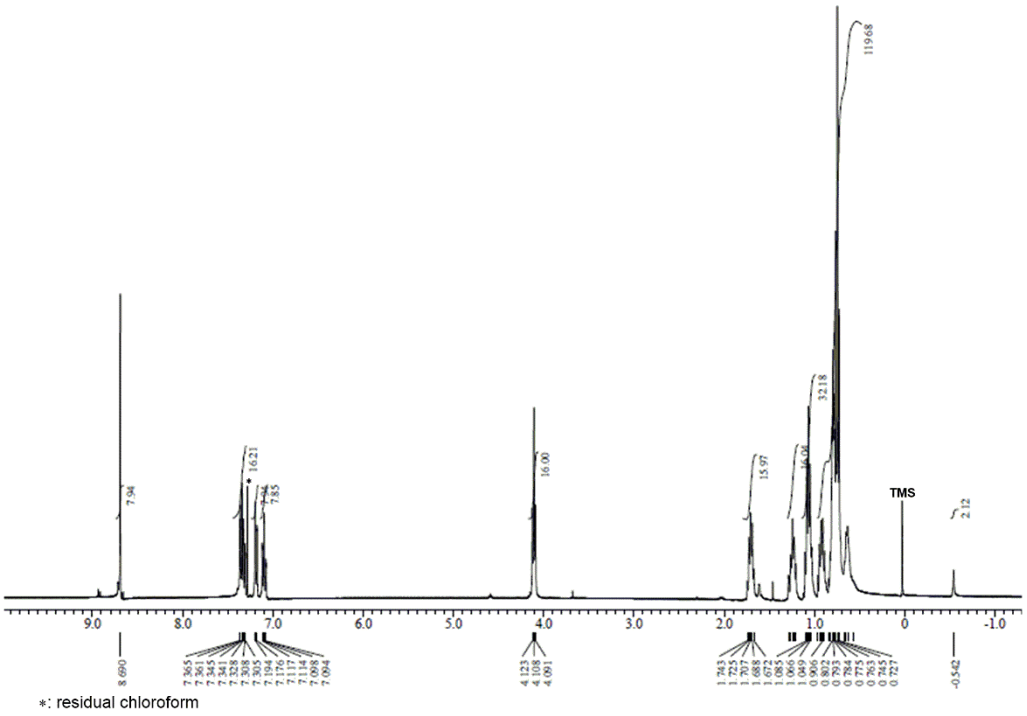

Figure 4-2. ^{1}H NMR spectrum of **2** in $CDCl_3$.

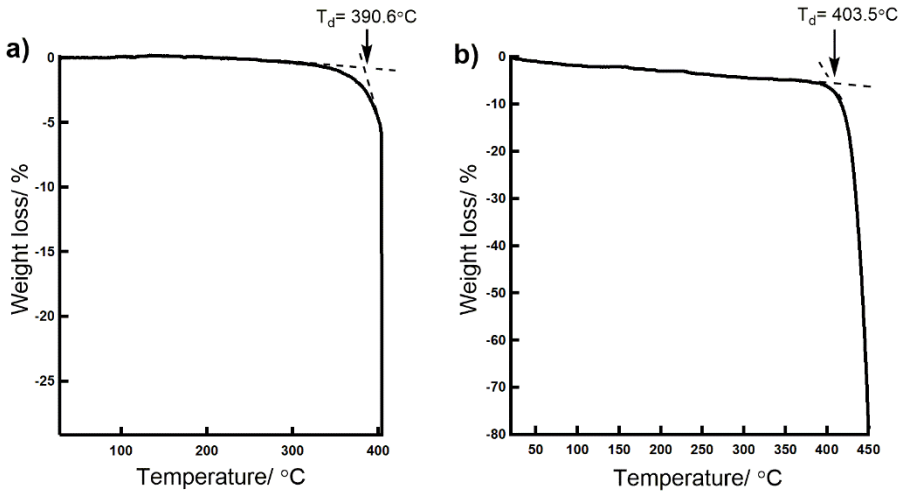

Figure 4-3. TGA profiles for **1** (a) and **2** (b) under N_2 atmosphere (scan rate: 10 °C /min).

4.3.2. Aggregation property

The shape and position of the Q-bands are known to be an indicator for analyzing the aggregation behavior of MPcs.[8] Figures 4-4a and 4-4b show the absorption spectra of **1** and **2** in THF and n-hexane. For **2** in the THF solution, two split Q-bands were observed at 704 and 668 nm, while **1** in THF had a strong sharp peak at 681 nm. The spectral shapes, Q-band position, and ε values for **1** and **2** nearly agreed with the reported values of monomeric metal-free Pcs and CuPcs.[7f,9] The Q bands of **1** and **2** in nonpolar *n*-hexane were broadened by decreasing the absorption intensities relative to the THF solutions, and new small shoulder peaks at around 640 nm appeared. The absorbance ratio between two peaks at 681 and 640nm decreased with increasing the concentration of **1** in *n*-hexane (Figure 4-5). These changes arose from the interaction between neighboring excitons, indicating the formation of aggregates through intermolecular π-π interactions among Pc units.[8] The inset of Figure 4-4b shows the UV-visible absorption spectra of neat samples **1** or **2** sandwiched by two quartz glasses. The sharp Q-bands as observed in the THF solutions almost disappeared and broadened, and new blue-shifted peaks appeared at around 640 nm. These spectral shapes indicate the stacking of Pcs with face-to-face arrangements.[10] When the UV-visible absorption spectra of the thin films of **1** and **2** were monitored by heating from room temperature (r.t.) to 90 °C, there was no appearance of sharper Q-bands which indicates the stability of aggregates without remarkable dissociation (Figure 4-6). In other words, these imply the formation of thermally-stable face-to-face stacks through π-π interactions among planar Pc rings in their condensed phase.

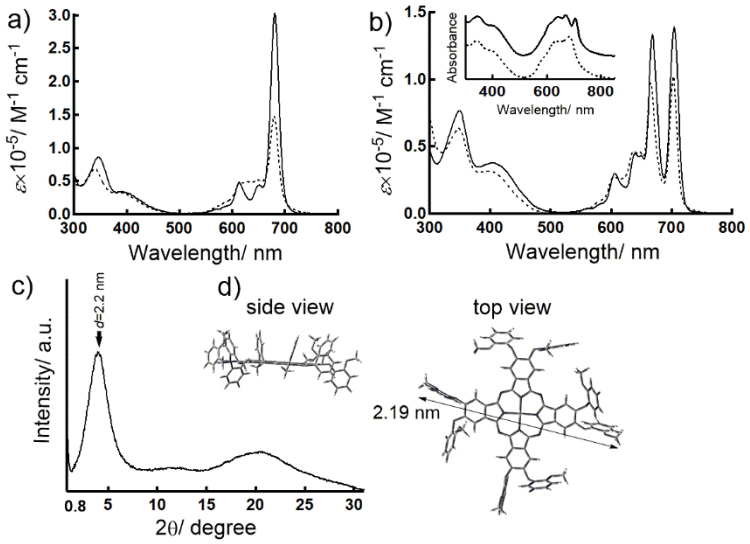

Figure 4-4. UV-visible absorption spectra of **1** (a) and **2** (b) in THF (solid line) and *n*-hexane (dashed line). The inset of (b) shows UV-visible absorption spectra of neat samples of **1** (dashed line) and **2** (solid line). c) SAXS pattern for **1** at r. t. d) An optimized structure of **1** estimated by DFT calculation. Dodecyl chains were omitted for DFT calculation.

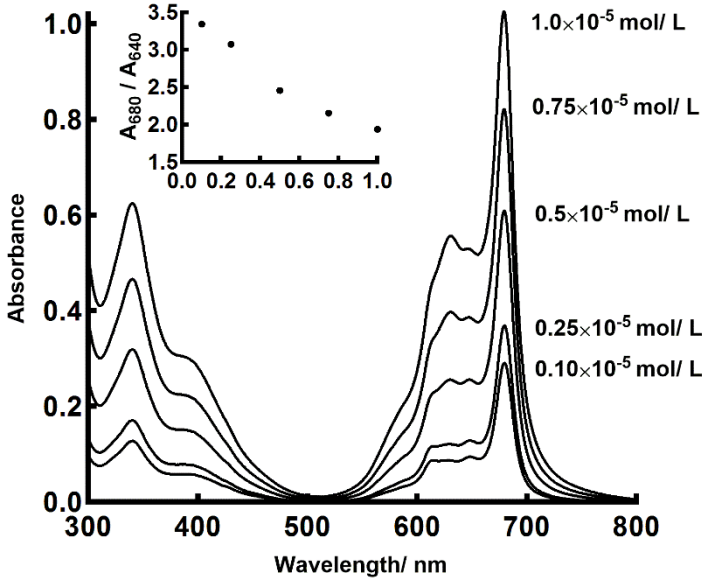

Figure 4-5. Concentration dependence of UV-visible absorption spectra of **1** in *n*-hexane. The inset shows the plots of absorbance ratios between two peaks at 681 and 640 nm vs. [**1**].

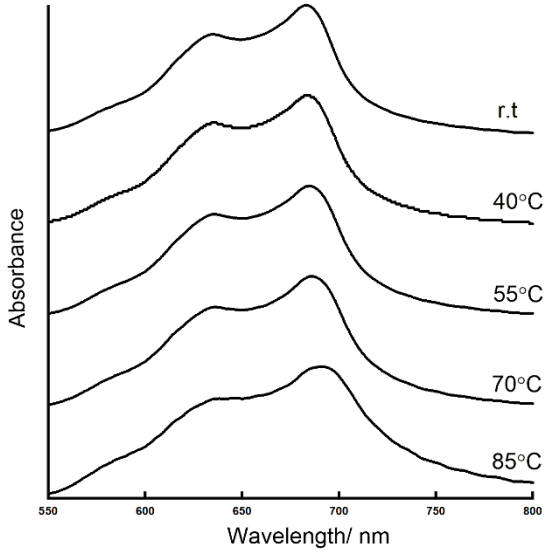

Figure 4-6. Absorption spectra of Q-band region of **1** measured at r.t., 40, 55, 70, and 85 °C.

4.3.3. Liquid property

No birefringence was observed for either **1** or **2** even though these neat samples are sheared or pushed under POM observation, revealing the absence of optically long-range-ordered structures (Figure 4-7).[6c] Differential scanning calorimetry (DSC) measurements were performed for **1**, **2**, and **3** to identify their thermal phase transition behavior (Figure 4-8). Both compounds **1** and **2** possess only a glass transition (T_g) at 9.2 and 6.1 °C, respectively. The T_g values of **1** and **2** were much higher than that of **3** (T_g = 139 °C), revealing that T_g was significantly increased by the tetramerization. Figure 4-4c shows a small-angle X-ray scattering (SAXS) pattern for **1** at r.t. A relatively broad reflection at 2θ = 1.3-7.9 degrees having a peak at d = 2.2 nm was observed, and the d spacing is almost compatible to the molecular diameter of the rigid Pc core decorated with eight phenoxy units (2.19 nm) estimated by the density functional theory (DFT) calculation (Figure 4-4d). This can be attributed to the reflection from the average center-to-center distance of neighboring Pc molecules. Furthermore, the observed reflection peak is broader than the d_{100} peaks for liquid crystalline Pcs reported previously, [11] suggesting that the center-to-center distance in **1** fluctuates in the condensed state. The broad halo observed at around 2θ = 15-20 degrees is characteristic of the molten state of alkyl chains. In addition, no intermolecular π-π stacking distance was observed around 2θ = 20 degrees as a peak, indicating the absence of a long-range order between Pc rings through π-π stacking.[9] The SAXS pattern of **1** did not change with increasing temperature from r.t. to 90 °C, indicating no structural change in this temperature range (Figure 4-9). These SAXS patterns for **1** and **2** (Figure 4-10) are similar to the reported patterns of porphyrin derivatives with long alkyl chains.[12]

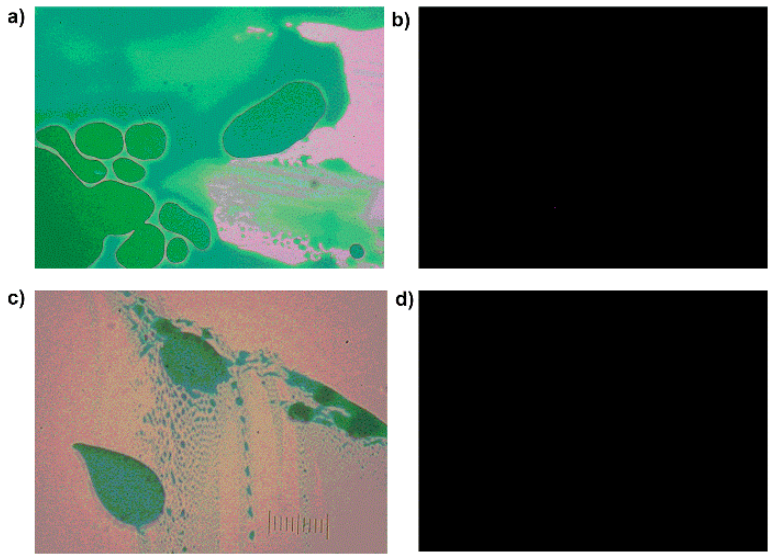

Figure 4-7. Optical micrographs of **1** (a, b) and **2** (c, d) at 25 °C. Images of (b) and (d) were taken under crossed polarizer.

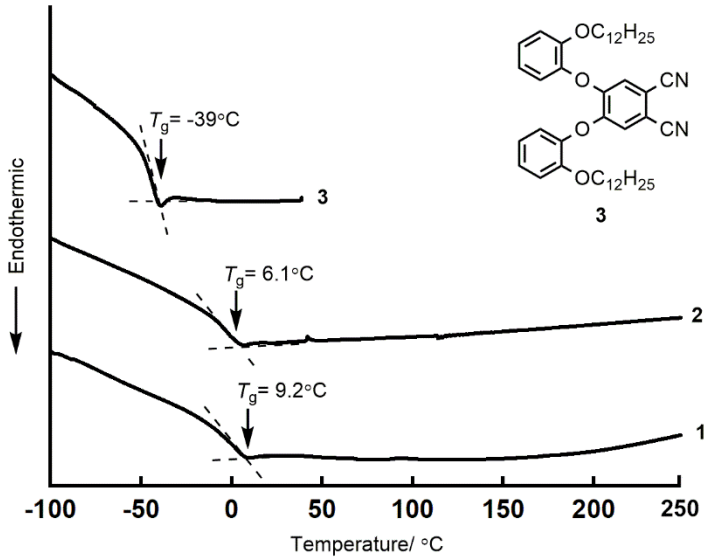

Figure 4-8. DSC profiles for **1**, **2** and **3** on a heating trace under N_2 atmosphere (scan rate: 10 °C /min).

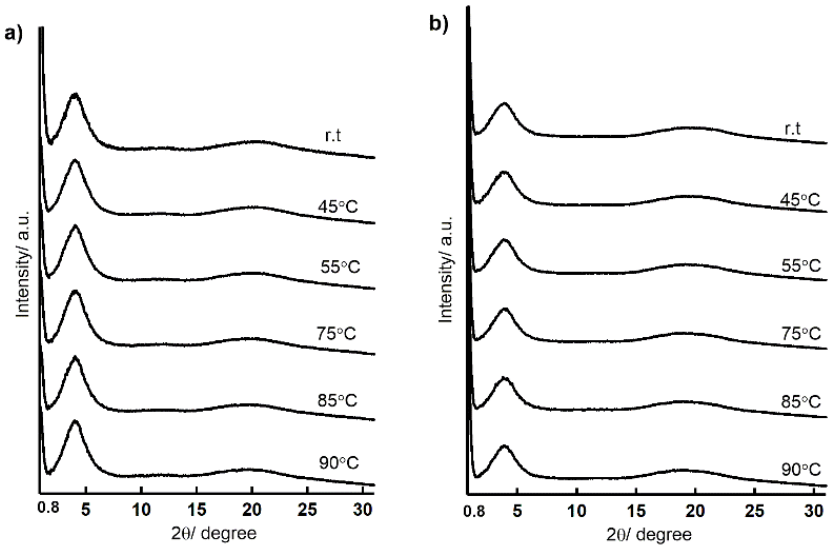

Figure 4-9. SAXS patterns for **1** (a) and **2** (b) measured at r. t., 45, 55, 75, 85, and 90 °C.

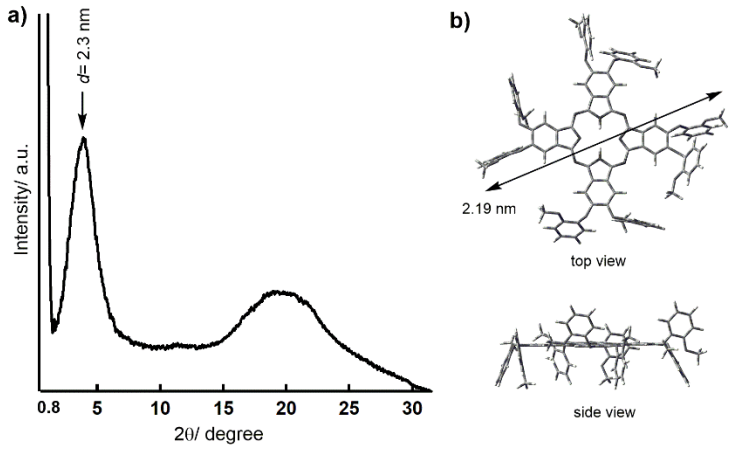

Figure 4-10. (a) SAXS pattern for **2** at r. t. (b) Optimized molecular structure of **2** estimated by DFT calculation. Dodecyl chains were omitted for DFT calculation.

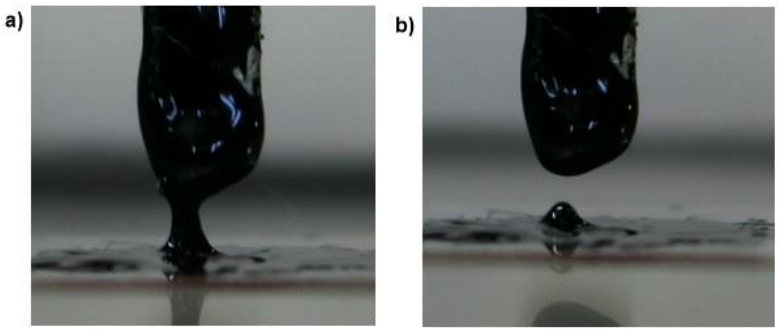

Figure 4-11. Apparent viscosity change of **1** by heating from 25 ºC (a) to 45 ºC (b).

Viscous fluid **2** formed a thread through mechanical pulling at 25 °C, and this thread was broken by being heated up to 45 °C (Figure 4-11). The origin of this behavior can be seen as a decreasing of the viscosity of **2** accompanied by heating. Rheological measurements were performed for **1** and **2** to investigate their rheological properties.[3] For both samples, strain amplitude (γ) scans were firstly performed to determine the linear-viscoelastic region. For both samples strain amplitude (γ) of 0.1% and 50% were within this linear viscoelastic region (Figure 4-12). Figure 4-13a shows the angular frequency (ω) dependence of storage elastic modulus (G') and viscous loss modulus (G'') at a shear strain of γ = 0.1% on double logarithmic plots. Both **1** and **2** displayed higher G'' values than the G' values in the whole measured ω range at 25 °C, which is typical of liquid-like behavior.[3] The double logarithmic plots of G' vs. ω for **1** and **2** have two slopes with the inflection point around ω = 5 s^{-1},

revealing a slow relaxation process below this point.[13] Figure 4-13b shows ω dependence of the complex viscosity (η^*) measured at 25 °C at γ = 0.1% and 50%. Zero-shear viscosities (η_0) given by $\lim_{\omega \to 0} |\eta^*|$ 1.60 × 10^4 and 1.03 × 10^4 Pa•s for **1** and **2** at γ = 0.1%.[13] These η_0 values are seven orders of magnitude higher than the viscosity of water (about 1 × 10^{-3} Pa•s), and the η_0 values of **2** are slightly higher than that of **1**. The η^* values of **1** and **2** were almost independent of ω at γ = 0.1% (Figure 4-13b). In contrast, the η^* value decreased as ω increased at the high shear strain (γ = 50%), indicating shear-thinning behavior.[13] Shear-thinning behavior is a typical behavior for liquids containing non-spherical materials and aggregates.[14] The observed shear-thinning behavior suggests the formation of rod-like clusters composed of short Pc-stacks with axial ratios, and these aggregates collapse into smaller clusters with increasing angular frequency under high shear force. The shear-thinning behavior at γ = 50% disappeared by heating above 35 °C, and the ω dependencies of η^* at 35-90 °C showed plateau Newtonian-like liquid profiles (Figure 4-14). The η_0 values of **1** and **2** at γ = 0.1% significantly decreased by four orders of magnitude as the temperature rose to 90 °C (Figure 4-13c). Thus, Pc-based molecular liquids exhibited a significant change of viscosity in response to the changes of temperature and shear force.

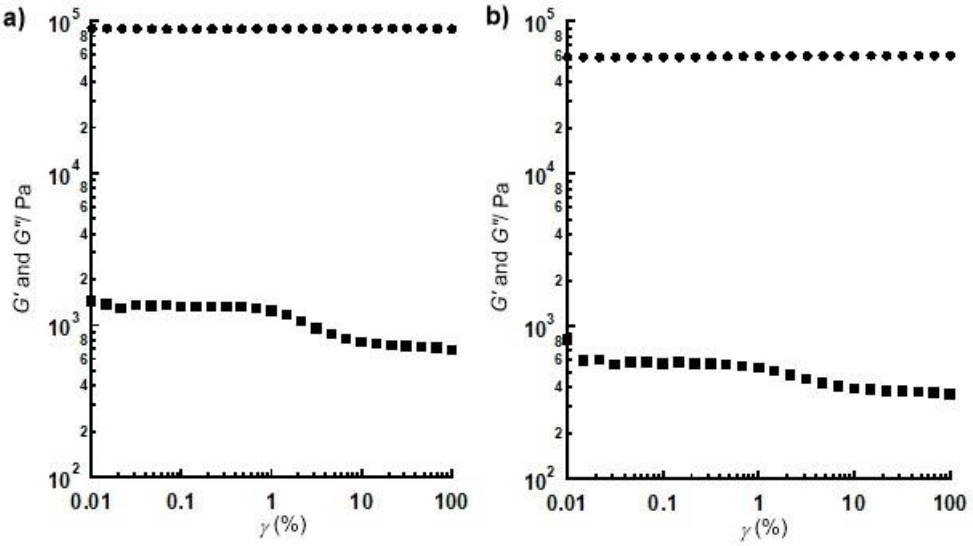

Figure 4-12. Storage elastic modulus (G': ■) and viscous loss modulus (G'': ●) vs. strain amplitude (γ) for **1** (a) and **2** (b).

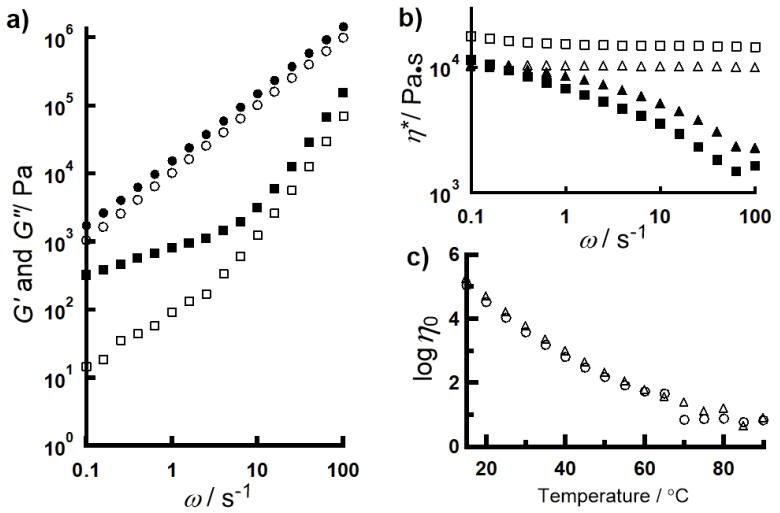

Figure 4-13. a) Storage elastic modulus (G') and viscous loss modulus (G'') vs. angular frequency (ω) on double logarithmic scale at 25°C (γ = 0.1%). ●: G'' for **1**, ■: G' for **1**, ○: G'' for **2**, □: G' for **2**. b) Complex viscosity (η^*) vs. ω on double logarithmic scale. □: **1** (γ = 0.1%), ■: 1 (γ = 50%), △: **2** (γ = 0.1%), ▲: **2** (γ = 50%). c) Plots of log η_0 vs. temperature at γ = 0.1% for **1** (△) and **2** (○).

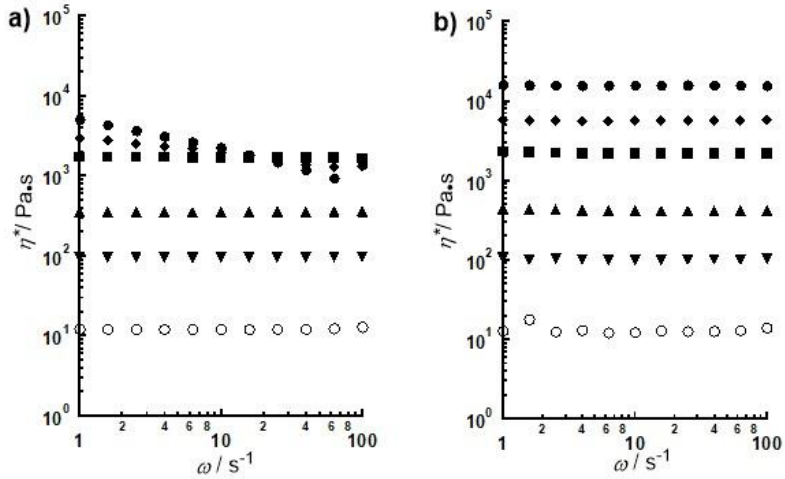

Figure 4-14. Complex viscosity (η^*) vs. angular frequency (ω) for **1** at γ = 50% (a) and 0.1% (b). ●: 25 ºC, ♦: 30 ºC, ■: 35 ºC, ▲: 45 ºC, ▼: 55 ºC, ○: 75 ºC.

4.4. Conclusion

In summary, we have investigated the rheological properties of Pc-based molecular liquids. The highly viscous liquids displayed only a glass transition at below 10 °C. The absorption spectra revealed the formation of face-to-face aggregations. Furthermore, SAXS patterns did not show the reflection from the long-range stacking distance. From these results, we can conclude that **1** and **2** form short rod-like nanoaggregates made of π-π stacks, and the aggregates were thermally stable. Rheological analyses revealed their liquid-like behavior, and significant viscosity changes by external inputs of temperature and shear force.

We propose a mechanism of the stimuli-responsive rheological properties observed for Pc-based molecular liquids schematically illustrated in Figure 4-15. First, monomeric Pcs aggregate into the short stacks with face-to-face conformations. Second, these stacks entangle each other and organize large rod-like clusters as observed in the broad SAXS reflection corresponding to the molecular diameter of the rigid Pc core. This is one reason for the high viscosities of **1** and **2**. The size of the cluster is reduced by increasing the temperature or shear force, and the viscosities dramatically decrease as a response to these external inputs. The alkylated-π FMLs have great potential for the fabrication of optoelectronic molecular devices.[15] The near-IR absorbing Pc-based molecular liquids with unique rheological properties will provide new opportunities for realizing these devices utilizing the near-IR light region.

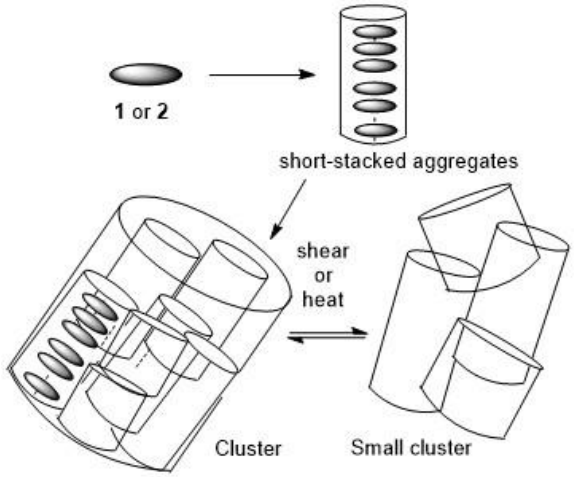

Figure 4-15. Stimuli-responsive structural change in Pc-based molecular liquids.

References

1. S. S. Babu, T. Nakanishi, *Chem. Commun*., 2013, **49**, 9373.
2. S. Laschat, A. Baro, N. Steinke, F. Giesselmann, C. Hägele, G. Scalia, R. Judele, E. Kapatsina, S. Sauer, A. Schreivogel, M. Tosoni, *Angew. Chem. Int. Ed*., 2007, **46**, 4832.
3. a)T.Michinobu, T. Nakanishi, J. P. Hill, M. Funahashi, K. Ariga, *J. Am. Chem. Soc*., 2006, **128**, 10384. b) S. S. Babu, J. Aimi, H. Ozawa, N. Shirahata, A. Saeki, S. Seki, A. Ajayaghosh, H. Möhwald, T. Nakanishi, *Angew. Chem., Int. Ed*., 2012, **51**, 3391. c) S. S. Babu, M. J. Hollamby, J. Aimi, H. Ozawa, A. Saeki, S. Seki, K. Kobayashi, K. Hagiwara, M. Yoshizawa, H. Möhwald, T. Nakanishi, *Nat. Commun.* 2013, **4**, 1969. d) C. Allain, J. Piard, A. Brosseau, M. Han, J. Paquier, T. Marchandier, M. Lequeux, C. Boissière, P. Audebert, *ACS Appl. Mater. Interfaces,* 2016, **8**, 19843. e) F. Lu, T. Takaya, K. Iwata, I. Kawamura, A. Saeki, M. Ishii, K. Nagura, T. Nakanishi, *Sci. Rep.,* 2017, **7**, 3416.
4. *Phthalocyanines: Properties and Applications*, ed. by. C. C. Leznoff, A. B. P. Lever, VCH, Weinheim, Germany, 1989, Vol. 14.
5. W.Pisula, X. Feng, K. Müllen, *Adv. Mater.*, 2010, **22**, 3634.
6. a) K. Ohta, H.-D. Nguyen-Tran, L. Tauchi, Y. Kanai, T. Megumi, Y. Takagi, in *Handbook of Porphyrin Science*, ed. by K. M. Kadish, K. M. Smith, R. Guilard, Word Scientific, Singapore, 2010, Vol. 12, Chap. 53, pp. 1120. b) T. Basova, A. Hassan, M. Durmuƒ, A. G. Gürek, V. Ahsen, *Coord. Chem. Rev*. 2016, **310**, 131. c) R. D. George, A. W. Snow, *Chem. Mater.,* 1994, **6**, 1587. d) M. Brewis, G. J. Clarkson, M. Helliwell, A. M. Holder, N. B. McKeown, *Chem.-Eur. J*., 2000, 6**,** 4630. e) N. Zharnikova, N. Usol'tseva, E. Kudrik, M. Thelakkat, *J. Mater. Chem.,* 2009*,* **19**, 3161.
7. a) E. M. Maya, J. S. Shirk, A. W. Snow, G. L. Roberts, *Chem. Commun*., 2001, 615. b) E. M. Maya, A. W. Snow, J. S. Shirk, R. G. S. Pong, S. R. Flom, G. L. Roberts, *J. Mater. Chem.*, 2003, **13**, 1603. c) E. M. Maya, A. W. Snow, J. S. Shirk, S. R. Flom, R. G. S. Pong, J. H. Callahan, *J. Porphyrins Phthalocyanines,* 2002, **6**, 463. d) M. Durmuş, C. Lebrun, V. Ahsen, *J. Porphyrins Phthalocyanines,* 2004, **8**, 1175. e) A. G. Gürek, M. Durmus, V. Ahsen, *New J. Chem.,* 2004, **28**, 693. f) M. Ichihara, A. Suzuki, K. Hatsusaka, K. Ohta, *J. Porphyrins Phthalocyanines,* 2007, **11**, 503.
8. N. Kobayashi, A. B. P. Lever, *J. Am. Chem. Soc*., 1987, **109**, 7433.
9. H. Sato, K. Igarashi, Y. Yama, M. Ichihara, E. Itoh, K. Ohta, *J. Porphyrins Phthalocyanines*, 2012, **16**, 1148.
10. K. Hatsusaka, K. Ohta, I. Yamamoto, H. Shirai, *J. Mater. Chem.,* 2001, **11**, 423.
11. K. Ohta, T. Watanabe, S. Tanaka, T. Fujimoto, I. Yamamoto, P. Bassoul, N. Kucharczyk, J. Simon, *Liq. Cryst*., 1991, **10**, 357.
12. M. Morisue, I. Ueno, T. Nakanishi, T. Matsui, S. Sasaki, M. Shimizu, J. Matsui, Y. Hasegawa, *RSC Adv*., 2017, **7**, 22679.
13. H. Watanabe, Y. Matsumiya, Q. Chen, W. Yu, in *Polymer Science: A Comprehensive Reference*,

ed. By K. Matyjaszewski, M. Möller, Elsevier, Amsterdam, Netherlands, 2012, Vol. 2, Chap. 28, pp. 683722.

14. a) H.-N. Xu, Y.-Y. Tang, X.-K. Ouyang, *Langmuir*, 2017, **33**, 235. b) K. Tsuchiya, Y. Orihara, Y. Kondo, N. Yoshino, T. Ohkubo, H. Sakai, M. Abe, *J. Am. Chem. Soc.*, 2004, **126**, 12282. c) L. Rose J., B. V. R. Tata, V. K. Aswal, P. A. Hassan, Y. Talmon, L. Sreejith, *Eur. Phys. J. E*, 2015, **38**, 4. d) A. Narayanan, F. Mugele, M. H. G. Duits, *Langmuir* 2017, **33**, 1629. e) J. S. Weston, D. Venkataramani, C. P. Aichele, B. P. Grady, J. Harwell, D. Resasco, *Langmuir*, 2014, **30**, 14982.
15. a) S. Hirata, K. Kubota, H. H. Jung, O. Hirata, K. Goushi, M. Yahiro, C. Adachi, *Adv. Mater.* 2011, **23**, 889. b) P. Duan, N. Yanai, N. Kimizuka, *J. Am. Chem. Soc*., 2013, **135**, 19056.

Chapter 5

A near-infrared fluorescent phthalocyanine liquid developed through controlling intermolecular interactions

Summary: Novel liquid phthalocyanines **1** and **2** were synthesized, and the correlation between their molecular structure and intermolecular interactions in the solvent-free state was investigated. H-aggregates were formed in **1**, and a monomeric non-aggregate state emitting in the near-infrared (NIR) spectral range was developed in **2**, enabling its application in NIR-technology.

5.1. Introduction

A combination of π-conjugated units and flexible units such as alkyl chains produces functional soft materials such as optoelectronically-active gels, [1] polymers, [2] and liquid crystals.[3] In particular, solvent-free functional molecular liquids (FMLs) have emerged as a new class of soft materials due to their non-volatility, processability, free deformability, improved stability to oxidation, solvent-like functions, and other properties. [4] One of the fascinating features of FMLs is their luminescence property in the liquid state. Various solvent-free luminous molecular liquids (LMLs)[5] have been reported over the past decade, which are regarded as good candidates for active components in light-emitting devices. [6, 7] In this context, development of near-infrared (NIR) luminous solvent-free liquids is an attractive avenue for realizing conversion systems of photon energy in the NIR spectral region[8] and light- weight/bendable/wearable light-emitting device[9] applicable in biomedicine and biosensing. However, most of the LMLs reported so far were composed of a relatively small π-conjugate molecular unit with branched alkyl side chains and exhibited luminescence limited to the visible light region. Most of the molecules with NIR absorption and luminescence have a rigid planar structure due to their large π-conjugation.[10] Therefore, precise control of molecular interactions in the liquid state is required for sufficient isolation of the large π-unit to avoid self-quenching of the emission due to the formation of face-to-face (H-) aggregates. For these reasons, development of NIR LMLs is quite challenging. As a good reference example, a molecular design focusing on the control of π-π interactions in the liquid state was developed by using the pyrene core as a fluorescent probe.[11] Recently, intermolecular interactions in liquid porphyrins have been successfully tuned on the basis of alkyl-π engineered molecular design.[12] Peripheral modification of a large π-conjugated unit with bulky yet flexible alkyl side chains could be a potential methodology for developing solvent-free NIR LMLs.

Phthalocyanines (Pcs) have been paid much attention for their NIR absorption and potential application in luminous dyes due to their photo- and chemical stability, tunability of their absorption and emission properties through structural modification, and complexation with various metals.[13] There are several reports on liquefaction of Pcs.[14] However, H-aggregates were noticed in their solvent-free liquid state, which are not desirable for NIR luminous properties. Dendrons have been used as axial or peripheral substituents of Pcs for suppressing face-to-face π-π interactions among Pc cores in the condensed state.[15, 16] In this approach, isolation of the Pc unit was successful, but liquefaction and NIR emission were not. In addition, six-coordinate central metals such as silicon and ruthenium were used, and much effort was required to synthesize the entire molecule. Therefore, liquefaction and isolation of the Pc core through structural modification of a metal-free Pc (H_2Pc) would be a priority in developing solvent-free NIR LMLs.

We designed H_2Pc **1** and **2** with bulky yet flexible 3,5- or 2,5-di(2-hexyldecyloxy)phenyl groups[11, 12] at non-peripheral (α)-positions[17] on a Pc ring for effective liquefaction of the molecules and isolation of the Pc unit (Scheme 5-1); we aim to clarify their aggregation properties. We discuss how the substituent pattern at the α-position on the Pc ring and the aggregation structure correlate, as well as the NIR fluorescence properties in the solvent-free liquid state.

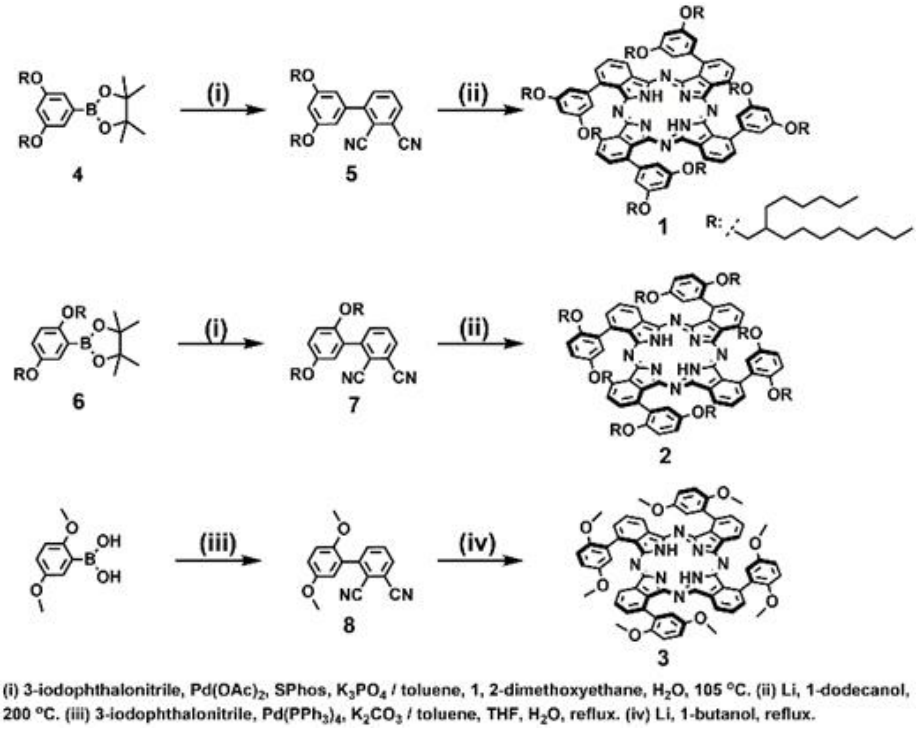

Scheme 5-1. Molecular structure and synthetic route for **1**, **2,** and **3**.

5.2. Experimental

5.2.1. Materials

All commercial available chemicals were used without further purifications unless otherwise noted. 4A molecular sieves and potassium acetate (AcOK) were dried at 200 °C *in vacuo* in prior to use. 1-Butanol and 1-dodecanol for synthesis of phthalocyanines was dried over 4A molecular sieves in prior to use. 2-Dicyclohexylphosphino-2′,6′-dimethoxybiphenyl (Sphos) and tetrakis(triphenylphosphine)palladium (0) ($Pd(PPh_3)_4$) were purchased from Sigma Aldrich. Palladium acetate ($Pd(OAc)_2$), dichlorobis-(triphenylphosphine)palladium (II) ($PdCl_2(PPh_3)_2$), AcOK, tripotassium phosphate (K_3PO_4), potassium carbonate (K_2CO_3), Li metal, and all solvents were purchased from WAKO pure chemical. Bis(pinacolato)diboron was purchased from Matrix Scientific. 2-Hexyldecylbromide and 2, 5-dimethoxyphenyl boronic acidwerepurchased from Tokyo Chemical Industry.

5.2.2. Synthesis

3,5-Di(2-hexyldecyloxy)benzeneboronic acid pinacol ester (4 in **Scheme 5-1)[11]**

The title compound was prepared by palladium-catalyzed Miyaura-Ishiyama borylation.[18] A flask containing 3,5-di(2-hexyldecyloxy)bromobenzene[11] (612mg, 0.960 mmol), AcOK (280 mg, 2.85 mmol, 3eq.), bis(pinacolato)diboron (B_2pin_2) (366 mg, 1.43 mmol, 1.5eq.) and $PdCl_2(PPh_3)_2$(73mg, 0.095 mmol, 0.1eq.) was filled with Ar. Deoxygenaized dioxane (3.2 mL) was added to the mixture with syringe through septum. The mixture was heated at 80 °C for 72 h. After cooling to r.t, the reaction mixture was diluted with *n*-hexane. This mixture was filtrated to remove insoluble chemicals. The filtrate was washed with water and brine. The organic layer was dried over Na_2SO_4. After filtration, the solvent was evaporated *in vacuo*. The crude product was purified with recycling preparative HPLC ($CHCl_3$) to obtain colorless oil. Yield: 67%

^{1}H-NMR (400.13 MHz, $CDCl_3$) δ (ppm): 6.92(d, *J* = 2.4 Hz, Ar*H*, 2H), 6.56(t, *J* = 2.2 Hz, Ar*H*, 1H), 3.84(d, *J* = 5.6 Hz, -OCH_2-, 4H), 1.74(brs, -OCC*H*-, 2H), 1.43-1.27(m, -(CH_2)$_{12}$-and -CH_3 of pinacol unit, 60H), 0.90-0.86(m, -CH_3, 12H).

^{13}C-NMR (100.16 MHz, $CDCl_3$) δ (ppm):160.65, 112.63, 105.35, 84.15, 71.07, 38.54, 32.35, 32.32, 32.30, 31.88, 30.47, 30.14, 30.04, 29.77, 27.31, 25.25, 23.11, 14.52.

HR-APCI-TOF-Mass (positive) found *m/z*: 683.6046, calcd. for $C_{44}H_{81}O_4B$ *m/z*: 683.6259 $[M]^+$.

2,5-Di(2-hexyldecyloxy)benzeneboronic acid pinacol ester (6 in **Scheme 5-1)[11]**

The synthetic method was the same for that of **4**. 2,5-di(2′-hexyldecyloxy)bromobenzene[11] was used as the starting material instead of 3,5-di(2-hexyldecyloxy)bromobenzene. The target compound was obtained as colorless oil. Yield: 51%

^{1}H-NMR (400.13 MHz, $CDCl_3$) δ (ppm): 7.18(d, *J* = 3.2 Hz, Ar*H,* 1H), 6.89(dd, *J* = 3.2, 5.6 Hz, Ar*H*, 1H), 6.75(d, *J* = 9. 2Hz, Ar*H*, 1H), 3.78(d, *J* = 5.2 Hz, -OCH_2-, 4H), 1.78-1.56(m, -OCC*H*-, 2H), 1.54-1.32(m, -(CH_2)$_{12}$-and -CH_3 of pinacol unit, 60H), 0.89-0.86(m, -CH_3, 12H).

^{13}C-NMR (100.16 MHz, $CDCl_3$) δ (ppm):158.61, 153.34, 122.33, 118.68, 115.78, 113.18, 83.70, 72.18, 71.81, 38.77, 38.60, 32.35, 32.33, 32.30, 31.83, 31.58, 30.59, 30.13, 30.09, 30.02, 29.79, 29.76, 27.36,27.32, 27.29, 25.31, 23.09, 14.52.

HR-APCI-TOF-Mass (positive) found *m/z*: 683.6341, calcd. for $C_{44}H_{81}O_4B$ *m/z*: 683.6259 $[M]^+$.

3-[3′,5′-Di(2-hexyldecyloxy)phenyl)phthalonitrile (5 in **Scheme 5-1)**

The title compound was prepared by palladium-catalyzed Suzuki-Miyaura coupling in using SPhos as a ligand.[19] The reaction condition was followed to previous report.[20] A flask containing 3-iodophthalonitrile[21] (118 mg, 0.454 mmol, 1.3eq.), 3,5-Di(2-hexyldecyloxy)benzeneboronic acid pinacol ester(**4**) (245 mg, 0.358 mmol), K_3PO_4 (310 mg, 1.40 mmol, 4eq.), $Pd(OAc)_2$(14 mg, 0.035 mmol, 0.1eq.) and SPhos (29 mg, 0.070 mmol, 0.2eq.) was filled with Ar. 6.9 mL of deoxygenaized

mixed solvent (toluene / 1, 2-dimethoxyehane (DME) / H_2O, 1:1:2, v/v/v) was added to the mixture with syringe through septum. The mixture was refluxed for 72 h. The reaction mixture was cooled to r.t, and extracted with ethyl acetate. The organic layer was washed with water and brine. The organic layer was dried overNa_2SO_4. After filtration, the solvent was evaporated *in vacuo*. The crude product was purified with silica gel column chromatography (R_f = 0.33, AcOEt: *n*-hexane = 1: 15, v/v) and recycling preparative HPLC ($CHCl_3$) to obtain as colorless oil. Yield: 65%

^{1}H-NMR (400.13 MHz, $CDCl_3$) δ (ppm): 7.82-7.73(m, Ar*H*, 3H), 6.65-6.59(m, Ar*H*, 3H), 3.89(d, *J* = 7.2 Hz, -OC*H*$_2$-, 4H), 1.81-1.78(m, -OCC*H*-, 2H), 1.49-1.30(m,-(C*H*$_2$)$_{12}$-, 48H), 0.92-0.88(m, -C*H*$_3$, 12H).

^{13}C-NMR (100.16MHz, $CDCl_3$) δ (ppm):160.86, 147.54, 137.98, 134.04, 132.68, 132.01, 117.27, 115.71, 115.15, 114.50, 107.24, 102.54, 71.23, 37.97, 31.91, 31.86, 31.37, 30.01, 29.68, 29.58, 29.33, 26.85, 26.83, 22.68, 14.11.

HR-APCI-TOF-Mass (negative) found *m/z*: 684.5661, calcd. for $C_{46}H_{72}N_2O_2$ *m/z*: 684.5588 $[M]^-$.

FT-IR (ATR) *v*/ cm^{-1}: 2233.57 (-CN)

3-[2′,5′-Di(2-hexyldecyloxy)phenyl]phthalonitrile (7 in **Scheme 5-1)**

The synthetic method and purifications were the same for that of **5.** 2,5-Di(2-hexyldecyloxy)benzeneboronic acid pinacol etster (**6**) was used as the starting material instead of 3, 5-di(2′-hexyldecyloxy)benzeneboronic acid pinacol ester. The target compound was obtained as colorless oil. Yield: 45% TLC (silica gel): R_f = 0.55 (AcOEt: *n*-hexane = 1: 30, v/v)

^{1}H-NMR (400.13 MHz, $CDCl_3$) δ (ppm): 7.76-7.67(m, Ar*H*, 3H), 6.97-6.91(m, Ar*H*, 2H), 6.82(d, *J* = 2.8Hz, Ar*H*, 1H), 3.80-3.79(m, -OC*H*$_2$-, 4H), 1.77-1.73(m, -OCC*H*-, 1H), 1.62(brs, -OCC*H*-, 1H), 1.46-1.18(m,-(C*H*$_2$)$_{12}$-, 48H), 0.90-0.85(m, -C*H*3, 12H).

^{13}C-NMR (100.16 MHz, $CDCl_3$) δ (ppm):153.67, 150.35, 145.12, 135.62, 132.45, 132.06, 126.64, 117.18, 117.11, 116.70, 116.16, 115.49, 113.86, 72.18, 38.47, 38.32, 32.31, 32.26, 32.21, 31.86, 31.77, 30.43, 30.39, 30.10, 30.04, 29.97, 29.73, 27.23, 27.15, 23.08, 14.51.

HR-APCI-TOF-Mass (negative) found *m/z*: 684.5552, calcd. for $C_{46}H_{72}N_2O_2$*m/z*: 684.5588 $[M]^-$.

FT-IR (ATR) *v*/ cm^{-1}: 2233.55 (-CN)

3-(2′,5′-Dimethoxyphenyl)phthalonitrile (8 in **Scheme 5-1)**

A flask containing 3-iodophthalonitrile[21] (401 mg, 1.58 mmol), 2,5-dimethoxyphenylboronic acid (373 mg, 2.05 mmol), K_2CO_3 (468 mg, 3.39 mmol) and $Pd(PPh_3)_4$ (181 mg, 0.156 mmol) was filled with Ar. Degassed mixed solvent (5.6ml, toluene/THF/H_2O (3: 1: 1.6, v/v/v))was added to the mixture. The mixture was refluxed for 36 h under Ar atmosphere. The reaction mixture was cooled to room temperature, and extracted with ethyl acetate. The organic layer was washed with water and brine, and dried over Na_2SO_4. After filtration, the solvent was evaporated *in vacuo*. The crude product was

purified with column chromatography (SiO_2, eluent: CH_2Cl_2: AcOEt = 20: 1) and recycling preparative HPLC ($CHCl_3$) to obtain a white solid (62%).

^{1}H-NMR (400.13 MHz, $CDCl_3$); δ (ppm): 7.77-7.69(m, Ar*H*, 3H), 6.97(m, Ar*H*, 2H), 6.81-6.80(m, Ar*H*, 1H), 3.78(s, -OC*H*$_3$, 3H), 3.77(s, -OC*H*$_3$, 3H).

^{13}C-NMR (100.16 MHz, $CDCl_3$); δ (ppm): 154.03, 150.80, 144.58, 135.66, 133.24, 132.34, 126.44, 116.86, 116.83, 116.71, 116.43, 116.39, 115.78, 113.04, 56.35, 56.28.

HR-APCI-TOF-Mass (negative); found *m/z*: 264.0880, calcd. for $C_{16}H_{12}O_2N_2$ *m/z*: 264.0893 $[M]^{-\cdot}$

FT-IR (ATR); *v* /cm^{-1}: 2233.57 (-CN).

1, 8, 15, 22-Tetra[3′,5′-di(2-hexyldecyloxyphenyl)]phthalocyanine (1 in **Scheme 5-1)**

The title compound was prepared by Linstead's method.[22] Li metal (27 mg, 3.9 mmol) was dissolved in dry 1-dodecanol (3.5 mL) at 100 °C under Ar. After Li was perfectly dissolved, the mixture was cooled to r.t. To this mixture 3-[3′,5′-di(2-hexyldecyloxyphenyl)]phthalonitrile (**5**) (239mg, 0.349 mmol) was added. The mixture was heated at 200 °C for 10h under Ar. After cooling to r.t, the reaction mixture was diluted with methanol. The precipitate was collected with filtration and residue was washed with methanol several times. The crude product was purified with column chromatography (Al_2O_3/ CH_2Cl_2, R_f =1.0). Further purification was carried out with recycling preparative HPLC ($CHCl_3$). The title Pc derivative was obtained as dark green viscous oil. Yield: 29%

^{1}H-NMR (400.13 MHz, $CDCl_3$) δ (ppm): 8.87(dd, *J* = 2.0, 3.2 Hz, $H_{Pc\text{-}\alpha}$, 4H), 8.10-8.07(m, $H_{Pc\text{-}\beta}$, 8H), 7.41(d, *J* = 2.0 Hz, Ar*H*,8H), 6.97(t, *J* = 2.2 Hz, Ar*H,* 4H), 3.99(d, *J* = 5.6 Hz, -OC*H*$_2$-, 16H), 1.81(quin, *J* = 6.0 Hz, -OCC*H*-, 8H), 1.46-0.61(m, aliphatic -C*H*$_2$-, 240H), -0.23(s, -N*H,* 2H).

HR-APCI-Mass (negative) found *m/z*: 2740.2675, calcd.for $C_{184}H_{290}N_8O_8$ *m/z*: 2740.2526 $[M]^-$.

UV-vis (in $CHCl_3$): λ_{max} /nm (logε) = 715(4.99), 681 (4.96), 653 (4.55), 619(4.38), 341(4.79).

Fluorescence (in $CHCl_3$, λ_{ex} = 625 nm): λ_{FL} = 718 nm.

1, 8, 15, 22-Tetra[2′,5′-di(2-hexyldecyloxyphenyl)]phthalocyanine (2 in **Scheme 5-1)**

The synthetic method and purifications were the same for that of **1**. 2′,5′-Di(2-hexyldecyloxy-phenyl)]phthalonitrile (**7**) was used as the starting material instead of **5.** The title Pc derivative was obtained as dark green oil. Yield: 6%

^{1}H-NMR (400.13 MHz, $CDCl_3$) δ (ppm): 8.72(br, $H_{Pc\text{-}\alpha}$, 4H), 8.04(br, $H_{Pc\text{-}\beta}$, 8H), 7.58-7.29(m, Ar*H,* 12H), 3.99-3.59(m, -OC*H*$_2$-, 16H), 1.83(br, *exo*-OCC*H*-, 4H), 1.48-0.15(m, aliphatic -C*H*$_2$-, 244H), -0.51(s, -N*H,* 2H).

HR-APCI-Mass (negative) found *m/z*: 2740.2132, calcd.for $C_{184}H_{290}N_8O_8$ *m/z*: 2740.2526 $[M]^-$.

UV-vis (in $CHCl_3$): λ_{max} /nm (logε) = 707(5.05), 673 (5.00), 646(4.54), 611(4.37), 346(4.75).

Fluorescence (in $CHCl_3$, λ_{ex} = 625nm): λ_{FL} =709 nm.

1, 8, 15, 22-Tetra(2′,5′-dimethoxyphenyl)phthalocyanine (3 in **Scheme 5-1)**

Li metal (13 mg, 1.9 mmol) was dissolved in dry 1-butanol (3.8 mL) at 70 °C under Ar. The mixture was cooled to room temperature, and 3-(2′,5′-dimethoxyphenyl)phthalonitrile (**8)** (100 mg, 0.378 mmol) was added to this mixture. The mixture was refluxed for 4h under Ar. After cooling to room temperature, the reaction was quenched with acetic acid and methanol. The precipitate was collected with filtration, and washed with methanol for several times. The crude product was purified with the recrystallization (CH_2Cl_2/ acetone) to isolate C_{4h}-regioisomer, and the precipitated solid was collected with filtration. Yield: 13%

^{1}H-NMR (400.13 MHz, $CDCl_3$); δ (ppm): 8.70(d, J = 7.2 Hz, $H_{Pc\text{-}\alpha}$, 4H), 8.11 (t, J = 7.4Hz, $H_{Pc\text{-}\beta}$,4H), 8.05 (d,J = 7.2 Hz, $H_{Pc\text{-}\beta}$, 4H), 7.48-7.33(m, ArH,12H), 3.96(s, -OCH_3,12H), 3.48(brs, -OCH_3,12H), -0.49(s, -NH, 2H).

HR-APCI-TOF-Mass (negative); found *m/z*: 1058.3760, calcd. for $C_{64}H_{50}N_8O_8$ *m/z*: 1058.3746 $[M]^-$.

UV-Vis (in $CHCl_3$): λ_{max} /nm (logε) = 707(5.09), 672 (5.06), 643 (4.60), 610 (4.44), 346 (4.81).

Fluorescence (in $CHCl_3$, λ_{ex} = 625 nm): λ_{FL} = 709 nm.

5.3. Results and discussion

5.3.1. Synthesis

H_2Pc **1** and **2** were synthesized according to Scheme 5-1. The phthalonitrile precursors **5** and **7** for **1** and **2**, respectively, were synthesized by Suzuki-Miyaura coupling between 3-iodophthalonitrile and the corresponding boronic acid esters (**4** and **6**) in the presence of palladium acetate and Buchwald ligand (SPhos)[19]. **1** and **2** were obtained through cyclotetramerization of **5** and **7**, respectively, in the presence of lithium alkoxide.[22] The reaction is usually conducted in the presence of 1-butanol, pentanol, or hexanol; however, cyclotetramerization of **5** and **7** did not proceed in the presence of 1-hexanol due to the presence of a bulky substituent near the nitrile groups. Therefore, 1-dodecanol was chosen as a solvent with a higher boiling point, which achieves cyclotetramerization of **5** and **7**. The crude product of **1** and **2** was purified with Al_2O_3 column chromatography and recycling preparative high performance liquid chromatography in conjunction with a size-exclusive column to obtain a dark green oil. The mass spectrometry of **1** and **2** showed $[M]^+$ peaks at *m/z* 2740.2675 and 2740.2132, respectively, which agrees with their calculated molecular weights. Cyclotetramerization of the 3-substituted phthalonitrile provides four possible regioisomers of the Pc.[23] The ^{1}H NMR spectrum of **1** shows simple peaks (Figure 5-1). This suggests that **1** was obtained as a single regioisomer. The ^{1}H NMR spectrum of **2** was also simple (Figure 5-2), which suggests the formation of a single regioisomer. Steric repulsion between bulky substituents on the 3-position in phthalonitriles can control the distribution of the Pc regioisomer during cyclotetramerization, which provides a single regioisomer of C_{4h}-symmetry.[24] Considering these early studies and the molecular structure of phthalonitriles **5** and **7**

with bulky substituents, it was assumed that **1** and **2** were composed of a single C_{4h}-symmetrical isomer. The proton resonance of methylene protons in –OCH_2– among branched alkyl chains shifted up-field and broadened, as compared with that of **1**. This result suggests that the presence of conformational isomer originated from a rotational barrier of the asymmetrical 2,5-substitution pattern on the phenyl side groups; the chemical shifts of the methylene groups near the Pc core are affected by a ring-current effect of π-conjugated units (Figure 5-2 and 5-3).[11, 12] Thermogravimetric analysis (TGA) was performed for **1** and **2** to confirm the absence of impurities such as solvents, by-products, and unreacted precursors (Figure 5-4). In both TGA results, only decomposition-triggered weight losses were observed around 360 and 400 °C for **1** and **2**, respectively. Therefore, the fluid states as shown in Figure 5-6a and 5-6b are intrinsic properties of pure **1** and **2** without contamination of residual solvents and impurities. **3** was synthesized as a control sample for evaluating the difference of steric wrapping of the Pc core; it was purified with recrystallization to isolate the C_{4h}-symmetrical isomer (Figure 5-5), and obtained as a solid.

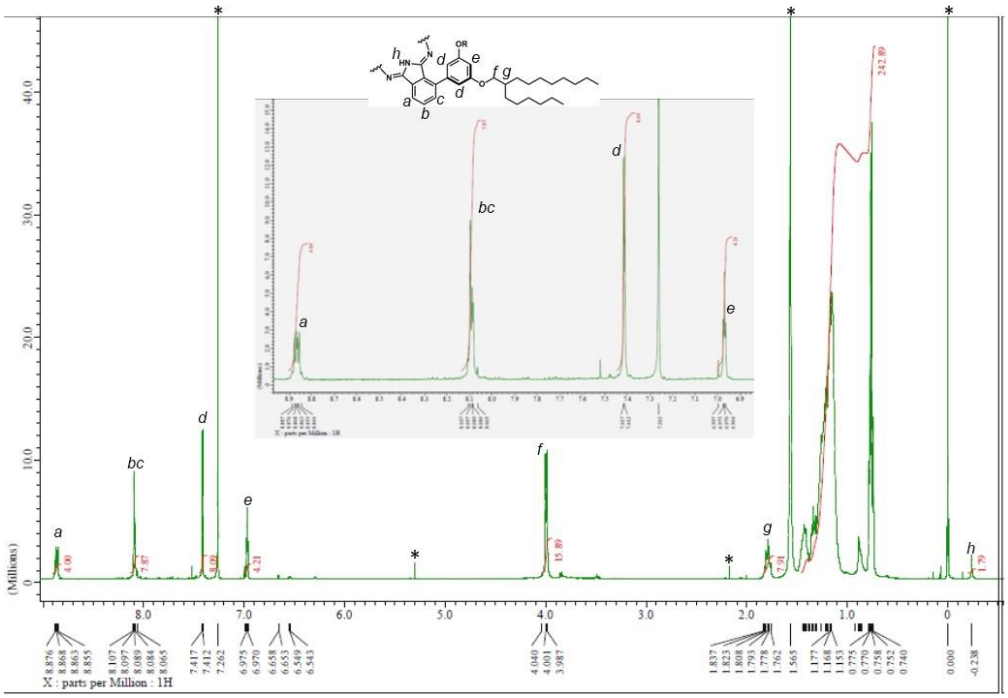

Figure 5-1. ^{1}H NMR spectrum of **1** in $CDCl_3$. Peaks marked with asterisk denote residual solvent and internal standard.

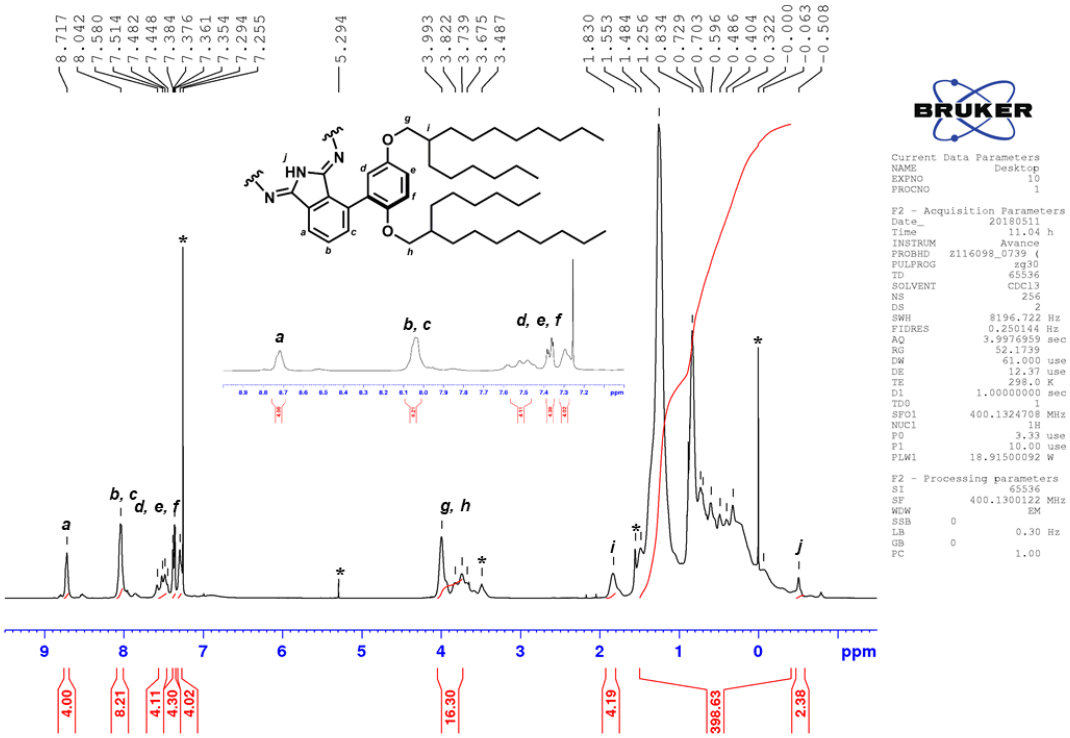

Figure 5-2. ^{1}H NMR spectrum of **2** in $CDCl_3$. Peaks marked with asterisk denote residual solvents and internal standard.

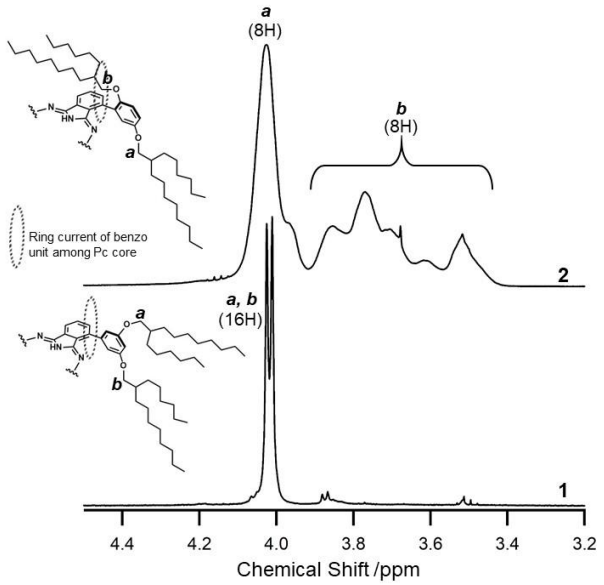

Figure 5-3. Selected region of ^{1}H NMR spectra for **1** (lower) and **2** (upper) in $CDCl_3$. Insets mean side group conformation relative to Pc core.

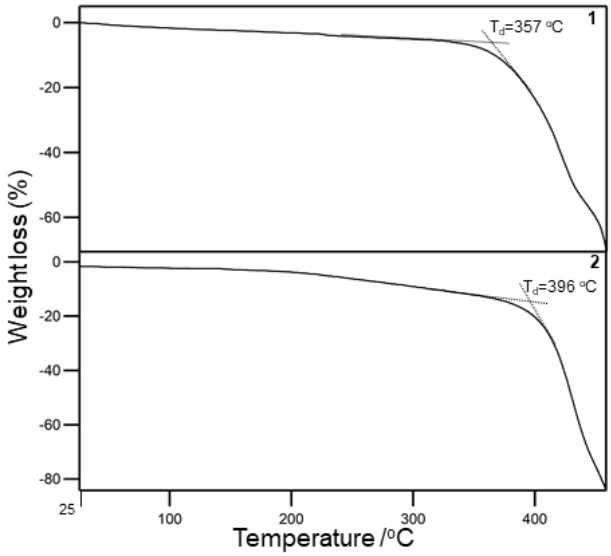

Figure 5-4. Thermogravimetric analysis curve for **1**and **2** (under N_2 atmosphere, scan rate 10 °C /min).

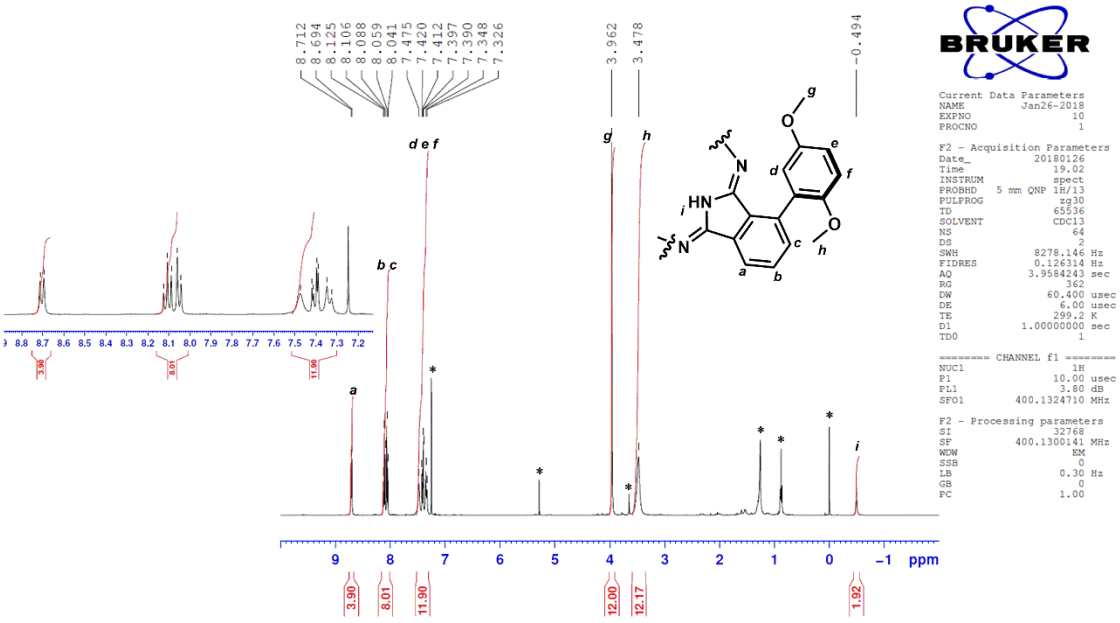

Figure 5-5. ^{1}H NMR spectrum for **3** in $CDCl_3$. Peaks marked with asterisk denote residual solvents and internal standard.

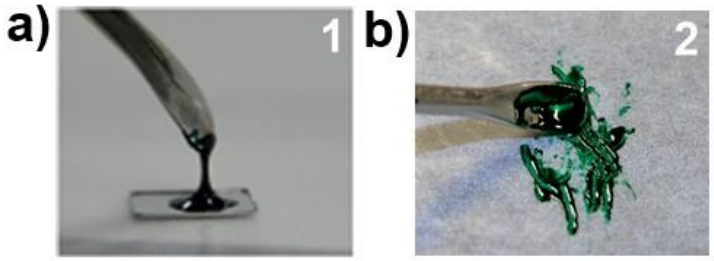

Figure 5-6. a) and b) Photographs of **1** and **2** as viscous fluids.

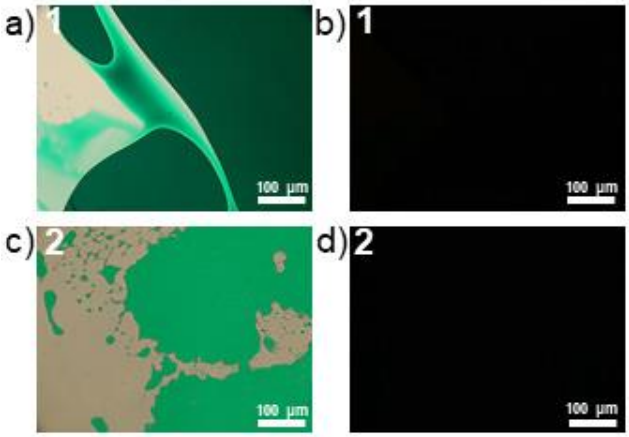

Figure 5-7. Polarizing optical microscopic images for **1**and **2** at room temperature. Images a) and c) were taken under open polarizer. Images b) and d) were taken under crossed polarizer.

5.3.2. Amorphous feature

No birefringence was observed for **1** and **2** even though these samples were sheared or pushed under polarizing optical microscope observation, revealing the absence of optically long-range-ordered structures (Figure 5-7).[14] Differential scanning calorimetry (DSC) analysis was performed for **1** and **2** to identify their thermal phase transition behavior (Figure 5-8 and 5-9). **1** and **2** showed only a broad shift of the baseline around -45 and -38 °C, respectively, in both the heating and cooling processes, which is a typical signal for glass transition. Thanks to their fluid feature at room temperature, **1** and **2** can be easily painted as solvent-free inks over a quartz plate by rubbing to form green liquid films (Figure 5-10). Figure 5-11 shows X-ray diffraction (XRD) patterns for **1** and **2** of their liquid films at room temperature. A broad reflection at 2θ = 2.8-7.1 degrees having a peak at d = 21 Å was observed, which corresponds to the average distance between the centers of neighboring Pc units.[14] The observed reflection peak is broader than the d_{100} reflections for previously reported liquid crystalline Pcs [25], suggesting that the center-to-center distance and conformations in **1** fluctuate in the solvent-free liquid

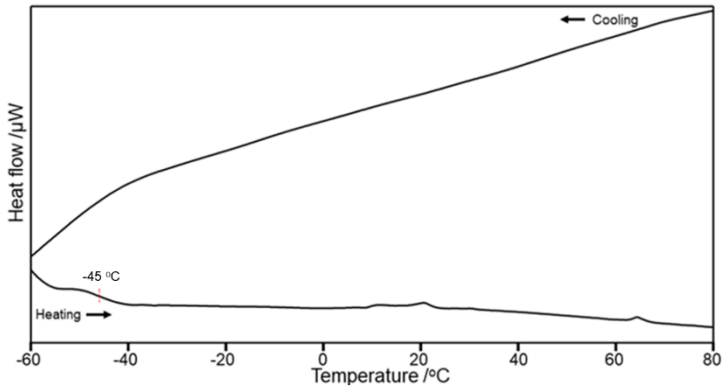

Figure 5-8. DSC profiles for **1** at scan rate 10 °C /min under N_2 flow.

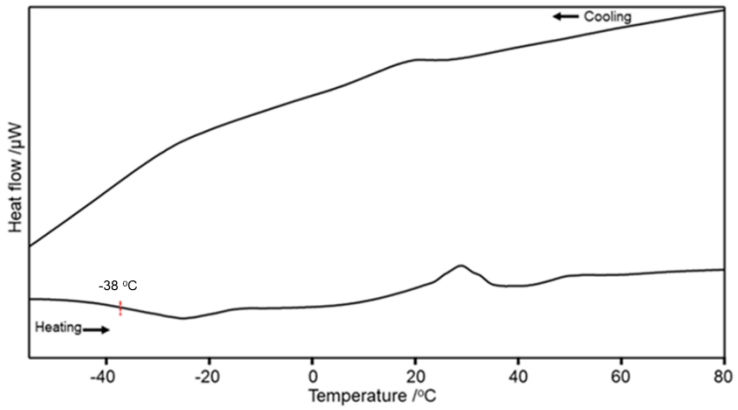

Figure 5-9. DSC profiles for **2** at scan rate 10 °C /min under N_2 flow.

state. The broad halo observed at around 2θ = 15-25 degrees is characteristic of the molten state of alkyl chains. In addition, no intermolecular π-π stacking distance was observed around 2θ = 20 degrees as a peak[14], suggesting the absence of a regular long-range order between the Pc cores through π-π stacking. This XRD pattern reflects the disordered state and the absence of long-range ordered structure in **1**. In contrast, the XRD pattern of **2** did not show clear reflections in the small-angle region, suggesting that the ordering between the centers of neighboring Pc molecules is negligible. It has been concluded that the structural regularity of the aggregates in **1** and **2** in the solvent-free liquid state depends on the substitution pattern of their branched alkyl chains. It can be qualitatively interpreted that **2** has a greater disorder state than **1**.

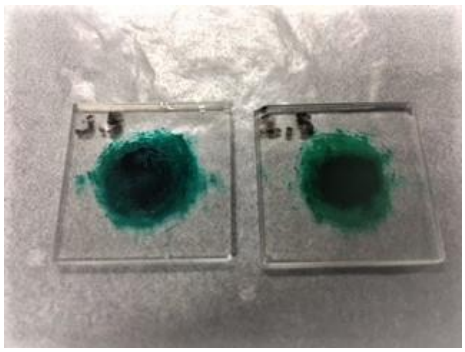

Figure 5-10. Liquid thin film sandwiched by two quartz plates for **1** (left) and **2** (right).

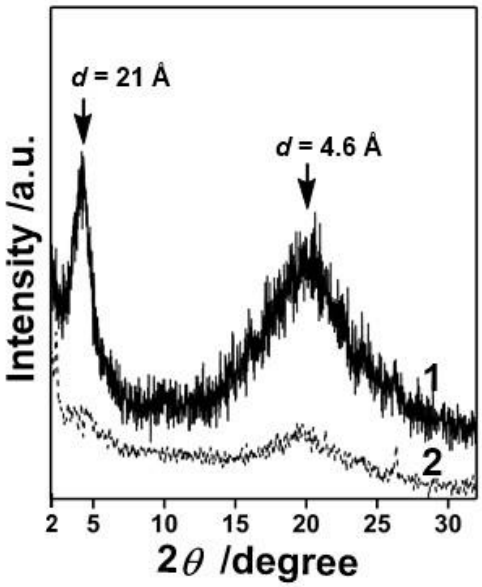

Figure 5-11. XRD patterns for **1** (solid line) and **2** (dashed line) at room temperature.

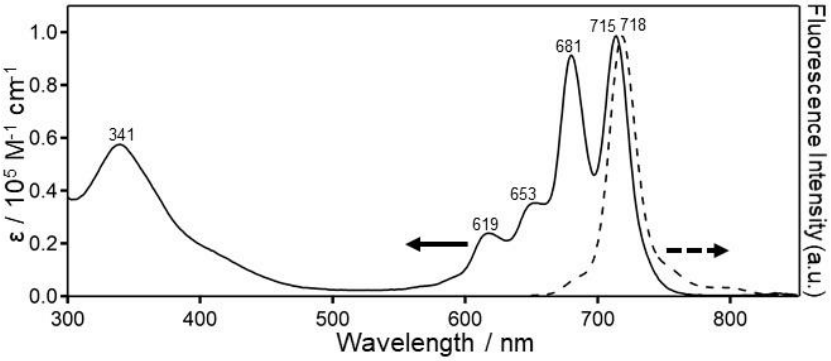

Figure 5-12. UV-vis absorption (solid line) and fluorescence (dashed line) spectra for **1** in chloroform solution. ε means molar extinction coefficient. Excitation wavelength for fluorescence spectrum was 625 nm.

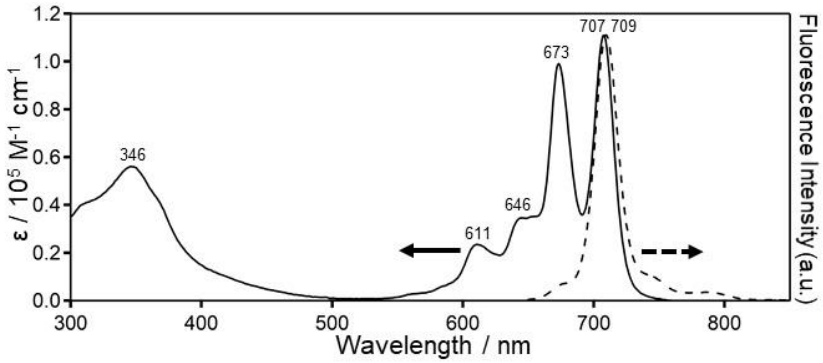

Figure 5-13. UV-vis absorption (solid line) and fluorescence (dashed line) spectra for **2** in chloroform solution. ε means molar extinction coefficient. Excitation wavelength for fluorescence spectrum was 625 nm.

5.3.3. Aggregation property

UV-visible-NIR absorption spectral measurements in both solution and solvent-free liquid states for **1** and **2** were conducted to obtain information on the π-π interactions among Pcs. The NIR absorption bands around 700 nm (Q-band) originated from the HOMO-LUMO electronic transition of Pcs. Therefore, the shapes and positions of the Q-bands are indicators for qualitative analysis of the aggregation behavior of Pcs with Kasha's exciton coupling theory.[26, 27] The absorption spectra for **1** and **2** in dilute chloroform solution showed two clear split Q-bands. The spectral shapes, positions and molar extinction coefficients (**1**: 9.12×10^4, **2**: 1.12×10^5) were exactly the same as the values of the previously reported monomeric H_2Pc derivatives (Figure 5-12 and 5-13).[24a] The results indicate that the Pc cores of **1** or **2** were molecularly dispersed in chloroform. Figures 5-14a and 5-14b show visible-

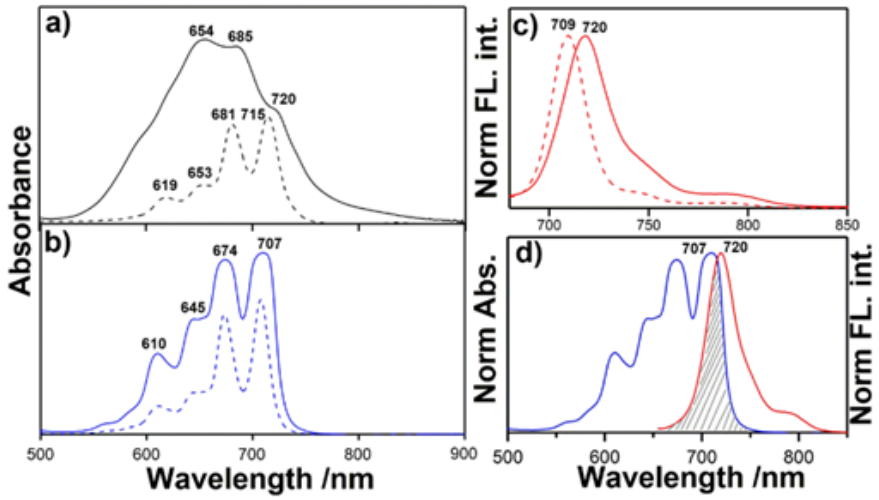

Figure 5-14. (a and b) Visible-NIR absorption spectra for **1** (a, black lines) and **2** (b, blue lines). Solid line: liquid film. Dashed line: chloroform solution (c = 1.26 $\times 10^{-5}$ and 1.03×10^{-5} M for **1** and **2**, respectively). (c) Fluorescence spectra for **2**. Solid line: liquid film. Dashed line: chloroform solution (c = 10^{-6} M). (d) Spectral overlap between absorption (blue line) and fluorescence (red line) bands in liquid film of **2**. The samples were excited at 625 nm in the fluorescence spectra.

NIR absorption spectra in solvent-free liquid samples for **1** and **2** sandwiched by two quartz plates. The spectral shape was broadened, and new blue-shifted peaks were observed for **1** (Figure 5-14a). These spectral features indicate the presence of H-aggregates among Pcs.[14a] On the other hand, the spectral shape for **2** was slightly broadened yet sharp even in the solvent-free liquid state, suggesting that there were aggregated species; however, the π-π interactions were relatively weaker, and there was no formation of H-aggregates (Figure 5-14b). Fluorescence spectral measurements in solution and solvent-free liquid states were conducted for **2** to obtain insight into the environment surrounding the Pc cores in the excited state (Figure 5-14c). A sharp and clear fluorescence emission band for **2** in the chloroform solution was observed at 709 nm (dashed line in Figure 5-14c), indicating a molecularly dispersed state in the dilute chloroform solution. The Stokes shift of the fluorescence band is a small value of 2 nm, reflecting the small change of atomic coordinates through a photo-excitation process due to the rigid planar structure of the Pc. The relative fluorescence quantum yields (Φ) were calculat

$$\Phi = \Phi_{st}\left(\frac{FA}{FA_{st}}\right)\left(\frac{A_{st}}{A}\right) \qquad \text{(Equation 1)} \ ^{28}$$

-ed from eqn 1 (Φ = 0.38 for **1**, 0.51 for **2**, and 0.57 for **3**). Fluorescent solvatochromism was not observed for these Pcs (Table 1). In the solvent-free liquid state, fluorescence emission was observed at 720 nm (solid line in Figure 5-14c). The fluorescence band was slightly broadened and red-shifted due to the surrounding environment or the presence of the dimeric or oligomeric species as in J-type

arrangement of the Pc core. Heat treatment was applied to the liquid film of **2** to get further insight into the red shift of the fluorescence peak compared with that in the solution state (Figure 5-15). No significant shifts of the fluorescence maximum were observed during heating from 25 to 200 °C, suggesting the absence of specific aggregated species such as J-type dimers or oligomers. This result reveals that the red shift of the fluorescence maximum in the liquid film originates from the surrounding environment of the Pc core. The face-to-face π-π interactions of the Pc cores in **2** were almost suppressed even in the solvent-free liquid state, which was enough to contribute to NIR-fluorescence emission, although approximately 50% of the emission was self-quenched due to its small Stokes shift (Figure 5-14d). Steric wrapping by bulky yet flexible chains can protect the π-conjugated unit from reactive species.[29] Photostability experiments were conducted by irradiating dilute chloroform solutions (c = 10^{-5} M) of the samples under simulated sunlight. The photo-degradation rate monitored by the absorption and fluorescence spectral change of **2** was about two times slower than that of the control sample (**3**) (Figure 5-16). This result clearly indicates that the enhanced stability of the Pc core is related to the wrapping by bulky alkyl side chains.

Table 5-1. Polarity effect of solvents on wavelength of fluorescence.

	λ_{FL} /nm			
Sample	*n*-hexane[a]	toluene[b]	$CHCl_3$[c]	THF[d]
1	714	718	718	717
2	706	709	709	708
3	n.d.[e]	709	709	707

[a] ε = 1.90. [b] ε = 2.38. [c] ε = 4.70. [d] ε = 18.5. [e] The datum was not obtained due to the insolubility. ε means dielectric constant of solvent.

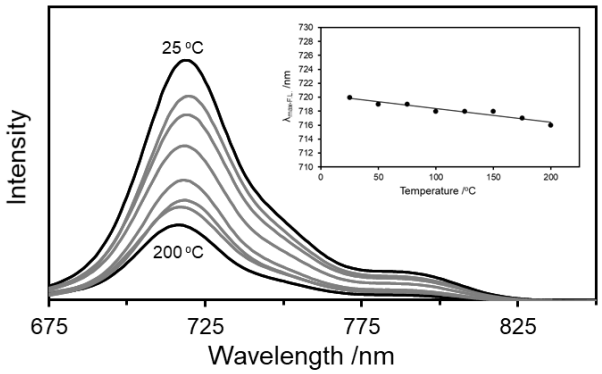

Figure 5-15. Fluorescence spectra for heating liquid film of **2**. Liquid film sandwiched by two quartz plates was used for this measurement. The liquid film was heated by hot stage (METTLER TOLEDO FP82HT) for 10 minutes, then the sample was quickly transferred from hot stage to spectrometer and fluorescence of the sample was measured.

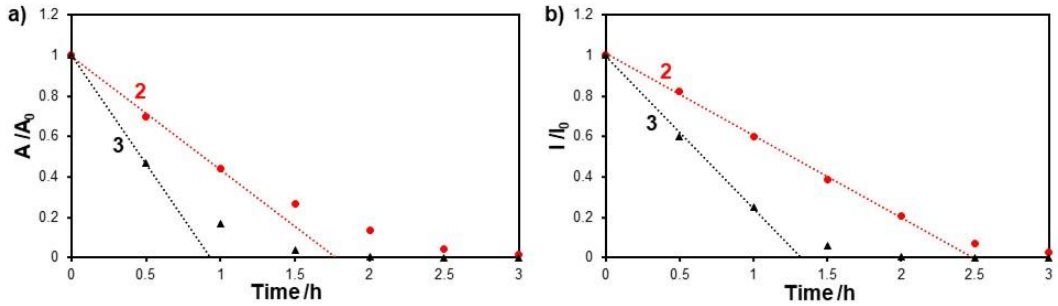

Figure 5-16. Time-dependent change of absorbance (a) or fluorescence intensity (b) ratio at 707 nm. The slopes of least squares line mean photo-degradation rate of the samples.

The aggregation properties through intermolecular π-π interactions of **1** and **2** in the liquid state depend on the substitution pattern of their branched alkyl chains. Figure 5-17 shows a proposed schematic illustration for the molecular structure-aggregation property relationship. As **1** with 2-hexyldecyl branched chains at the 3,5-positions in the phenyl side groups has a space over the Pc core, there is a chance for the face-to-face approach of the Pc core. Therefore, **1** forms H-aggregates in the solvent-free liquid state. On the other hand, the Pc core of **2** was efficiently covered by 2-hexyldecyl branched chains at the 2-position in the phenyl side groups as confirmed by ^{1}H NMR and photostability experiments in the solution state. The configurations of the branched alkyl chains prohibit the face-to-face arrangement approach of the Pc cores even in the condensed solvent-free liquid state. Therefore, face-to-face π-π interactions in **2** are suppressed, and the NIR fluorescence emission from the liquid sample of **2** can be preserved.

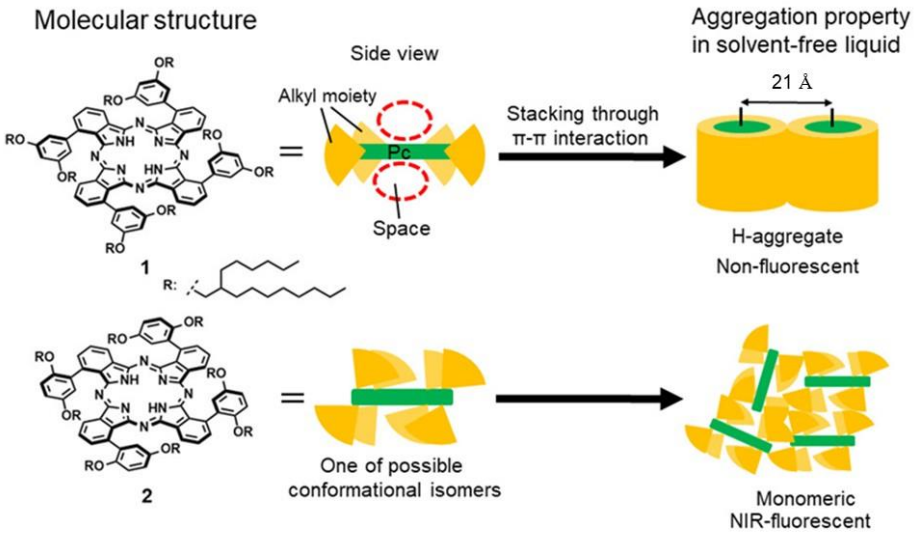

Figure 5-17. Schematic representation of the molecular structure-aggregation property relationship for **1** and **2.**

5.4. Conclusion

Pcs **1** and **2** substituted with four di(2-hexyldecyloxy)phenyl units at the non-peripheral positions were synthesized, and the correlation between their molecular structure and aggregation property was investigated. The substitution pattern of the 2-hexyldecyl branched chains on the non-peripheral phenyl units affected the aggregation property in the solvent-free liquid state. The neat-state XRD and absorption spectral experiments can provide sufficient information on the Pc-core environment. The non H-aggregated species, as well as enhanced photostability, are due to the steric wrapping effect with 2-hexyldecyl branched chains on the Pc surface, which can greatly contribute to the NIR-fluorescence in the solvent-free liquid state of **2**, albeit its partial self-quenching originated from the small Stokes shift. On the other hand, the fluorescence of **1** was completely quenched due to the formation of H-aggregates. The rational molecular design is helpful toward the steric protection of the Pc core and tuning of the aggregation property in Pc liquids. The NIR-fluorescent Pc-based molecular liquid will enable the application of NIR-technology in light-emitting devices and photon up conversion systems. As future prospects, molecular design and/or metal ion-complexation for increasing the NIR-emissive component should be explored to contribute to the development of soft materials including solvent-free liquids with potential for efficient utilization of photon energy in the NIR spectral region.

References

1. (a) A. Dawn, T. Shiraki, S. Haraguchi, S. Tamaru, and S. Shinkai, *Chem. –Asian J.*, 2011, **6**, 266; (b) S. S. Babu, V. K. Praveen, and A. Ajayaghosh, *Chem. Rev.*, 2014, **114**, 1973.
2. (a) A. T. Kleinschmidt and D. J. Lipomi, *Acc. Chem. Res.*, 2018, **51**, 3134; (b) A. Shinohara, C. Pan, Z. Guo, L. Zhou, Z. Liu, L. Du, Z. Yan, F. J. Stadler, L. Wang, and T. Nakanishi, *Angew. Chem. Int. Ed.*, 2019, **58**, 9581.
3. (a) S. Sergeyev, W. Pisula, and Y. H. Geerts, *Chem. Soc. Rev.*, 2007, **36**, 1902; (b) H. K. Bisoyi and Q. Li, *Chem. Rev.*, 2016, **116**, 15089; (c) T. Kato, J. Uchida, T. Ichikawa, and T. Sakamoto, *Angew. Chem. Int. Ed.*, 2018, **57**, 4355.
4. Recent review for solvent-free molecular liquids: A. Ghosh and T. Nakanishi, *Chem. Commun.*, 2017, **53**, 10344.
5. Review for solvent-free luminous molecular liquids: F. Lu and T. Nakanishi, *Adv. Opt. Mater.*, 2019, 1900176.
6. P. Duan, N. Yanai, and N. Kimizuka, *J. Am. Chem. Soc.*, 2013, **135**, 19056.
7. (a) S. Hirata, K. Kubota, H. H. Jung, O. Hirata, K. Goushi, M. Yahiro, and C. Adachi, *Adv. Mater.*, 2011, **23**, 889; (b) N. Kobayashi, T. Kasahara, T. Edura, J. Oshima, R. Ishimatsu, M. Tsuwaki, T. Imato, S. Shoji, and J. Mizuno, *Sci. Rep.*, 2015, **5**, 14822.

8. (a) T. N. Singh-Rachford, A. Nayak, M. L. Muro-Small, S. Goeb, M. J. Therien, and F. N. Castellano, *J. Am. Chem. Soc.*, 2010, **132**, 14203; (b) S. Amemori, Y. Sasaki, N. Yanai, and N. Kimizuka, *J. Am. Chem. Soc.*, 2016, **138**, 8702.
9. Recent review for NIR-OLED: A. Zampetti, A. Minotto, and F. Cacialli, *Adv. Funct. Mater.*, 2019, 29, 1807623.
10. (a) J. Fabian, H. Nakazumi, and M. Matsuoka, *Chem. Rev.*, 1992, **92**, 1197; (b) G. Qian and Z. Y. Wang, *Chem. –Asian J.*, 2010, **5**, 1006.
11. F. Lu, T. Takaya, K. Iwata, I. Kawamura, A. Saeki, M. Ishii, K. Nagura, and T. Nakanishi, *Sci. Rep.*, 2017, **7**, 3416.
12. A. Ghosh, M. Yoshida, K. Suemori, H. Isago, N. Kobayashi, Y. Mizutani, Y. Kurashige, I. Kawamura, M. Nirei, O. Yamamuro, T. Takaya, K. Iwata, A. Saeki, K. Nagura, S. Ishihara, and T. Nakanishi, *Nat. Commun.*, 2019, **10**, 1.
13. (a) N. Kobayashi, H. Ogata, N. Nonaka, and E. A. Luk'yanets, *Chem. –Eur. J.*, 2003, **9**, 5123; (b) A. Muranaka, M. Yonehara, and M. Uchiyama, *J. Am. Chem. Soc.*, 2010, **132**, 7844; (c) T. Furuyama, K. Satoh, T. Kushiya, and N. Kobayashi, *J. Am. Chem. Soc.*, 2014, **136**, 765.
14. (a) Y. Chino, A. Ghosh, T. Nakanishi, N. Kobayashi, K. Ohta, and M. Kimura, *Chem. Lett.*, 2017, **46**, 1539; (b) A. Zielinska, A. Takai, H. Sakurai, A. Saeki, M. Leonowicz, and T. Nakanishi, *Chem. –Asian J.*, 2018, **13**, 770.
15. (a) M. Brewis, G. J. Clarkson, M. Helliwell, A. M. Holder, and N. B. McKeown, *Chem. –Eur. J.*, 2000, **6**, 4630; (b) R. R. Dasari, M. M. Sartin, M. Cozzuol, S. Barlow, J. W. Perry, and S. R. Marder, *Chem. Commun*., 2011, **47**, 4547.
16. (a) C. A. Kernag and D. V. McGrath, *Isr. J. Chem.*, 2009, **49**, 9; (b) X. Chen, N. Fernando, and D. V. McGrath, *Macromolecules*, 2010, **43**, 5512.
17. A. W. Snow, in *The Porphyrin Handbook, Phthalocyanines: Properties and Materials*, ed. K. M. Kadish, K. m. Smith, R. Guilard, Elsevier Science, San Diego, USA, 2003, Vol. 17, pp. 129-176.
18. T. Ishiyama, M. Murata, and N. Miyaura, *J. Org. Chem.*, 1995, **60**, 7508.
19. R. Martin and S. L. Buchwald, *Acc. Chem. Res.*, 2008, **41**, 1461.
20. H. Suzuki, K. Kawano, K. Ohta, Y. Shimizu, N. Kobayashi, and M. Kimura, *ChemistryOpen,* 2016, **5**, 150.
21. H. A. Moynihan and G. Claudon, *CrystEngComm*, 2010, **12**, 2695.
22. P. A. Barrett, D. A. Frye, and R. P. Linstead, *J. Chem. Soc.*, 1938, 1157.
23. G. Schmid, M. Sommerauer, M. Geyer, and M. Hanack, in *Phthalocyanines: Properties and Applications*, ed. C. C. Leznoff, and A. B. P. Lever, VCH, Weinheim, 1996, Vol. 4, pp. 5-18.
24. (a) J. Ranta, T. Kumpulainen, H. Lemmetyinen, and A. Efimov, *J. Org. Chem.*, 2010, **75**, 5178; (b) P. Apostol, A. Bentaleb, M. Rajaoarivelo, R. Clérac, and H. Bock, *Dalton Trans*., 2015, **44**, 5569; (c) S. Yamamoto, K. Kuribayashi, T. N. Murakami, E. Kwon, M. J. Stillman, N. Kobayashi,

H. Segawa, and M. Kimura, *Chem. –Eur. J.*, 2017, **23**, 15446.

25. (a) S. Kawano, Y. Yamada, S. Rongfang, Y. Ishihara, and K. Tanaka, *Chem. Lett.*, 2018, **47**, 1262; (b) M. Lehmann, M. Dechant, M. Holzapfel, A. Schmiedel, and C. Lambert, *Angew. Chem. Int. Ed.*, 2019, **58**, 3610.
26. M. Kasha, H. R. Rawls, and M. A. El-Bayoumi, *Pure Appl. Chem.*, 1965, **11**, 371.
27. (a) K. Hatsusaka, K. Ohta, I. Yamamoto, and H. Shirai, *J. Mater. Chem.*, 2001, **11**, 423; (b) P. Kasprzycki, L. Sobotta, S. Lijewski, M. Wierzchowski, T. Goslinski, J. Mielcarek, C. Radzewicz, and P. Fita, *Phys. Chem. Chem. Phys.*, 2017, **19**, 21390.
28. *β*-Tetra-*tert*-butylphthalocyanine was used as a standard sample (Φ_{st}=0.67 in toluene: See reference, D. M. Guldi, I. Zilbermann, A. Gouloumis, P. Vázquez, and T. Torres, *J. Phys. Chem. B*, 2004, **108**, 18485). Where Φ and Φ_{st} are fluorescence quantum yield for unknown sample and standard sample, respectively, FA and FA_{st} are integrated area of fluorescence spectra for unknown sample and standard sample, respectively, A and A_{st} are absorbance at excitation wavelength (625 nm) for unknown sample and standard sample, respectively. All fluorescence spectra were recorded in toluene. The samples were excited at 625 nm.
29. S. S. Babu, M. J. Hollamby, J. Aimi, H. Ozawa, A. Saeki, S. Seki, K. Kobayashi, K. Hagiwara, M. Yoshizawa, H. Möhwald, and T. Nakanishi, *Nat. Commun.*, 2013, **4**, 1969.

Chapter 6

Conclusion

6.1. Summary and conclusion

The main objective of the present thesis was to reveal the relationship between the molecular structures and aggregation structures through controlling intermolecular interactions of Pc in liquid crystalline and solvent-free liquid state. The author focused on the molecular design based on combination of flexible units and Pc as π-conjugated units. The positions of alkyl chains on phenyl ether groups have been changed from *m*-positon (**Chapter 3**) to *o*-position (**Chapter 4**), leading to reduction of π-π interactions between Pc cores. Detailed analysis have been conducted for the Pc's aggregates in columnar liquid crystalline (**Chapter 3**) and solvent-free liquid state (**Chapter 4**). Moreover, the author have focused to the structures of bulky yet flexible units, and the bulky unit's positon on Pc ring (**Chapter 5**). The relationship between the molecular structures and aggregation property have been investigated. These works are summarized in the following section.

Chapter 3 describes the synthesis, characterization, mesomorphism of novel octa(*m*-alkoxyphenyl-thio) copper Pcs. The structure of π-π stacks and liquid crystalline phase depended on the ether-linkers (O in previous work, S in this work) and length of alkyl chains. Each of the present longer alkoxy-substituted *phenylthio* derivatives (*m*-C_nOPhS)$_8$PcCu (n = 4~16) showed only rectangular columnar (Col_{ro}(P2m)) phase (tilted π-π stack), whereas each of the previous longer alkoxy-substituted *phenoxy* derivatives (*m*-C_nOPhO)$_8$PcCu (n = 10~20) showed only a hexagonal columnar (Col_{ho}) phase (face-to-face π-π stack). The different mesophase appearance may be originated from the difference of interaction among the Pc cores having steric hindrance of the peripheral substituents (PhO and PhS).

Chapter 4 investigates the detailed liquid property of octa(*o*-dodecyloxyphenoxy) copper Pc and the metal-free derivative. The result of absorption spectra in liquid film indicated that face-to-face (H-) aggregates were formed in the solvent-free liquid state. Polarizing optical microscopic and rheology experiments suggested the presence of nano-sized rod-like cluster, and the clusters collapsed in response to external inputs of temperature and shear force.

In **Chapter 5**, the synthesis and relationship between the molecular structures and aggregation property for novel liquid Pcs, 1, 8, 15, 22-tetra[3′, 5′-(2″-hexyldecyloxyphenyl)]-phthalocyanine (**1**) and 1, 8, 15, 22-tetra[2′, 5′-(2″-hexyldecyloxyphenyl)]phthalocyanine (**2**) are reported. **1** formed H-aggregates in solvent-free liquid state. On the other hand, **2** remained monomeric non-aggregated state in the solvent-free state, which contribute to NIR-fluorescence emission in the liquid state. In addition, enhanced photosatbility in relative to the control sample was found in **2** due to steric wrapping effect of the branched alkyl chains.

Table 6-1. Relationship between molecular structure-aggregation structure and functions.

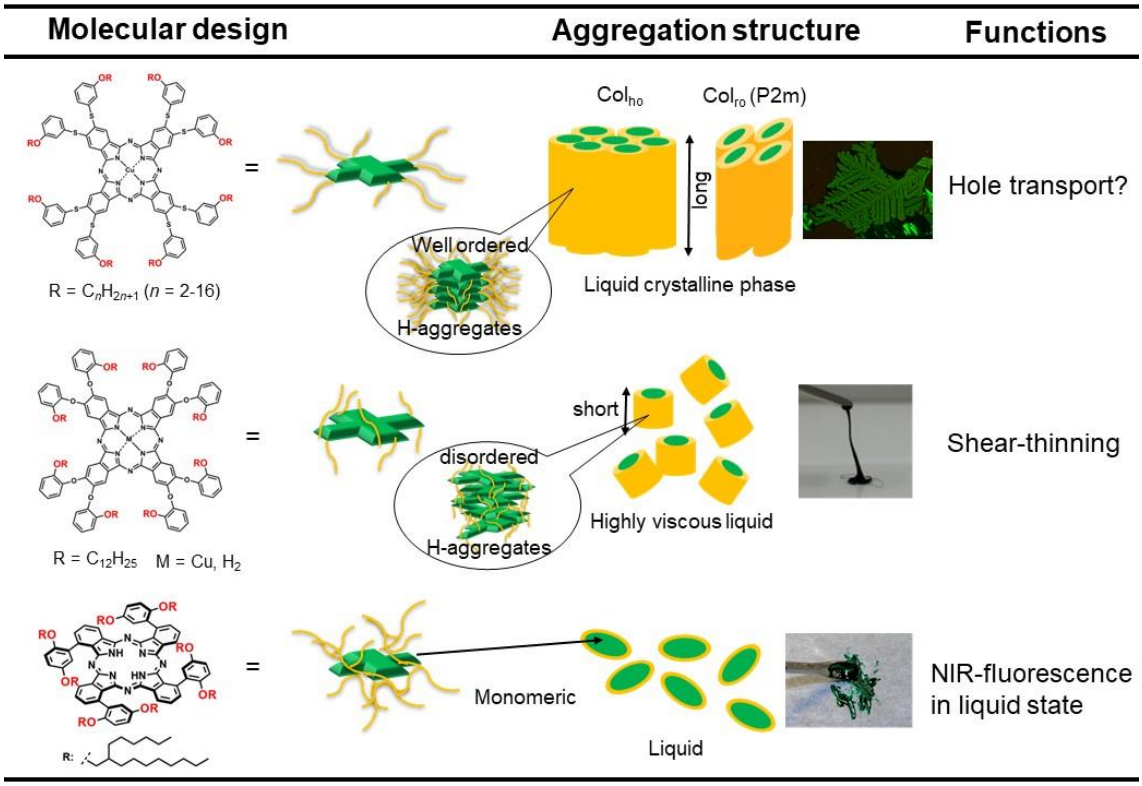

In this thesis, the author investigated the relationship between the molecular structure and the aggregation structures in liquid crystalline and liquid state. The relationship between molecular design and the properties is summarized in Table 6-1. The extending of alkyl chains in flexible units (*m*-alkoxyphenylthio groups) to outer side in Pc core provides a space over the core, which induces face-to-face stacking of the Pc core in macroscopically ordered columnar structure as well as the flexible chains are melted by heating (**Chapter 3**). The self-assembled structure potentially have hole-transport property. In contrast to that of **chapter 3**, the dodecyl chains in phenoxy groups are extend to inner side of Pc core (*o*-substitution) (**Chapter 4**). The *o*-substitution of dodecyl chains weaken π-π interactions between Pc cores, which inhibit from growing into macroscopically ordered columns. Therefore, the Pc derivatives can exhibit highly viscous liquid state. However, short columnar structure was remained in the highly viscous liquid due to the feebly survived π-π interactions. The stimuli-responsive rheological properties can be originated from the survived short columnar structure. The introduction of two-typed bulky yet flexible units (3,5- and 2,5-substitution) to *α*-positions on Pc core provided different aggregated states (**Chapter 5**). The extending of branched alkyl chains to outer side reduce their π-π interactions but provides a space over the Pc core. Therefore, short columnar structure through their feeble π-π interactions are remained in the liquid state. In contrast to the design, asymmetrical 2,5-substitution leads to isolate Pc core thanks to the steric wrapping by branched alkyl chains. Therefore, NIR-fluorescence in the liquid state is preserved and the enhanced photostability is

observed.

In conclusion, the aggregation structures of the Pc derivatives are dependent in the surface coverage of Pc core by alkyl chains. The surface coverage of Pc core can be tuned through changing the position of side groups and alkyl chains. When the Pc core is not covered, the Pc cores are face-to-face stacked each other and one-dimensionally columnar structures are formed. The columns grow into macroscopically ordered columns and the one-dimensionally long columns are self-assembled into two-dimensionally columnar lattice. In contrast to this, when Pc core is insufficiently covered, short columns are formed through feeble face-to-face π-π interactions in liquid state. The highly viscosity of the liquid Pcs are originated from the presence of short columns in the liquid state. Moreover, stimuli-responsive rheological properties are induced through the collapse of the clusters. Introducing the bulky yet flexible units to Pc core, the Pc core was sterically wrapped by branched alkyl chains, which leads to isolate the Pc core. As the result, NIR-fluorescence was preserved in the solvent-free liquid state.

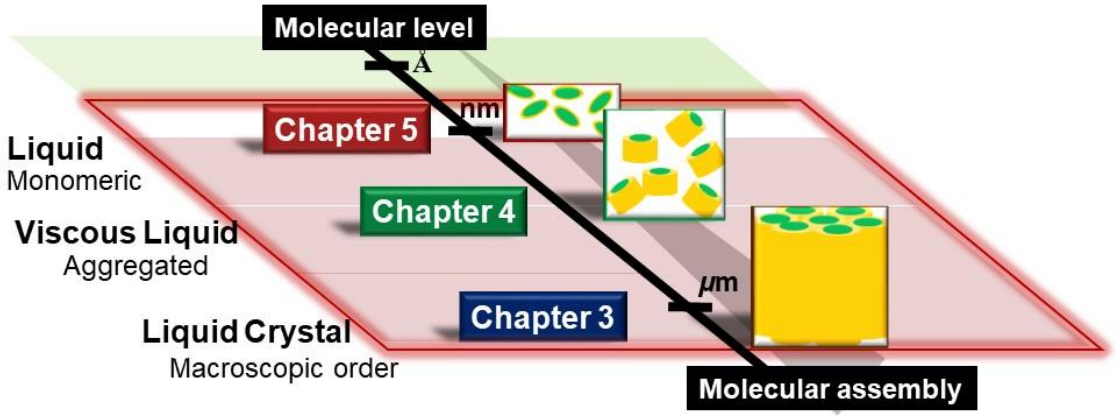

Figure 6-1. Aggregation structures and their size in each chapter.

The results of each chapter are summarized in the view of molecular assembly's size (Figure 6-1). The size of molecular assembly is gradually decrease with the increasing surface coverage of Pc core by alkyl chains. No surface coverage of Pc core provide **micro meter-sized** self- assemble state. In the lower surface coverage, **nano meter-sized** columns are formed through face-to-face π-π interactions. On the other hand, in the higher surface coverage, Pc cores are **near molecularly dispersed** in the solvent free liquid. The structures and size of aggregates affect the functions of molecular assembly and materials. In the result of this dissertation, it is revealed that the functions of the Pc-based materials transfer from that of molecular assembly to that of near molecular level with decreasing the size of molecular assembly.

Publications

1. Yoshiaki Chino, Kazuchika Ohta, Mutsumi Kimura, and Mikio Yasutake, **Discotic liquid crystals of transition metal complexes, 53: synthesis and mesomorphism of phthalocyanines substituted by *m*-alkoxyphenylthio groups,** *J. Porphyrins Phthalocyanines*, 2017, **21**, 159-178. *Selected as cover article
2. Yoshiaki Chino, Avijit Ghosh, Takashi Nakanishi, Nagao Kobayashi, Kazuchika Ohta, and Mutsumi Kimura, **Stimuli-responsive Rheological Properties for Liquid Phthalocyanines**, *Chem. Lett.*, 2017, **46**, 1539-1541.
3. Yoshiaki Chino, Takashi Nakanishi, and Mutsumi Kimura, **A near-infrared fluorescent phthalocyanine liquid developed through controlling intermolecular interactions**, *New J. Chem.*, 2020, **44**, 1689-1693.

Other papers

1. Takahiro Kawata, Yoshiaki Chino, Nagao Kobayashi, and Mutsumi Kimura, **Increased Light-Harvesting in Dye-Sensitized Solar Cells through Förster Resonance Energy Transfer within Supramolecular Dyad Systems**, *Langmuir*, 2018, **34,** 7274-7300.
2. Fengniu Lu, Keumhee Jang, Izabela Osica, Keita Hagiwara, Michito Yoshizawa, Masashi Ishii, Yoshiaki Chino, Kazuchika Ohta, Kinga Ludwichowska, Krzysztof Jan Kurzydłowski, Shinsuke Ishihara, and Takashi Nakanishi, **Supercooling of functional alkyl-π molecular liquids**, *Chem. Sci.*, 2018, **9**, 6774-6778.
   *Hot article, Backside back cover, Highlighted in ChemSci Pick of the week

Conference proceeding

International symposium

1. Kazuchika Ohta, Toshiki Nishizawa, Takahiro Nishiguchi, Yoshiaki Chino, Ryo Shimizu, Yoshiyuki Hattori, Shuji Inoue, Masakazu Katayama, Kazuhiko Mizu-uchi, and Takumi Kono, **Synthesis of carbon nanotubes by microwave energy**, Pacifichem2015, December 15-20, 2015, Hawaii, USA, Oral.
2. Yoshiaki Chino, Takashi Nakanishi, and Mutsumi Kimura, **Control of intermolecular interactions in phthalocyanine liquids**, MANA international symposium 2019, National Institute of Material Science, Tsukuba, Ibaraki, Japan, March 5, 2019, Poster.

Domestic symposium

1. Yoshiaki Chino, Takahiro Nishiguchi, Yasufumi Takagi and Kazuchika Ohta, **Synthesis of carbon nanotubes by microwave heating and its surface functionalization by solution plasma**, JEMEA symposium, O28, Sophia University, Japan, November 20, 2015, Oral.
2. Yoshiaki Chino and Kazuchika Ohta, **Discotic Liquid Crystals of Organic Metal Complexes (118); Synthesis and Columnar Mesomorphism of Novel (*m*-C_nOPhS)$_8$PcCu Complexes**, The Chemical Society of Japan, The 96th Annual Meeting, 3E4-45, Doshisya University, Japan, March 26, 2016, Oral.
3. Yoshiaki Chino, Mutsumi Kimura, **Stimulus Response of Viscoelastic Property for Liquid Phthalocyanines**, Nanofiber society, The 8th Annual Meeting, , Tokyo Institute of Technology, Japan, July 14, 2017, Poster.
4. Mutsumi Kimura, Yoshiaki Chino, **Liquid phthalocyanines having near-infrared light absorption proprety**, The 2nd workshop for "functional liquids", National Institute of Materials Science, Japan, Novemver 10, 2018, Oral.
5. Yoshiaki Chino, Takashi Nakanishi, and Mutsumi Kimura, **Stimuli-responsive liquid phthalocynanine**, The Chemical Society of Japan, The 98th Annual Meeting, 2F4-43, Nihon University, Japan, March 21, 2018, Oral.
6. Yoshiaki Chino, Takashi Nakanishi, and Mutsumi Kimura, **Stimuli-responsive liquid phthalocynanine**, The Chemical Society of Japan, The 98th Annual Meeting, 1PC-075, Nihon University, Japan, March 20, 2018, Poster.
7. Ryota Kudo, Yoshiaki Chino, Nagao Kobayashi, Mutsumi Kimura, **Multi-dimensional Organized Structures formed by Octopus-type Phthalocyanines,** The Chemical Society of Japan, The 98th Annual Meeting, 2F5-38, Nihon University, Japan, March 21, 2018, Oral.

Acknowledgements

I would like to thank Prof. Mutsumi Kimura for his limitless patience, understanding and honest support. I also would like to thank Prof. Kazuchika Ohta for his recommendation for doctoral studies, lecture of analytical methods for liquid crystalline material, and his kindness supports and advices. I also would like to thank Dr. Takashi Nakanishi of frontier molecules group in National Institute of Material Science (NIMS) for his lecture of analytical methods for liquid material, giving me chances to study in NIMS and to attend international symposium, his kindness supports, advices and fruitful discussions. I also would like to thank Prof. Nagao Kobayashi for his kindness supports and advices for phthalocyanine chemistry. I also would like to thank Assoc. Prof. Yu Kitazawa for his kindness supports and advices.

I would like to extend my special thanks to Prof. Shigeyuki Yagi of Osaka Prefecture University, Prof. Naoki Asao, Prof. Yoshiyuki Hattori, Prof. Yasushi Nomura for reviewing my thesis.

I would like to thank my colleagues in Kimura Lab, who are still here or left including Ana Carolina Cons Bacilla, Ryota Kudo, Mizuki Goto, Masahiro Sonobe, Yosuke Karasawa, Tatsuya Yosii, Akane Imazu, Yuhi Ito, Yoshino Ohgami, Satsuki Yoshida, Teruaki Ohshima, Saki Takahashi, Takahiro Kawata, Kengo Kuribayashi, Takeshi Sii, Takuro Ikeuchi, and Dr. Satoshi Yamamoto who made my Ph. D. journey much more enjoyable. I am also very thankful to all members of frontier molecules group in NIMS including Dr. Avijit Ghosh and Dr. Fengniu Lu for their kindness supports, advices, and fruitful discussions.

Finally, I am greatly indebted to my parents Yoshihiro and Michiko Chino for their moral supports and warm encouragements.

March 19, 2020

Yoshiaki Chino